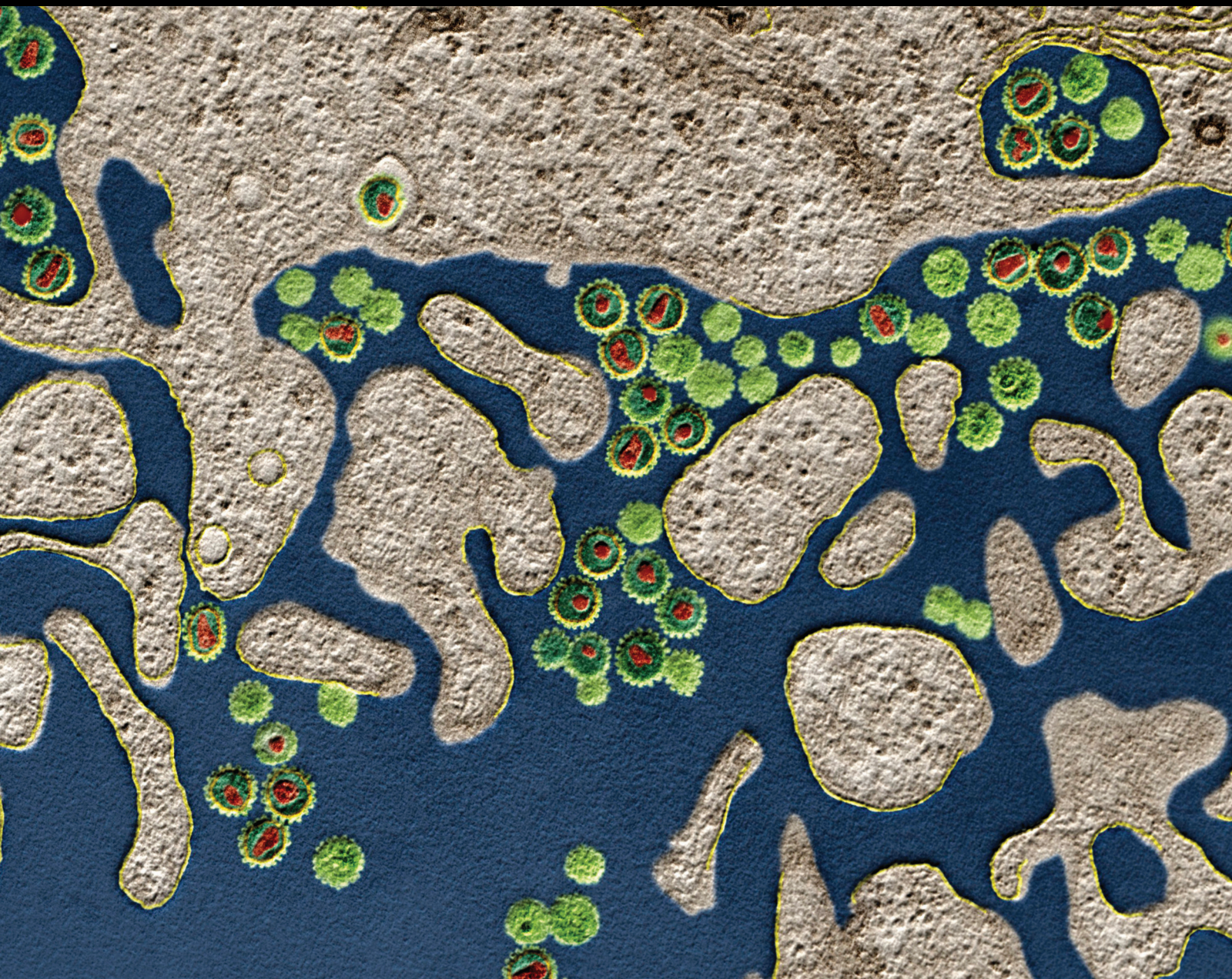


# New Insights into Immune-based Diagnosis, Therapy and Prophylaxis for Infectious Diseases 2020

Special Issue Editor in Chief: Giuseppe A. Sautto

Guest Editors: Roberta Antonia Diotti and Kristen Michelle Kahle





---

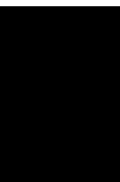
**New Insights into Immune-based Diagnosis,  
Therapy and Prophylaxis for Infectious  
Diseases 2020**

Journal of Immunology Research

---

**New Insights into Immune-based  
Diagnosis, Therapy and Prophylaxis for  
Infectious Diseases 2020**

Special Issue Editor in Chief: Giuseppe A. Sautto  
Guest Editors: Roberta Antonia Diotti and Kristen  
Michelle Kahle



---

Copyright © 2021 Hindawi Limited. All rights reserved.

This is a special issue published in "Journal of Immunology Research." All articles are open access articles distributed under the Creative Commons Attribution License, which permits unrestricted use, distribution, and reproduction in any medium, provided the original work is properly cited.

# Chief Editor

Martin Holland, United Kingdom

## Editorial Board

Jagadeesh Bayry, France  
Payam Behzadi, Iran  
Kurt Blaser, Switzerland  
Dimitrios P. Bogdanos, Greece  
Eduardo F. Borba, Brazil  
Carlo Cavaliere, Italy  
Cinzia Ciccacci, Italy  
Robert B. Clark, USA  
Nathalie Cools, Belgium  
Marco de Vincentiis, Italy  
M. Victoria Delpino, Argentina  
Roberta Antonia Diotti, Italy  
Lihua Duan, China  
Nejat K. Egilmez, USA  
Theodoros Eleftheriadis, Greece  
Eyad Elkord, United Kingdom  
Weirong Fang, China  
Elizabeth Soares Fernandes, Brazil  
Steven E. Finkelstein, USA  
Maria Cristina Gagliardi, Italy  
Luca Gattinoni, USA  
Alvaro González, Spain  
Antonio Greco, Italy  
Qingdong Guan, Canada  
Theresa Hautz, Austria  
Douglas C. Hooper, USA  
Giannicola Iannella, Italy  
Juraj Ivanyi, United Kingdom  
Ravirajsinh Jadeja, USA  
Peirong Jiao, China  
Liu Jinhui, China  
Vladimir JURISIC, Serbia  
Youmin Kang, China  
Alexandre Keller, Brazil  
Sung Hwan Ki, Republic of Korea  
Bogdan Kolarz, Poland  
Esther Maria Lafuente, Spain  
Natalie Lister, Australia  
Jinhui Liu, China  
Mahboobeh Mahdavinia, USA  
Daniele Maria-Ferreira, Saint Vincent and the Grenadines  
Eiji Matsuura, Japan  
François Meurens, Canada

Cinzia Milito, Italy  
Hector Mora-Montes, Mexico  
Chikao Morimoto, Japan  
Paulina Niedźwiedzka-Rystwej, Poland  
Paola Nistico, Italy  
Enrique Ortega, Mexico  
Felipe Passero, Brazil  
Keshav Raj Paudel, Australia  
Carlo Perricone, Italy  
Patrice Xavier Petit, France  
Somchai Pinlaor, Thailand  
Luis Alberto Ponce-Soto, Peru  
Massimo Ralli, Italy  
Pedro A. Reche, Spain  
Eirini Rigopoulou, Greece  
Ilaria Roato, Italy  
Aurelia Rughetti, Italy  
Francesca Santilli, Italy  
Takami Sato, USA  
Giuseppe A. Sautto, USA  
Senthamil R. Selvan PhD, USA  
Anquan Shang, China  
Amar Singh, USA  
Benoit Stijlemans, Belgium  
Jacek Tabarkiewicz, Poland  
Hiroshi Tanaka, Japan  
Bufu Tang, China  
Samanta Taurone, Italy  
Mizue Terai, USA  
Ban-Hock Toh, Australia  
Shariq M. Usmani, USA  
Shengjun Wang, China  
Ran Wang, China  
Paulina Wlasiuk, Poland  
Zhipeng Xu, China  
Baohui Xu, USA  
Huaxi Xu, China  
Xiao-Feng Yang, USA  
Qiang Zhang, USA  
Dunfang Zhang, China  
Jixin Zhong, USA



## Contents






### **New Insights into Immune-Based Diagnosis, Therapy and Prophylaxis for Infectious Diseases 2020**




Giuseppe A. Sautto , Roberta A. Diotti , and Kristen M. Kahle

Editorial (2 pages), Article ID 9767464, Volume 2021 (2021)

### **Epitope-Based Peptide Vaccine Design against Fructose Bisphosphate Aldolase of *Candida glabrata*: An Immunoinformatics Approach**

Lina Mohamed Elamin Elhasan , Mohamed B. Hassan , Reham M. Elhassan , Fatima A.

Abdelrhman , Essam A. Salih , Asma Ibrahim H , Amna A. Mohamed , Hozaira S. Osman ,

Marwa Saad M. Khalil , Athar A. Alsafi , Abeer Babiker Idris , and Mohamed A. Hassan

Research Article (19 pages), Article ID 8280925, Volume 2021 (2021)

### **Clinical Features and Risk Factors of Active Tuberculosis in Patients with Behçet's Disease**

Yaxu Liu , Lifan Zhang, Ziyue Zhou, Luxi Sun, Baotong Zhou, Xiaoqing Liu , and Wenjie Zheng 

Research Article (7 pages), Article ID 2528676, Volume 2020 (2020)

### **Elucidating the Pivotal Immunomodulatory and Anti-Inflammatory Potentials of Chloroquine and Hydroxychloroquine**


Seidu A. Richard , Sylvanus Kampo, Maite Esquijarosa Hechavarria, Marian Sackey, Alexis D. B.

Buunaaim, Eugene Dogkotenge Kuugbee, and Thomas Winsum Anabah

Review Article (13 pages), Article ID 4582612, Volume 2020 (2020)





### **Comprehensive Screening of Mouse T-Cell Epitopes in Human Herpesvirus 6B Glycoprotein H/L/Q1/Q2 Tetramer Complex**


Mie Okutani, Akiko Kawabata, Mitsuhiro Nishimura, Satoshi Nagamata, Soichiro Kuwabara, Yasunari

Haseda, Lisa Munakata, Ryo Suzuki, Yasuko Mori, and Taiki Aoshi 

Research Article (13 pages), Article ID 4697529, Volume 2020 (2020)


### **The Pathogenesis of Coronavirus Disease 2019 (COVID-19): Evaluation and Prevention**

Hayat Ouassou , Loubna Kharchoufa , Mohamed Bouhrim , Nour Elhouda Daoudi , Hamada

Imtara , Nouredine Bencheikh , Amine ELbouzidi , and Mohamed Bnouham 

Review Article (7 pages), Article ID 1357983, Volume 2020 (2020)

### **Immunotherapy with IgY Antibodies toward Outer Membrane Protein F Protects Burned Mice against *Pseudomonas aeruginosa* Infection**

Fatemeh Norouzi, Bahador Behrouz, Mahya Ranjbar, and Seyed Latif Mousavi Gargari 

Research Article (8 pages), Article ID 7840631, Volume 2020 (2020)

## Editorial

# New Insights into Immune-Based Diagnosis, Therapy and Prophylaxis for Infectious Diseases 2020

Giuseppe A. Sautto <sup>1</sup>, Roberta A. Diotti <sup>2,3</sup> and Kristen M. Kahle<sup>4</sup>

<sup>1</sup>Center for Vaccines and Immunology, University of Georgia, Athens, GA 30602, USA

<sup>2</sup>Laboratory of Medical Microbiology and Virology at “Vita-Salute” San Raffaele University, 20132 Milan, Italy

<sup>3</sup>Pomona Ricerca S.r.l., Turin, Italy

<sup>4</sup>Spark Therapeutics, Inc., Philadelphia, PA, USA

Correspondence should be addressed to Giuseppe A. Sautto; [gasautto@uga.edu](mailto:gasautto@uga.edu)

Received 6 December 2021; Accepted 6 December 2021; Published 30 December 2021

Copyright © 2021 Giuseppe A. Sautto et al. This is an open access article distributed under the Creative Commons Attribution License, which permits unrestricted use, distribution, and reproduction in any medium, provided the original work is properly cited.

Immune-based diagnostic, therapeutic, and prophylactic tools have played a central role in medicine since the discovery of antibodies at the end of the 19<sup>th</sup> century.

Since then, more and more sophisticated antibody-based approaches have been developed allowing to easily diagnose different types of disorders spanning from infectious diseases to premalignant, malignant, and autoimmune diseases.

As an example, the enzyme-linked immunosorbent assay (ELISA) represents one of the simplest but still most powerful methods for the diagnosis of different types of diseases, and thanks to its versatility, multiple formats have been developed such as the competitive ELISA, the sandwich ELISA, and the indirect ELISA. Additionally, besides assessing the binding to an antigen, antibody-based method approaches can also have a prognostic value since they can assess the presence, for example, of neutralizing antibodies eliciting a protective effect. In this regard, the hemagglutination inhibition assay (HAI) represents the gold standard method to evaluate the efficacy of not only current standard of care but also underdevelopment next-generation influenza vaccines in eliciting a neutralizing and protective immune response. As for ELISA, the HAI has also been developed in different formats in order to dissect the antibody response, for example, following influenza infection or vaccination. In this context, our group recently described a competitive HAI-based assay using a combination of influenza virus and recombinant influenza hemagglutinin (HA) proteins to dissect the HAI functional activity of HA-specific antibody populations in a single assay format [1].

In parallel to their ease of manufacturing and deployment as highly specific molecules, antibodies represent also a fundamental tool for the development of prophylactic and therapeutic immune-based strategies. As an example, in this special issue, F. Norouzi et al. [2] described the use of egg yolk-specific antibodies (IgY) raised against the outer membrane protein F (OprF) of *Pseudomonas aeruginosa* in a murine burn model of infection. Importantly, immunotherapy with anti-OprF IgY resulted in a significant improvement in the survival of mice infected by *P. aeruginosa* and this phenomenon has been mechanistically confirmed *in vitro* using a A549 cell-based invasion assay. This work represents a further demonstration of the efficacy of antibody-based approaches in limiting infectious diseases. Additionally, thanks to the discovery of methods for developing monoclonal antibodies (mAbs), immune-based therapies are today routinely used in the context of autoimmune and oncologic diseases and are starting to be used more frequently in the clinical practice for the treatment of other types of disorders such as infectious diseases. The current COVID-19 pandemic has further demonstrated, thanks to the extraordinary advancements in the field, the faster discovery and effectiveness of antibody-based approaches as a rapid first-line developed antiviral molecules against SARS-CoV-2, as mentioned by H. Ouassou et al. in their review article of this special issue [3]. In fact, soon after the pandemic outbreak, a plethora of mAbs were soon described in the literature with some of them concomitantly entering in the clinical trial *iter* [4, 5].

In addition to their direct role as immunotherapeutic and immunoprophylactic molecules, antibodies play also a pivotal role as indirect tools to dissect the antibody response following infection or vaccination. In this context, our group recently described the development of mAbs against Computationally Optimized Broadly Reactive Antigens (COBRA) for influenza as a way to dissect the determinants of the humoral response and shed light on the mechanisms responsible of the broad antibody-mediated neutralization and protection conferred by COBRA-based influenza vaccines [6].

In addition to the B cell arm-based tools, the T cell-mediated components of the immune response play a central role not only in the context of our immunity but also as a valid instrument to develop diagnostic and prophylactic tools against infectious diseases. As an example, in this special issue, L. M. Elamin Elhasan et al. described through the use of immunoinformatic approaches the prediction of the most conserved and immunogenic B and T cell epitope peptides of the fructose biphosphate aldolase (Fba1) for the development of a *Candida glabrata* vaccine [7]. Similarly, M. Okutani et al. screened the CD4+ and CD8+ T cell epitopes in the gH/gL/gQ1/gQ2 tetrameric complex protein of the human herpesvirus 6 subtype B (HHV-6B) in a mice immunization model [8]. In particular, this group identified multiple CD4+ and CD8+ T cell-stimulating peptides both in BALB/c and C57BL/6 mouse strains, highlighting the potential of the gH/gL/gQ1/gQ2 tetramer-targeted strategy for the future development of T cell-based vaccine and immunotherapies against HHV-6B.

In this special issue, all these aspects are covered by two review articles and four research papers discussing how we can exploit and utilize the immune system to understand new host-pathogen relationships as well as for the development of novel prophylactic, therapeutic, and diagnostic tools. We hope that the readers of this special issue will appreciate the interesting findings and the reviewed concepts of the field discussed in these papers.

## Conflicts of Interest

The editors declare that they have no conflicts of interest regarding the publication of this special issue.

Giuseppe A. Sautto  
Roberta A. Diotti  
Kristen M. Kahle

## References



- [1] G. A. Kirchenbaum, G. A. Sautto, R. A. Richardson, J. W. Ecker, and T. M. Ross, "A competitive hemagglutination inhibition assay for dissecting functional antibody activity against influenza virus," *Journal of Virology*, vol. 95, no. 23, article JVI0237920, 2021.
- [2] F. Norouzi, B. Behrouz, M. Ranjbar, and S. L. Mousavi Gargari, "Immunotherapy with IgY antibodies toward outer membrane protein F protects burned mice against *Pseudomonas aeruginosa* infection," *Journal of Immunology Research*, vol. 2020, Article ID 7840631, 8 pages, 2020.

- [3] H. Ouassou, L. Kharchoufa, M. Bouhrim et al., "The pathogenesis of coronavirus disease 2019 (COVID-19): evaluation and prevention," *Journal of Immunology Research*, vol. 2020, Article ID 1357983, 7 pages, 2020.
- [4] E. Andreano, E. Nicastrì, I. Paciello et al., "Extremely potent human monoclonal antibodies from COVID-19 convalescent patients," *Cell*, vol. 184, no. 7, pp. 1821–1835.e16, 2021.
- [5] J. Dong, S. J. Zost, A. J. Greaney et al., "Genetic and structural basis for SARS-CoV-2 variant neutralization by a two- antibody cocktail," *Nature Microbiology*, vol. 6, no. 10, pp. 1233–1244, 2021.
- [6] G. A. Sautto, G. A. Kirchenbaum, R. B. Abreu et al., "A computationally optimized broadly reactive antigen subtype-specific influenza vaccine strategy elicits unique potent broadly neutralizing antibodies against hemagglutinin," *Journal of Immunology*, vol. 204, no. 2, pp. 375–385, 2020.
- [7] L. M. Elamin Elhasan, M. B. Hassan, R. M. Elhassan et al., "Epitope-based peptide vaccine design against fructose biphosphate aldolase of *Candida glabrata*: an immunoinformatics approach," *Journal of Immunology Research*, vol. 2021, Article ID 8280925, 19 pages, 2021.
- [8] M. Okutani, A. Kawabata, M. Nishimura et al., "Comprehensive screening of mouse T-cell epitopes in human herpesvirus 6B glycoprotein H/L/Q1/Q2 tetramer complex," *Journal of Immunology Research*, vol. 2020, Article ID 4697529, 13 pages, 2020.



## Research Article

# Epitope-Based Peptide Vaccine Design against Fructose Bisphosphate Aldolase of *Candida glabrata*: An Immunoinformatics Approach

Lina Mohamed Elamin Elhasan <sup>1</sup>, Mohamed B. Hassan <sup>2</sup>, Reham M. Elhassan <sup>3</sup>,  
Fatima A. Abdelrhman <sup>4</sup>, Essam A. Salih <sup>5</sup>, Asma Ibrahim H <sup>6</sup>, Amna A. Mohamed <sup>7</sup>,  
Hozaifa S. Osman <sup>2</sup>, Marwa Saad M. Khalil <sup>7</sup>, Athar A. Alsafi <sup>1</sup>, Abeer Babiker Idris <sup>8</sup>,  
and Mohamed A. Hassan <sup>4,9</sup>

<sup>1</sup>Faculty of Science and Technology, Department of Biotechnology, Omdurman Islamic University, Khartoum, Sudan

<sup>2</sup>Faculty of Medicine and Health Science, Omdurman Islamic University, Khartoum, Sudan

<sup>3</sup>Department of Pharmaceutical Chemistry, Faculty of Pharmacy, Sudan International University, Khartoum, Sudan

<sup>4</sup>Department of Biotechnology, Africa City of Technology, Khartoum, Sudan

<sup>5</sup>Biology and Technology Department, College of Applied and Industrial Sciences, University of Bahri, Khartoum, Sudan

<sup>6</sup>Faculty of Pharmacy, National Ribat University, Khartoum, Sudan

<sup>7</sup>Al-Neelain Medical Research Center, Al-Neelain University, Khartoum, Sudan

<sup>8</sup>Department of Medical Microbiology, Faculty of Medical Laboratory Sciences, University of Khartoum, Khartoum, Sudan

<sup>9</sup>Department of Translation Bioinformatics, Detavax Biotech, Kayseri, Turkey

Correspondence should be addressed to Lina Mohamed Elamin Elhasan; [lina2014371@gmail.com](mailto:lina2014371@gmail.com)

Received 10 July 2020; Revised 27 March 2021; Accepted 12 April 2021; Published 5 May 2021

Academic Editor: Roberta Antonia Diotti

Copyright © 2021 Lina Mohamed Elamin Elhasan et al. This is an open access article distributed under the Creative Commons Attribution License, which permits unrestricted use, distribution, and reproduction in any medium, provided the original work is properly cited.

**Background.** *Candida glabrata* is a human opportunistic pathogen that can cause life-threatening systemic infections. Although there are multiple effective vaccines against fungal infections and some of these vaccines are engaged in different stages of clinical trials, none of them have yet been approved by the FDA. **Aim.** Using immunoinformatics approach to predict the most conserved and immunogenic B- and T-cell epitopes from the fructose bisphosphate aldolase (Fba1) protein of *C. glabrata*. **Material and Method.** 13 *C. glabrata* fructose bisphosphate aldolase protein sequences (361 amino acids) were retrieved from NCBI and presented in several tools on the IEDB server for prediction of the most promising epitopes. Homology modeling and molecular docking were performed. **Result.** The promising B-cell epitopes were AYFKEH, VDKEPLYTK, and HVDKESLYTK, while the promising peptides which have high affinity to MHC I binding were AVHEALAPI, KYFKRMAAM, QTSNGGAAY, RMAAMNQWL, and YFKEHGEPL. Two peptides, LFSSHMLDL and YIRSIAPAY, were noted to have the highest affinity to MHC class II that interact with 9 alleles. The molecular docking revealed that the epitopes QTSNGGAAY and LFSSHMLDL have the lowest binding energy to MHC molecules. **Conclusion.** The epitope-based vaccines predicted by using immunoinformatics tools have remarkable advantages over the conventional vaccines in that they are more specific, less time consuming, safe, less allergic, and more antigenic. Further in vivo and in vitro experiments are needed to prove the effectiveness of the best candidate's epitopes (QTSNGGAAY and LFSSHMLDL). To the best of our knowledge, this is the first study that has predicted B- and T-cell epitopes from the Fba1 protein by using in silico tools in order to design an effective epitope-based vaccine against *C. glabrata*.

## 1. Introduction

Candidiasis is a fungal infection that has a high burden of morbidity and mortality in hospitalized and immunocompromised patients. It occurs in more than a quarter of a million patients every year with incidence rates for candidemia of 2–14 per 100,000 [1–4]. In general, *Candida* species infection ranges from superficial mucosal candidiasis such as vulvovaginal candidiasis and oropharyngeal candidiasis to serious systemic infection such as candidemia or fungemia [5–8]. Pathogenicity is facilitated by a number of virulence factors, most importantly its ability to adhere to host surfaces including medical devices, biofilm formation, and secretion of hydrolytic enzymes. Also, *Candida* cells elaborate polysaccharides, proteases, phospholipases, and hemolysins that cause host cell damage which leads to the increase in the incidence and antifungal resistance of NCAC species, specifically *C. glabrata*, and the unfortunate high morbidity and mortality associated with these species [8, 9].

*Candida glabrata* (*C. glabrata*) is a human opportunistic pathogen that can cause life-threatening systemic infections. *C. glabrata* is not polymorphic, grows as blastoconidia (yeast), and lacks pseudohyphal formation, so it is classified in the genus *Torulopsis*. *C. glabrata* cells (1–4  $\mu\text{m}$  in size) forms glistening, smooth, and cream-colored colonies [10, 11]. During the infection, *C. glabrata* pathogens invade the macrophages, which are considered part of the innate immune system which is the first line of defense against invading pathogens. *C. glabrata* is able to modify the macrophage's phagosomal compartment, avoiding full maturation and acidification, and thus prevents the forming of the phagolysosomal environment [12]. *C. glabrata* is able to invade the bloodstream and different organs in a mouse model that have intragastric infections [13].

*C. glabrata* has a haploid genome—published in 2004 by Dujon et al. [14]—that allows adaptation to a wide range of environments [9, 15, 16]. Also, its genome contains more tandem repeats of genes than the other *Nakaseomyces* [17] and covers 67 genes encoding putative adhesin (cell wall proteins), including the Epa family with 17 members [16, 18], such as epithelial adhesin 1 (Epa1p) [19] and fructose biphosphate aldolase protein (Fba1) which play an essential role in the pathogenicity of *Candida* species mainly in the adhesion of the pathogen to the host [20, 21].

Fba1 is a yeast cell wall protein which presents in multiple species of *Candida*, e.g., *C. glabrata*, *C. parapsilosis*, *C. tropicalis*, and *C. albicans* fungal pathogens [22–26]. Fba1 is an important enzyme in the glycolytic pathway [27–30] and is also a multifunctional protein [31] that can facilitate the attachment (adhesion) to human cells or abiotic surfaces [32–34], protects *Candida* cells from the host's immune system [33], and promotes the detoxification of the ROS generated during the respiratory burst [21, 33, 34]. However, proteomics analysis revealed that Fba1 is the most abundant and stable enzyme in *Candida*. Moreover, it is considered one of the main immunodominant proteins [35, 36] in *Candida* cells and has been tested in the murine model as a protected protein against *Candida* [37], especially *C. albicans*, and also introduced immunity to

*C. glabrata* [34]; therefore, Fba1 is a potential antifungal target in yeast [38]. Multiple vaccines used Fba1 as an immunogenic protein against different pathogens such as the lethal and challenging *S. pneumoniae*, *Salmonella* spp., and *M. bovis* [39, 40].

The incidence of fungal infection has been increasing in the last few years, due to several factors such as misuse of broad-spectrum antibiotics, cytotoxic chemotherapy, immunocompromised patients, and transplantations [15, 41]. Invasive fungal infections are a major cause of global morbidity and mortality, accounting for about 1.4 million deaths per year [42]. Systemic fungal infections cost the healthcare industry approximately \$2.6 billion per year in the USA alone [43]. However, *Candida* species pose a base problem in hospitals, according to Healthcare-Associated Infections (HAI) [19, 44–46]. Although there are multiple effective vaccines against fungal infections and some of these vaccines are engaged in different stages of clinical trials, none of them have yet been approved by the FDA [47]. Therefore, there is an urgent and crucial need to design vaccines against the *Candida* species that might improve the quality of life for immunosuppressed patients [48].

The aim of this study is to predict the most conserved and immunogenic B- and T-cell epitopes from the Fba1 protein of *C. glabrata* by using in silico tools with the immunoinformatics approach presented in the IEDB server [49, 50]. This approach has multiple benefits in comparison to other approaches by being affordable, safe, time-saving, and clinically applicable using different computational software techniques [51–53]. To the best of our knowledge, this is the first study that has predicted the best candidates of multiple epitopes for Fba1 protein against *C. glabrata*.

## 2. Materials and Methods

In this study, we have used a variety of bioinformatics databases and tools for the prediction of the most promising peptides, through three phases shown in Figure 1.

**2.1. Retrieval of Fructose Biphosphate Aldolase Protein Sequences.** 13 *Candida glabrata* fructose biphosphate aldolase protein sequences (361 amino acids) were retrieved from the NCBI (<https://www.ncbi.nlm.nih.gov/protein>) database on 21 January 2019. The accession numbers of fructose biphosphate aldolase protein sequences were CAG61849.1, XP\_448879.1, KTB01194.1, KTB08502.1, KTB09791.1, KTB12564.1, KTB19354.1, KTB25695.1, KTB27082.1, OXB40821.1, OXB46121.1, SLM13767.1, and SCV14850.1 [20].

**2.2. Determination of Conserved Regions.** Multiple sequence alignment (MSA) was used to determine the conserved regions; the retrieved sequences were aligned by MSA using Clustal W as applied in the BioEdit [54].

**2.3. Prediction of B-Cell Epitope.** The reference sequence of fructose biphosphate aldolase protein was submitted to the following B-cell tests [49, 50].

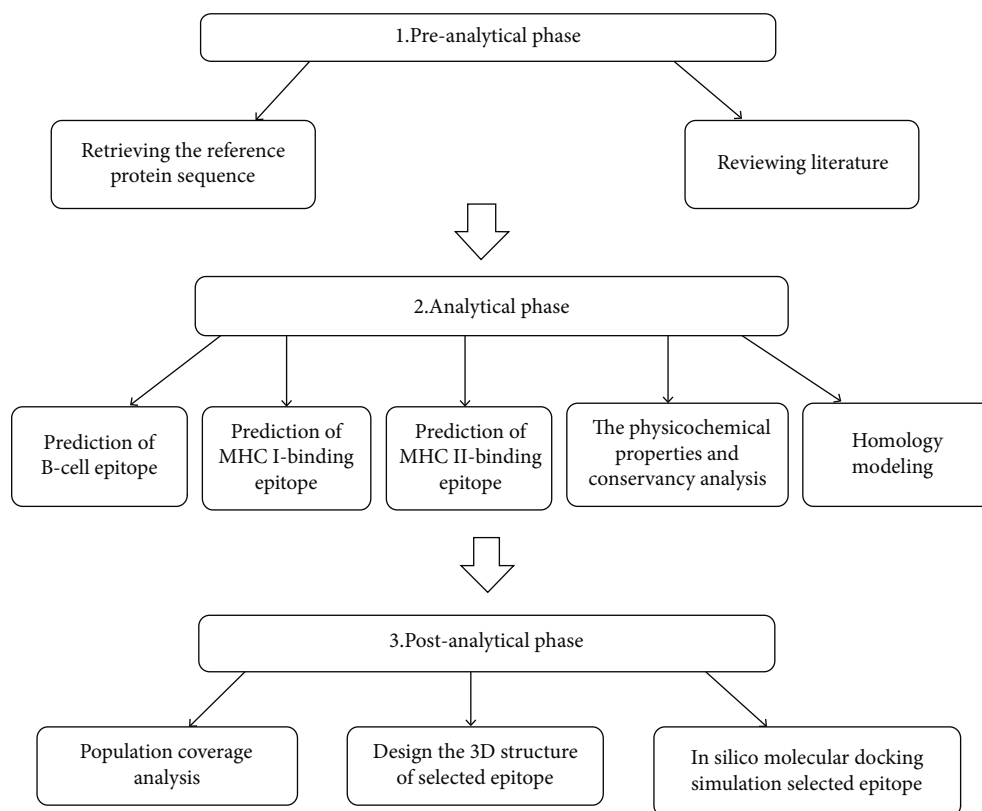


FIGURE 1: Schematic representation of the methodology phases.

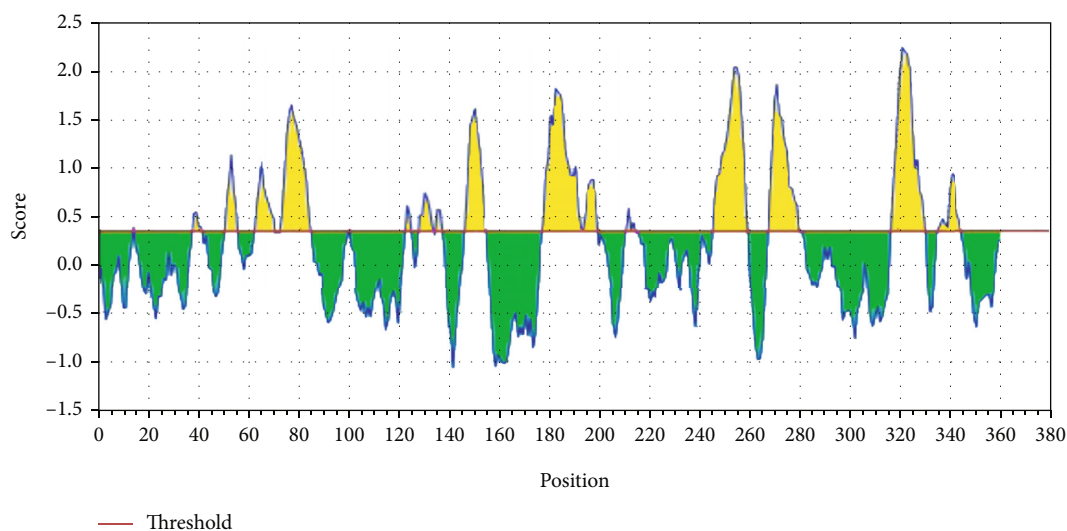


FIGURE 2: Bepired linear epitope prediction: the red line is the threshold; above (the yellow part) is proposed to be part of the B-cell epitope.

**2.3.1. Prediction of Linear B-Cell Epitopes.** A collection of methods to predict linear B-cell epitopes based on protein sequence characteristics of the antigen using amino acid scales and HMMs was used.

The Bepired tool from IEDB (<http://tools.iedb.org/bcell/result/>) was used to predict the linear B-cell epitopes

from the conserved region with a default threshold value of 0.35 [55–57].

**2.3.2. Prediction of Surface Accessibility.** Emini surface accessibility prediction tool of the Immune Epitope Database (IEDB) (<http://tools.iedb.org/bcell/result/>) was used to

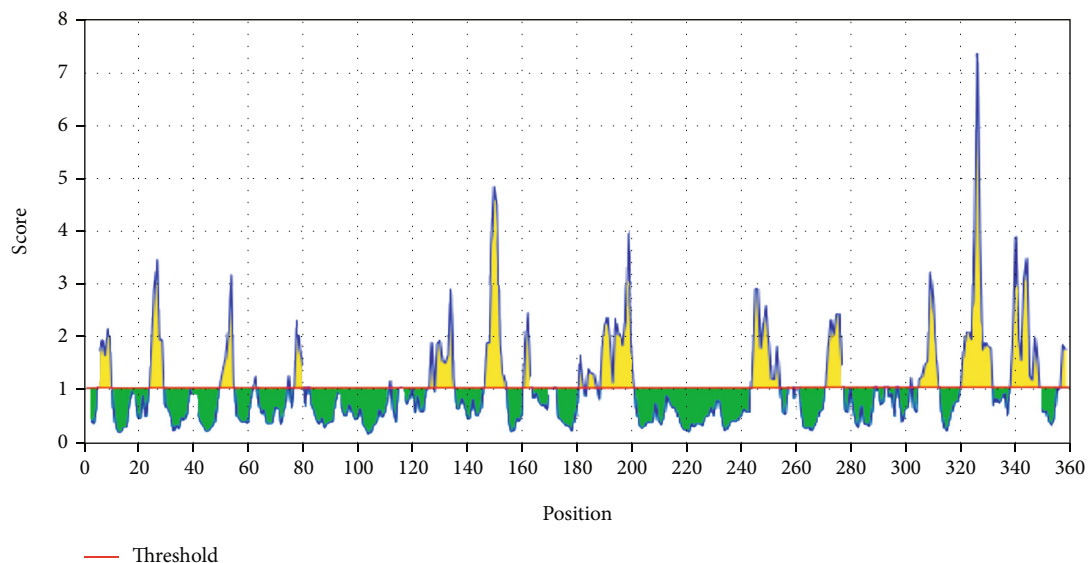


FIGURE 3: Emini's surface accessibility prediction test: the red line is the threshold; above (the yellow part) is proposed to be part of the B-cell epitope.

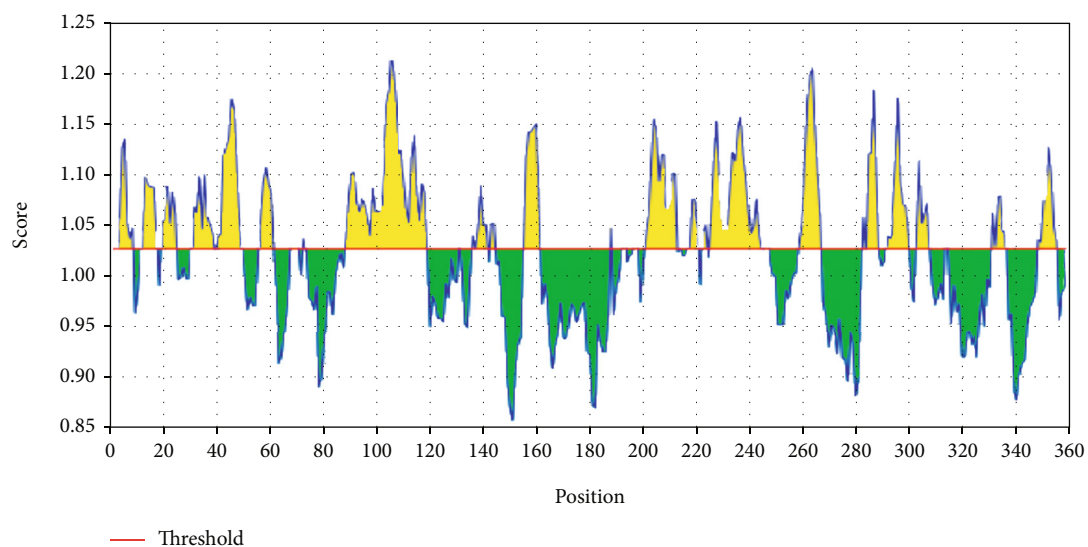


FIGURE 4: Kolaskar and Tongaonkar antigenicity prediction test: the red line is the threshold; above (the yellow part) is proposed to be part of the B-cell epitope.

TABLE 1: The proposed predicted antigenic B-cell epitopes; 9 antigenic sites were identified from fructose bisphosphate aldolase of *C. glabrata*.

Start	End	Peptide	Length
63	70	SNGGAAYF	8
73	84	KGVSNDGQNASI	12
129	134	AYFKEH	6
147	155	SEETDDENI	9
178	199	ITGGEEGDGVNNEHVDKESLYTK	22
247	260	KYAAEKTGAPAGSK	14
269	280	GSGSTQEEFNTG	12
318	331	GNPEGADKPNKKFF	14
336	345	WVREGEKTMS	10

to predict the surface epitopes from the conserved region with the default threshold value 1.0 [58].

**2.3.3. Prediction of Epitope Antigenicity.** The Kolaskar and Tongaonkar antigenicity method was used to detect the antigenic sites with a default threshold value of 1.025 (<http://tools.iedb.org/bcell/result/>) [59].

**2.3.4. Prediction of Discontinuous B-Cell Epitopes.** This method predicts epitopes based upon solvent-accessibility and flexibility. The methods are for modeling, docking of antibody, and protein 3D structures (<http://tools.iedb.org/bcell/result/>).

The modeled 3D structure was submitted to the ElliPro (<http://tools.iedb.org/elliPro/>) prediction tool to filter out the antigenic residues. The minimum score and maximum

TABLE 2: List of the most promising B-cell epitopes and their surface and antigenicity.

Start	End	Peptide	Length	Surface score (Emini's surface threshold = 1.000)	Antigenicity score (Kolaskar's test = 1.025)
129	134	AYFKEH	6	1.502	1.034
191	199	VDKESLYTK	9	2.48	1.032
190	199	HVDKESLYTK	10	2.648	1.04

TABLE 3: List of the promising discontinuous B-cell epitopes.

No.	Residues	Number of residues	Score
1	T300, G301, I302, R303, D304, Y305, V306, L307, N308, K309, K310, D311, Y312, I313, M314, S315, M316, V317, G318, N319, P320, E321, G322, A323, D324, K325, P326, N327, K328, K329, F330, F331, E339, K342	34	0.867
2	D332, P333, R334, V335, W336	5	0.749
3	V3, Q4, E5, V6, L7, K8, Y25, E28, H29, K30, F31, K55, S56, A156, T157, V159, K160, K163, G177, I178, T179, G180, G181, E182, E183, D184, G185, V186, N187, N188, E189, H190, V191, D192, K193, E194, S195, L196, Y197, T198, K199, P200, E201, F204, A205, E208, A209, A211, P212, I213, S214, P215, A222, F223, G224, Q231, A232, G233, N234, V235, V236, L237, S238, P239, E240, A243, D244, K247, Y248, A249, A250, E251, K252, T253, G254, A255, P256, A257, G258, S259, K260, P261, S272, T273, Q274, E275, N278, T279, N282, N283, T357, K358, N359, T360, L361	95	0.669
4	V15, G16, A71, G72, K73, G74, V75, S76, N77, D78, G79, Q80, N81, A82, I84, R85, C112, A113, K114, L117, P118, D121, G122, L124, E125, A126, E128, A129, Y130, F131, K132, E133, H134, G135, E136, P137, L138, R164, A166, A167, M168, N169, Q170	43	0.668
5	L146, S147, E148, E149, T150, D151, D152, E153	8	0.582
6	R9, K10, T11, G12, I14, R52, D53, A98, P99, A100, Y101, G102, I103	13	0.514

distance (Angstrom) were calibrated in the default mode with a score of 0.5 and 6, respectively [60].

**2.4. Prediction of MHC Class I Binding Epitopes.** The peptides' binding affinity to MHC I molecules was defined by the IEDB MHC I prediction tool at <http://tools.iedb.org/mhc1>. The binding affinity of fructose bisphosphate aldolase peptides to MHC I molecules was obtained using the artificial neural network (ANN) method. All conserved epitopes that bind to MHC I alleles at score  $\leq 500$  half-maximal inhibitory concentrations (IC<sub>50</sub>) with peptides that have a length of 9 amino acids were selected for further analysis [49, 61–66].

**2.5. MHC Class II Binding Predictions.** Prediction of peptide binding affinity to MHC II molecules was defined by the IEDB MHC II prediction tool at <http://tools.iedb.org/mhcii/result/>. MHC II molecules have the ability to bind peptides with different lengths which make the prediction accuracy debatable. For MHC II binding prediction, human allele reference sets were used. The prediction method was selected as NN-align to assess both the binding affinity and MHC II binding core epitopes with a length of 9 amino acid peptides at score IC<sub>50</sub> of 100 [49, 67].

**2.6. Population Coverage Calculation.** The candidate epitopes of MHC I and MHC II and combined binding of MHC I and MHC II alleles from *Candida glabrata* fructose bisphosphate aldolase protein were employed for population coverage, and the world population was set as a target population for the

selected MHC I and MHC II combined binding alleles using the IEDB population coverage calculation tool at <http://tools.iedb.org/population/> [49, 68].

**2.7. Homology Modeling.** The reference sequence of *Candida glabrata* fructose bisphosphate aldolase protein was applied to Raptor X for modeling at <http://raptorx.uchicago.edu/>. Then, the 3D structural model of the protein was visualized by using the Chimera tool powered by UCSF [69–73].

**2.8. Physicochemical Parameters.** The function of vaccines is to enhance the immunogenic response once introduced to the immune system. Thus, it is essential to recognize the physicochemical parameters of the protein using the protein program and BioEdit [54] (available at <https://web.expasy.org/protparam/> and <https://web.expasy.org/protscale/>) [74].

**2.9. Molecular Docking Analysis.** Molecular docking was performed using Moe 2007. The 3D structures of the promiscuous epitopes were predicted by PEP-FOLD. The crystal structures of HLA-A\*02:06 (PDB ID 3OXR) and HLA-DRB1\*01:01 (PDB ID 5JLZ) were chosen as a model for molecular docking and were downloaded in a PDB format from the RCSB PDB resource. However, the selected crystal structures were in a complex form with ligands. Thus, to simplify the complex structure of all water molecules, hetero groups and ligands were removed by Discovery Studio Visualizer 2.5. Partial charge and energy minimization were applied for ligands and targets. In terms of the identification

TABLE 4: Promising T-cell epitopes (class MHC I alleles) with their position and IC50 value.

Core epitope	Start	End	Allele	IC50
KYFKRMAAM	160	168	HLA-A*24:02	451.84
	160	168	HLA-A*30:01	232.12
	160	168	HLA-A*31:01	131.22
	160	168	HLA-B*14:02	427.02
	160	168	HLA-C*07:02	149.13
	160	168	HLA-C*12:03	240.46
	160	168	HLA-C*14:02	6.27
	205	213	HLA-A*02:01	154.37
AVHEALAPI	205	213	HLA-A*02:06	9.78
	205	213	HLA-A*30:01	20.96
	205	213	HLA-A*32:01	122.32
	205	213	HLA-A*68:02	55.22
RMAAMNQWL	164	172	HLA-A*02:01	52.44
	164	172	HLA-A*02:06	237.09
	164	172	HLA-A*32:01	79.39
	164	172	HLA-B*15:01	258
	164	172	HLA-C*14:02	482
	61	69	HLA-A*01:01	54.18
QTSNGGAAY	61	69	HLA-A*26:01	89.37
	61	69	HLA-A*29:02	56.68
	61	69	HLA-A*30:02	47.89
	61	69	HLA-B*15:01	111.57
	61	69	HLA-B*15:02	82.52
	61	69	HLA-B*35:01	99.45
YFKEHGEPL	130	138	HLA-B*08:01	295.97
	130	138	HLA-C*03:03	42.03
	130	138	HLA-C*07:02	319.29
	130	138	HLA-C*12:03	26.8
	130	138	HLA-C*14:02	18.47

of the binding groove, the potential binding sites in the crystal structure were recognized using the Alpha Site Finder. Finally, ten independent docking runs were carried out for each peptide. The results were retrieved as binding energies. Best poses for each epitope that displayed the lowest binding energies were visualized using UCSF Chimera 1.13.1 software [72, 75–78].

### 3. Result

**3.1. B-Cell Epitope Prediction.** The reference sequence of fructose bisphosphate aldolase from *C. glabrata* was analyzed using a Bepipred linear epitope prediction test; the average binder's score of the protein to B-cell was 0.199 and minimum was -0.009 and 2.424 for a maximum score; all values equal or greater than the default threshold 0.350 which were potentially linear epitopes are shown in Figure 2.

**3.1.1. Prediction of Surface Accessibility.** In Emini's surface accessibility prediction test, for a potent B-cell epitope, the average surface accessibility area of the Fba1 protein was

scored as 1.000, with a maximum of 7.725 and a minimum of 0.113; all values equal or greater than the default threshold 1.000 were potentially in the surface shown in Figure 3.

**3.1.2. Prediction of Epitope Antigenicity.** For the Kolaskar and Tongaonkar antigenicity prediction test, the average of antigenicity was 1.025, with a maximum of 1.223 and a minimum of 0.853; all values equal to or greater than the default threshold 1.025 are potential antigenic determinants (see Figure 4). The results of all proposed conserved predicted B-cell epitopes are shown in Table 1. The list of the most promising B-cell epitopes with their surface scores and antigenicity is shown in Table 2.

**3.1.3. Discontinuous B-Cell Epitope Prediction.** The modeled 3D structure of the Fba1 protein was submitted to the ElliPro prediction tool to filter out the antigenic residues. The minimum score and maximum distance (Angstrom) were calibrated in the default mode with a score of 0.5 and 6, respectively (see Table 3 for more illustrations).

### 3.2. T-Cell Peptide Prediction

**3.2.1. Prediction of MHC I Binding Profile for T Cytotoxic Cell Conserved Epitopes.** 114 epitopes were anticipated to interact with different MHC I alleles. The core epitopes KYFKRMAAM and QTSNGGAAY were noticed to be the dominant binders with 7 alleles for each (HLA-A\*24:02, HLA-A\*30:01, HLA-A\*31:01, HLA-B\*14:02, HLA-C\*07:02, HLA-C\*12:03, and HLA-C\*14:02) (HLA-A\*01:01, HLA-A\*26:01, HLA-A\*29:02, HLA-A\*30:02, HLA-B\*15:01, HLA-B\*15:02, and HLA-B\*35:01) followed by AVHEALAPI, RMAAMNQWL, and YFKEHGEPL which bind with five alleles; these findings are shown in Table 4.

**3.2.2. Prediction of MHC II Binding Profile for T Helper Cell Conserved Epitopes.** 102 conserved predicted epitopes were found to interact with MHC II alleles. The core epitope LFSSHMLDL is thought to be the top binder as it interacts with 9 alleles (HLA-DRB1\*07:01, HLA-DPA1\*01, HLA-DPB1\*04:01, HLA-DPA1\*01:03, HLA-DPB1\*02:01, HLA-DPA1\*02:01, HLA-DPB1\*01:01, HLA-DPA1\*03:01, and HLA-DPB1\*04:02), followed by IRGSIAAAH which binds to five alleles and VVAALEAAR which also binds with five alleles but with low frequency. Followed by YQAGNVVLS and IAPAYGIPV, these findings are shown in Table 5.

**3.3. Population Coverage.** The most interesting findings in this test is the population coverage analysis result for the most common binders to MHC I and MHC II alleles each and combined among the world, exhibiting an exceptional coverage with percentages 92.54%, 99.58%, and 98.5%, respectively.

**3.3.1. Population Coverage for Isolated MHC I.** Five epitopes are given to interact with the most frequent MHC class I alleles: AVHEALAPI, KYFKRMAAM, QTSNGGAAY, RMAAMNQWL, and YFKEHGEPL, representing a considerable coverage against the whole world population. The maximum population coverage percentage over these epitopes is 92.54% (see Figure 5).

TABLE 5: Promising T-cell epitope (class MHC II alleles) with their position and peptide sequence and IC50 value and rank.

Core sequence	Allele	Start	End	Peptide sequence	IC50	Rank
LFSSHMLDL	HLA-DRB1*07:01	132	146	KEHGEPLFSSHMLDL	17.8	3.37
	HLA-DPA1*01	135	149	GEPLFSSHMLDLSEE	93.6	5.05
	HLA-DPB1*04:01	135	149	GEPLFSSHMLDLSEE	93.6	5.05
	HLA-DPA1*01:03	133	147	EHGEPLFSSHMLDLS	46	4.82
	HLA-DPB1*02:01	133	147	EHGEPLFSSHMLDLS	46	4.82
	HLA-DPA1*02:01	134	148	HGEPLFSSHMLDLSE	59	6.3
	HLA-DPB1*01:01	134	148	HGEPLFSSHMLDLSE	59	6.3
	HLA-DPA1*03:01	135	149	GEPLFSSHMLDLSEE	12	1.14
	HLA-DPB1*04:02	135	149	GEPLFSSHMLDLSEE	12	1.14
IRGSIAAAH	HLA-DRB1*01:01	81	95	NASIRGSIAAAHYIR	31.5	15.98
	HLA-DRB1*04:01	81	95	NASIRGSIAAAHYIR	86.5	7.02
	HLA-DRB5*01:01	81	95	NASIRGSIAAAHYIR	7.3	1.55
	HLA-DQA1*01:02	80	94	QNASIRGSIAAAHYI	59.3	3.74
	HLA-DQB1*06:02	80	94	QNASIRGSIAAAHYI	59.3	3.74
	HLA-DQA1*05:01	81	95	NASIRGSIAAAHYIR	4.6	0.27
	HLA-DQB1*03:01	81	95	NASIRGSIAAAHYIR	4.6	0.27
YQAGNVVLS	HLA-DRB1*01:01	227	241	HGVYQAGNVVLSPEI	19.7	11.15
	HLA-DRB1*09:01	227	241	HGVYQAGNVVLSPEI	80.9	5.58
	HLA-DQA1*01:02	227	241	HGVYQAGNVVLSPEI	91.3	6.42
	HLA-DQB1*06:02	227	241	HGVYQAGNVVLSPEI	91.3	6.42
	HLA-DQA1*05:01	224	238	GNVHGVYQAGNVVLS	7.9	0.96
	HLA-DQB1*03:01	224	238	GNVHGVYQAGNVVLS	7.9	0.96
VVAALEAAR	HLA-DRB1*03:01	41	55	SSTVVAALEAARDAK	50.9	2.91
	HLA-DRB1*09:01	41	55	SSTVVAALEAARDAK	95.1	6.59
	HLA-DRB5*01:01	41	55	SSTVVAALEAARDAK	15	3.71
	HLA-DQA1*01:02	40	54	SSSTVVAALEAARDA	38.1	1.93
	HLA-DQB1*06:02	40	54	SSSTVVAALEAARDA	38.1	1.93
	HLA-DQA1*05:01	42	56	STVVAALEAARDAKS	16.2	2.87
IAPAYGIPV	HLA-DQB1*03:01	42	56	STVVAALEAARDAKS	16.2	2.87
	HLA-DRB1*01:01	94	108	IRSIAPAYGIPVVLH	12.1	6.74
	HLA-DRB1*07:01	91	105	AHYIRSIAPAYGIPV	34.1	6.37
	HLA-DRB1*15:01	94	108	IRSIAPAYGIPVVLH	79.2	8.07
	HLA-DQA1*05:01	94	108	IRSIAPAYGIPVVLH	16.5	2.94
	HLA-DQB1*03:01	94	108	IRSIAPAYGIPVVLH	16.5	2.94

3.3.2. *Population Coverage for Isolated MHC II.* Three epitopes were assumed to interact with the most frequent MHC class II alleles (IRGSIAAAH, LFSSHMLDL, and VVAALEAAR) with a percentage of 99.58%. The LFSSHMLDL epitope shows an exceptional result for the population coverage test for MHC II binding affinity of 96.60% globally (see Figure 6).

3.3.3. *Population Coverage for MHC I and MHC II Alleles Combined.* Regarding the combined MHC I and MHC II alleles, five epitopes were supposed to interact with the most predominant MHC class I and MHC class II alleles (IAPAYGIPV, AAFGNVHGV, VVAALEAAR, YIRSTIAPAY, and YQAGMVVLS), representing a significant global coverage by the IEDB population coverage tool which revealed coverage with percentage of 98.50% as shown in Figure 7.

3.4. *Homology Modeling.* The 3-dimensional structure of the fructose bisphosphate aldolase protein from *C. glabrata* and the most promising peptides binding to MHC class II by using the Chimera tool powered by UCSF are shown in Figure 8.

3.5. *Physicochemical Parameters.* The length of fructose bisphosphate aldolase protein is 361 amino acids, and its molecular weight is 39356.3. Theoretical pI is 5.49 which explain the pH of the protein. Total numbers of negatively and positively charged residues that contain the fructose bisphosphate aldolase protein are (Asp+Glu): 47 and (Arg+Lys): 35, respectively. Also, the number of atoms that compose this protein is 5488 which presented as flowing: carbon 1752, hydrogen 2716, nitrogen 470, oxygen 538, and sulfur

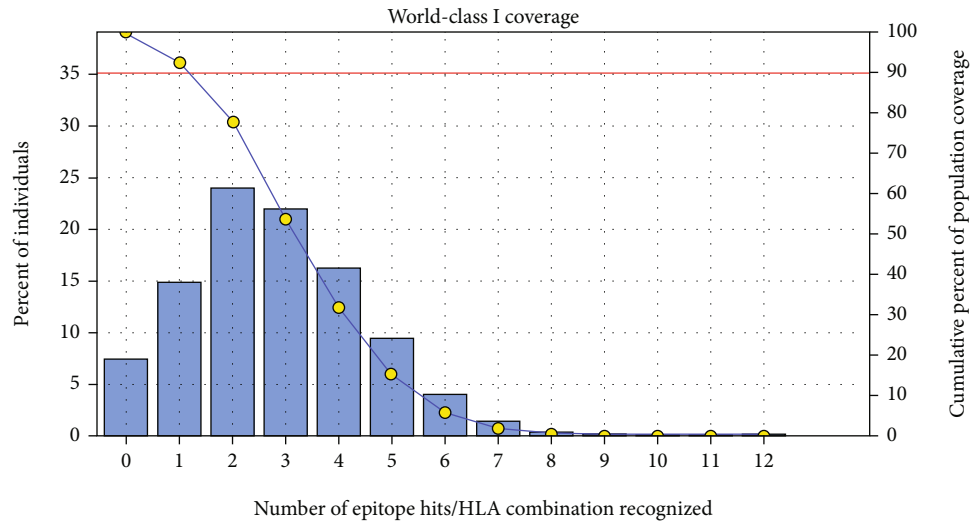


FIGURE 5: Global coverage for the top five MHC I peptides (AVHEALAPI, KYFKRMAAM, QTSNGGAAAY, RMAAMNQWL, and YFKEHGEPL). Note: in the graph, the line (-o-) represents the cumulative percentage of population coverage of the epitopes; the bars represent the population coverage for each epitope.

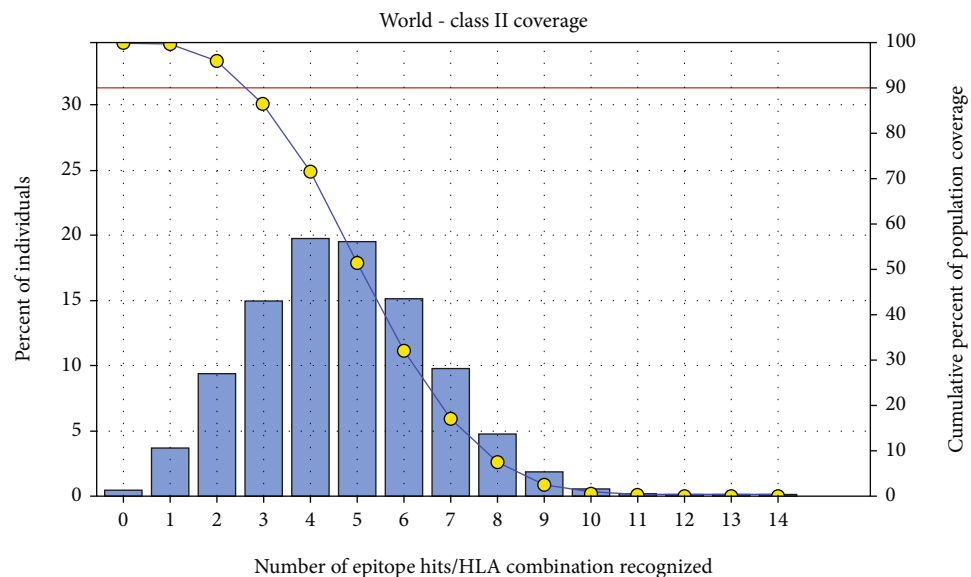


FIGURE 6: Global proportion for the top five MHC II IRGSIAAAH, LFSSHMLDL, and VVAALEAAR. Notes: in the graph, the line (-o-) represents the cumulative percentage of population coverage of the epitopes; the bars represent the population coverage for each epitope.

12. N-terminal of the sequence considered is M (Met). The half-life of the fructose biphosphate aldolase protein estimate is 30 hours (mammalian reticulocytes, in vitro) and more than 20 hours (yeast, in vivo). The aliphatic index and the grand average of hydropathicity (GRAVY) value of vaccine were determined as 80.55 and  $-0.264$ , respectively. Instability of the fructose biphosphate aldolase protein is computed to be 29.93, meaning the protein is stable [74]. The amino acids that compose the protein fructose biphosphate aldolase with their molecular weights are shown in Table 6 and Figure 9.

3.6. *Molecular Docking*. The best epitopes that displayed the lowest binding energies visualized by using UCSF chimera 1.13.1 software are shown in Table 7 and Figures 10–25.

#### 4. Discussion

In the present study, we predicted the most conserved and immunogenic B- and T-cell epitopes from Fba1 protein of *C. Glabrata* by using the immunoinformatics approach in order to develop an effective epitope-based vaccine against this fungal pathogen which has emerged in recent years as a



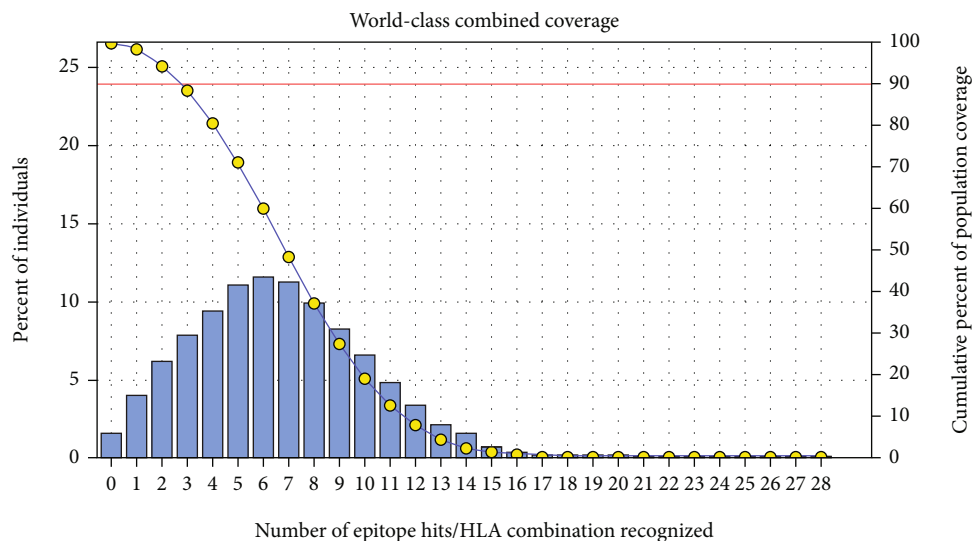


FIGURE 7: Global population proportion for the top five MHC I and II epitopes in combined mode (IAPAYGIPV, AAFGNVHGV, VVAALEAAR, YIRSTIAPAY, and YQAGMVVLS). Notes: in the graphs, the line (-o-) represents the cumulative percentage of population coverage of the epitopes; the bars represent the population coverage for each epitope.

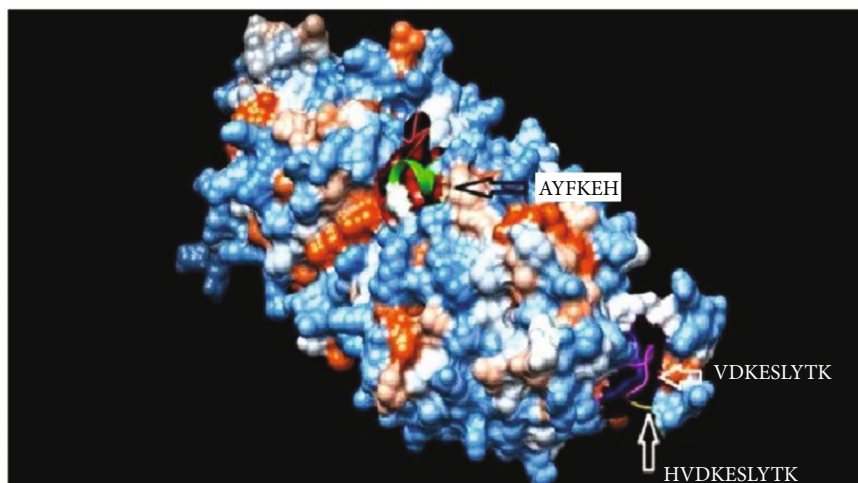


FIGURE 8: Structural position of the promising B-cell epitope (AYFKEH (in purple color), VDKESELYTK (in yellow color), and HVDKESELYTK (in red color)) in 3-dimensional structure of the fructose biphosphate aldolase protein from *C. glabrata* using Chimera tool powered by UCSF.

serious health problem especially among immunosuppressed and hospitalized patients [7]. A previous study conducted by de Klerk et al. [79] showed that the Fba1 protein has the ability to provoke immune responses in human against *M. mycetomatis* [79]. Also, several recent publications have used the Fba1 protein as a strong antigenic target for predicting B- and T-cell epitopes in order to design promising vaccines against fungal and bacterial pathogens such as *M. mycetomatis*, *P. aeruginosa*, *L. monocytogenes*, and *S. mansoni* by using in silico tools [80–83]. Hence, there are more studies to explore the fructose biphosphate aldolase protein immunogenic role and the possibility to find common conserved epitopes for different organisms.

The principle of using a cocktail of B- and T-cell epitopes in the epitope-based vaccine to trigger humoral as well as cellular mediated immune response is very promising to clear infection instead of humoral or cellular immunity alone, and it was applied before to enhance protection against different kinds of infectious diseases [84, 85]. In this study, the analysis of the Fba1 protein revealed 11 effective epitopes for B-cells (AYFKEH, VDKESELYTK, and HVDKESELYTK) and T-cells (AVHEALAPI, KYFKRMAAM, QTSNGGAAY, RMAAMNQWL, YFKEH-GEPL, IRGSIAAAH, LFSSHMLDL, and VVAALEAAR).

However, the molecular docking, which evaluates the binding affinity to MHC molecules [51, 52], showed that the peptides QTSNGGAAY and LFSSHMLDL are the best

TABLE 6: Amino acid composition of the protein (fructose biphosphate aldolase) with their number and molecular weight (Mol%) using BioEdit software version 7.0.5.3.

Amino acid	Number	Mol%	Amino acid	Number	Mol%
Ala A	39	10.80	Leu L	23	6.37
Cys C	3	0.83	Met M	9	2.49
Asp D	21	5.82	Asn N	19	5.26
Glu E	26	7.20	Pro P	15	4.16
Phe F	14	3.88	Gln Q	8	2.22
Gly G	30	8.31	Arg R	10	2.77
His H	12	3.32	Ser S	23	6.37
Ile I	20	5.54	Thr T	17	4.71
Lys K	25	6.93	Val V	29	8.03
Trp W	3	0.83	Tyr Y	15	4.16

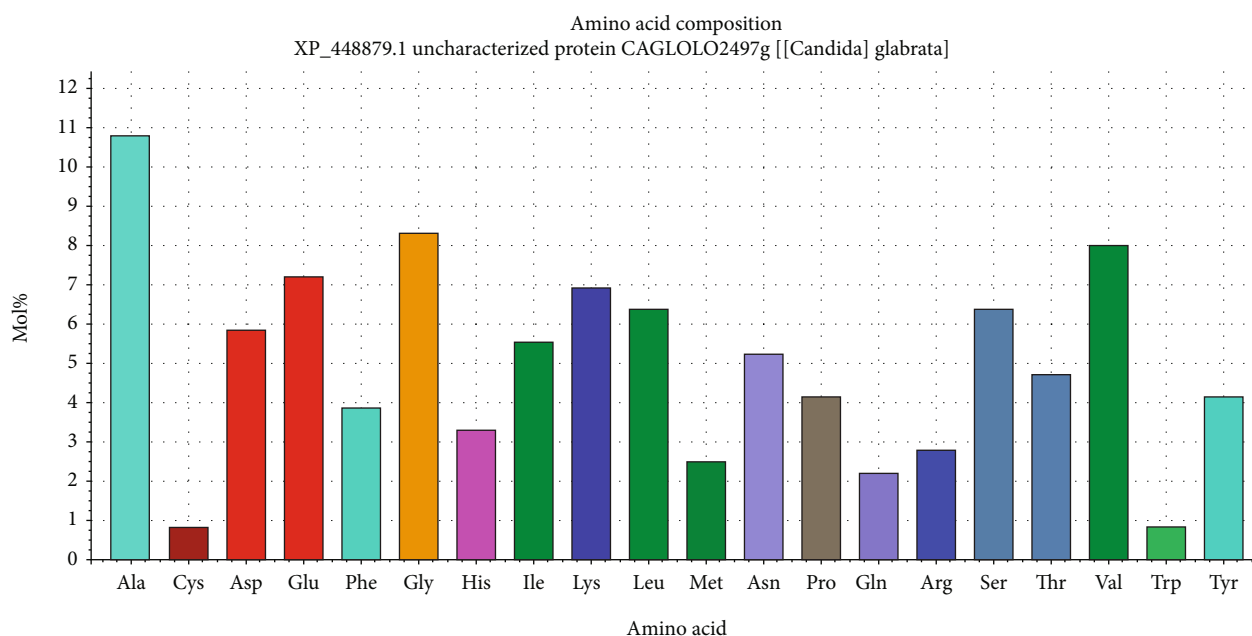


FIGURE 9: Graph showing amino acid composition of fructose biphosphate aldolase protein and their molecular weights using BioEdit software 7.0.5.3.

TABLE 7: Docking results of the most promiscuous epitopes that show the best binding affinity.

Epitope	Binding MHC molecule	Binding energy ( $\Delta G^*$ kcal/mol)
AVHEALAPI	HLA-A*02:06	-15.8010
KYFKRMAAM	HLA-A*02:06	-20.5935
QTSNGGAAY	HLA-A*02:06	-30.5467
RMAAMNQWL	HLA-A*02:06	-20.6392
YFKEHGEPL	HLA-A*02:06	-16.7505
IRGSIAAAH	HLA-DRB1*01:01	-20.6557
LFSSHMLDL	HLA-DRB1*01:01	-25.5732
VVAALEAAR	HLA-DRB1*01:01	-19.8404

\*Global energy: it is the energy required to estimate the strength of association between the epitope within the active.

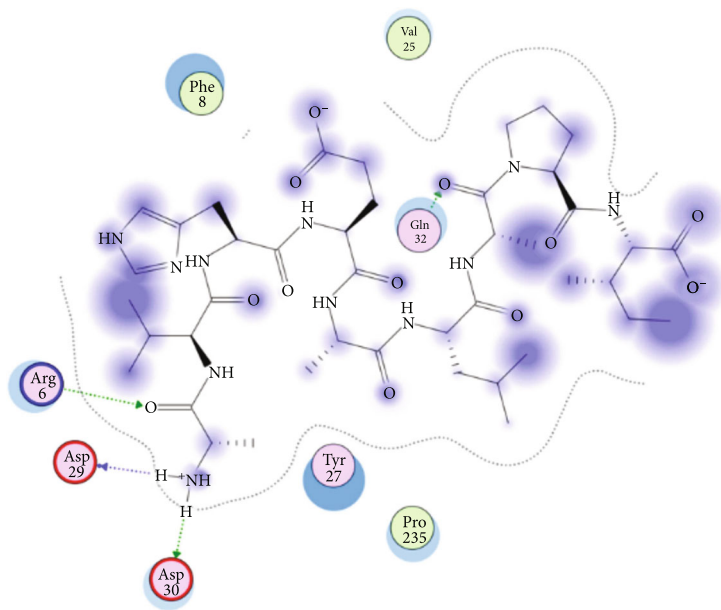


FIGURE 10: Illustration of the 2D interaction of the best docking poses of AVHEALAPI in the binding sites of HLA-A\*02:06.

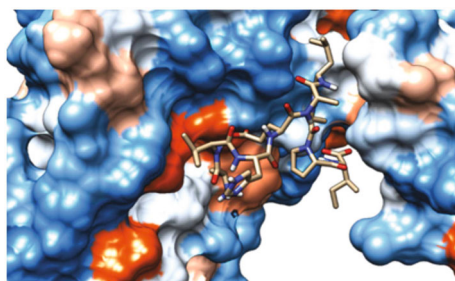


FIGURE 11: Illustration of the 3D interaction of the best docking poses of AVHEALAPI in the binding sites of HLA-A\*02:06.

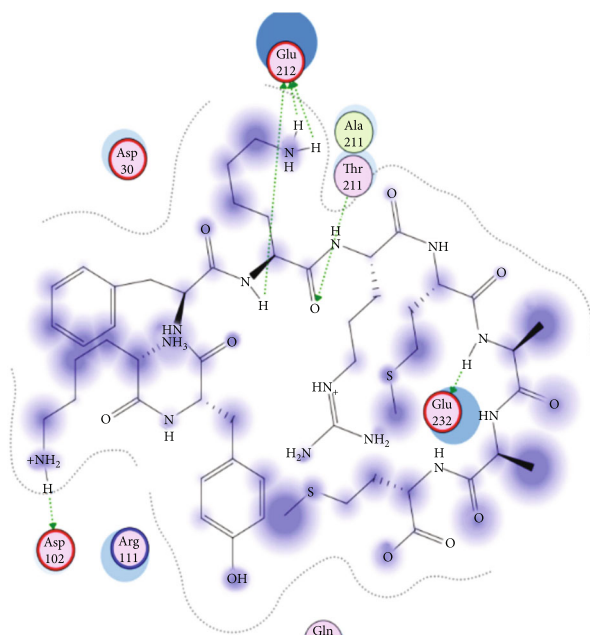


FIGURE 12: Illustration of the 3D interaction of the best docking poses of KYFKRMAAM in the binding sites of HLA-A\*02:06.

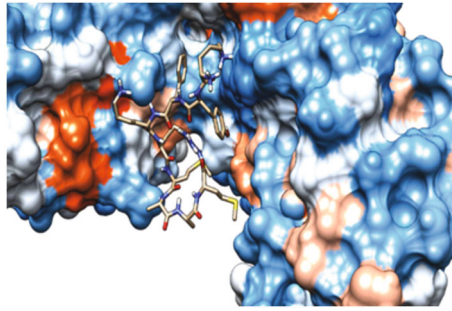


FIGURE 13: Illustration of the 3D interaction of the best docking poses of KYFKRMAAM in the binding sites of HLA-A\*02:06.

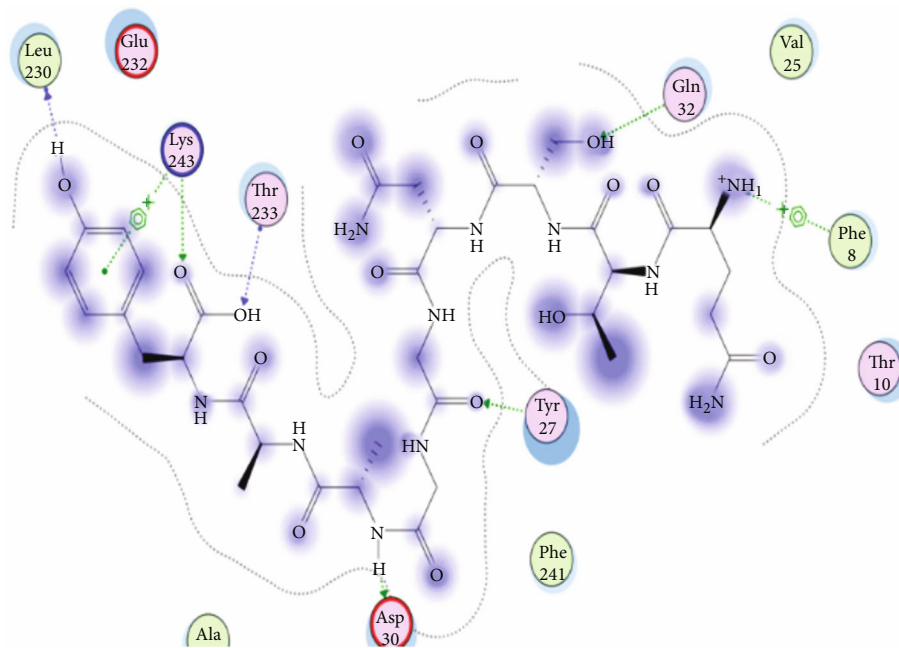


FIGURE 14: Illustration of the 2D interaction of the best docking poses of QTSNGGAAY in the binding sites of HLA-A\*02:06.

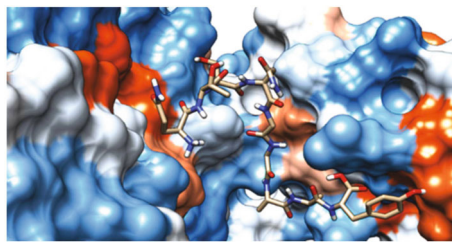


FIGURE 15: Illustrate the 2D interaction of the best docking poses of QTSNGGAAY in the binding sites of HLA-A\*02:06.

candidates for designing an effective epitope-based vaccine against *C. glabrata*.

After retrieving the various sequences of *C. glabrata* fructose biphosphate aldolase protein, the protein reference sequence was submitted to the Bepipred linear epitope prediction test, Emini surface accessibility test, and Kolaskar

and Tongaonkar antigenicity test in the IEDB, to determine the affinity of B-cell epitopes and their position regarding the surface and their immunogenicity. Three peptides have passed (AYFKEH, VDKEPLYTK, and HVDKEPLYTK) in all the prediction tests shown in Tables 1 and 2 and Figures 2–4. However, the MHC I binding prediction tool

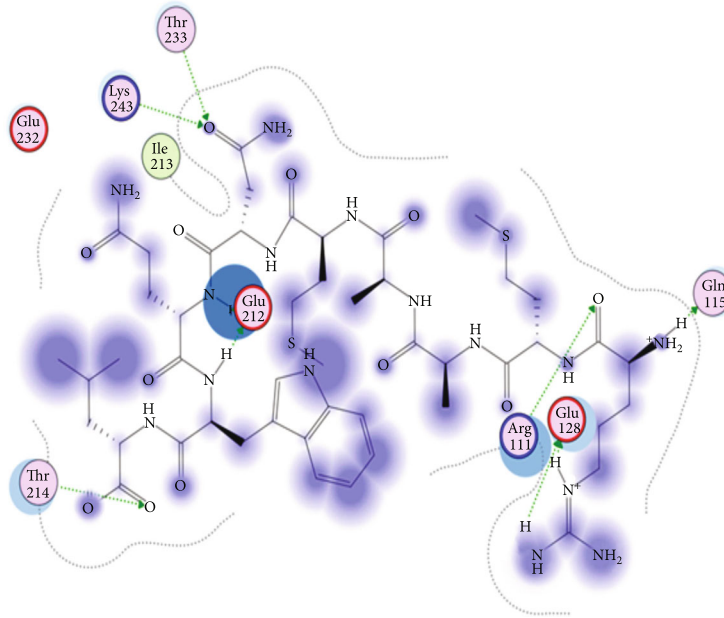


FIGURE 16: Illustration of the 2D interaction of the best docking poses of RMAAMNQWL in the binding sites of HLA-A\*02:06.

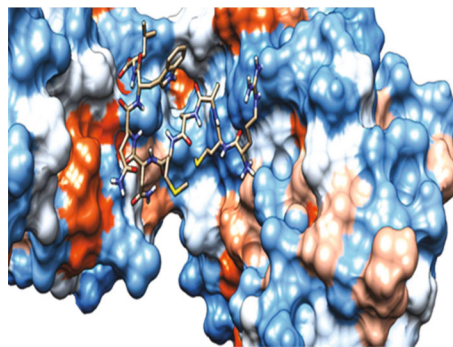


FIGURE 17: Illustration of the 2D interaction of the best docking poses of RMAAMNQWL in the binding sites of HLA-A\*02:06.

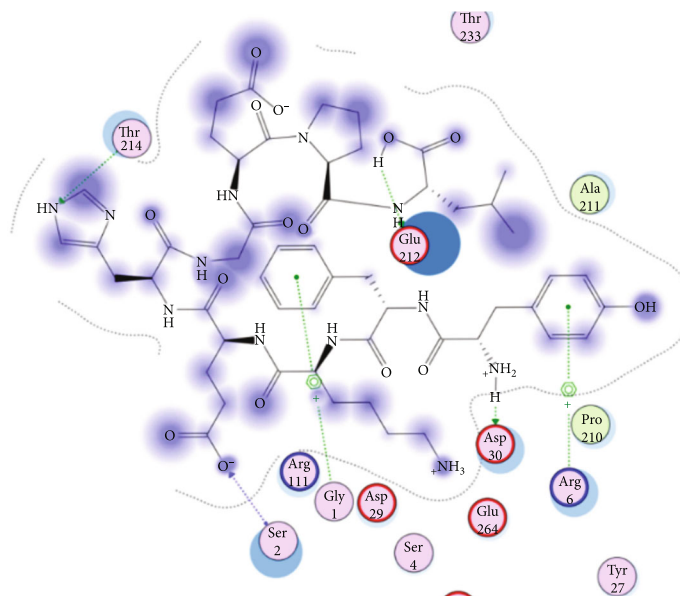


FIGURE 18: Illustration of the 3D interaction of the best docking poses of YFKEHGEPL in the binding sites of HLA-A\*02:06.

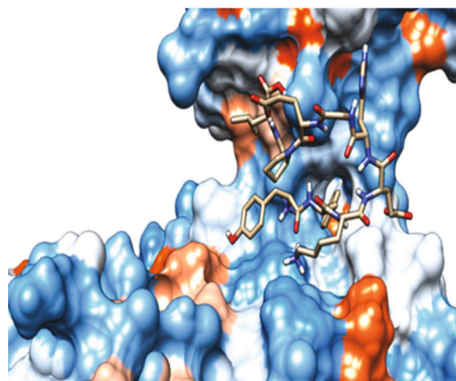


FIGURE 19: Illustration of the 3D interaction of the best docking poses of YFKEHGEPL in the binding sites of HLA-A\*02:06.

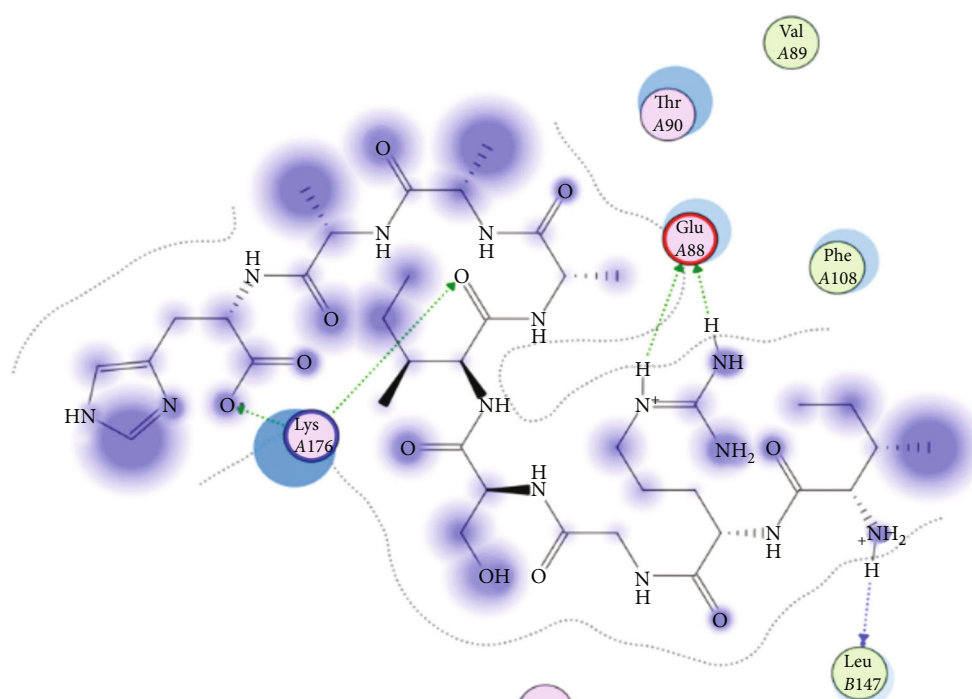


FIGURE 20: Illustration of the 3D interaction of the best docking poses of IRGSIAAAH in the binding sites of HLA-DRB1\*01:01.

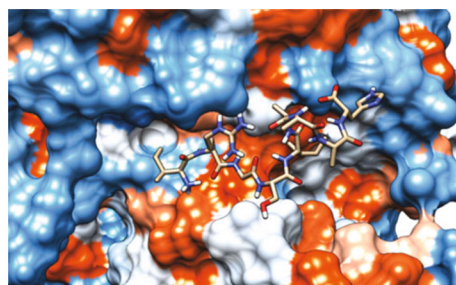


FIGURE 21: Illustration of the 3D interaction of the best docking poses of IRGSIAAAH in the binding sites of HLA-DRB1\*01:01.

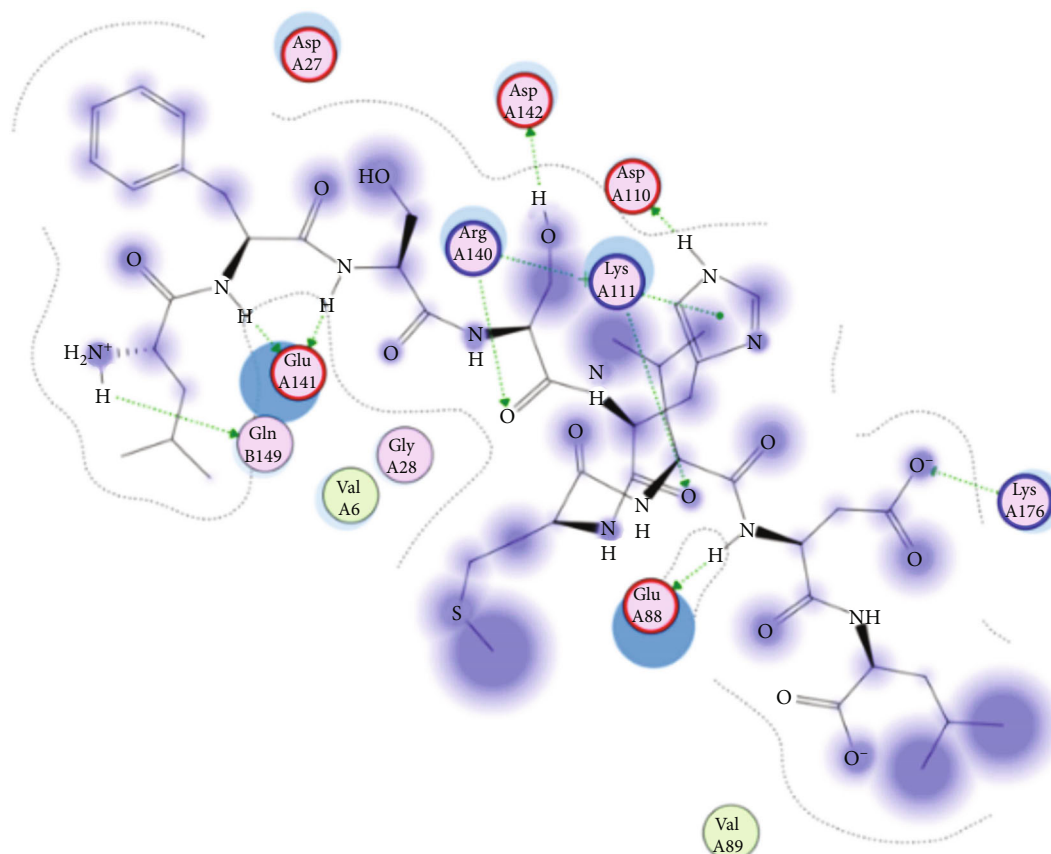


FIGURE 22: Illustration of the 3D interaction of the best docking poses of LFSSHMLDL in the binding sites of HLA-DRB1\*01:01.

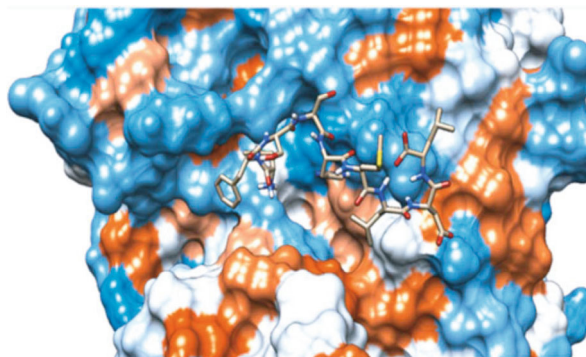


FIGURE 23: Illustration of the 3D interaction of the best docking poses of LFSSHMLDL in the binding sites of HLA-DRB1\*01:01.

using an artificial neural network (ANN) [61] with half maximal inhibitory concentration ( $IC_{50}$ )  $\leq 500$  revealed 114 conserved peptides interacting with various MHC I alleles. Three peptides were noticed to have the highest affinity in corresponding to their interaction with MHC I alleles. The peptide YIRSIAPAY from 93 to 101 had the affinity with 8 alleles to interact with HLA-A\*26:01, HLA-A\*29:02, HLA-B\*15:01, HLA-A\*30:02, HLA-B\*15:02, HLA-B\*35:01, HLA-C\*14:02, and HLA-C\*12:03, followed in order by KYFKRMAAM from 160 to 168 which interacts with 7 alleles

(HLA-A\*24:02, HLA-A\*31:01, HLA-A\*30:01, HLA-B\*14:02, HLA-C\*07:02, HLA-C\*14:02, and HLA-C\*12:03) and QTSNGGAAY from 61 to 69 which interacts with 7 alleles (HLA-A\*01:01, HLA-A\*26:01, HLA-A\*30:02, HLA-A\*29:02, HLA-B\*15:02, HLA-B\*15:01, and HLA-B\*35:01) (see Table 4), while MHC II binding prediction tool using NN-align [67] with half-maximal inhibitory concentration ( $IC_{50}$ )  $\leq 100$  revealed 102 conserved peptides that interact with various MHC II alleles. Two peptides (LFSSHMLDL and YIRSIAPAY) were noted to have the highest affinity in

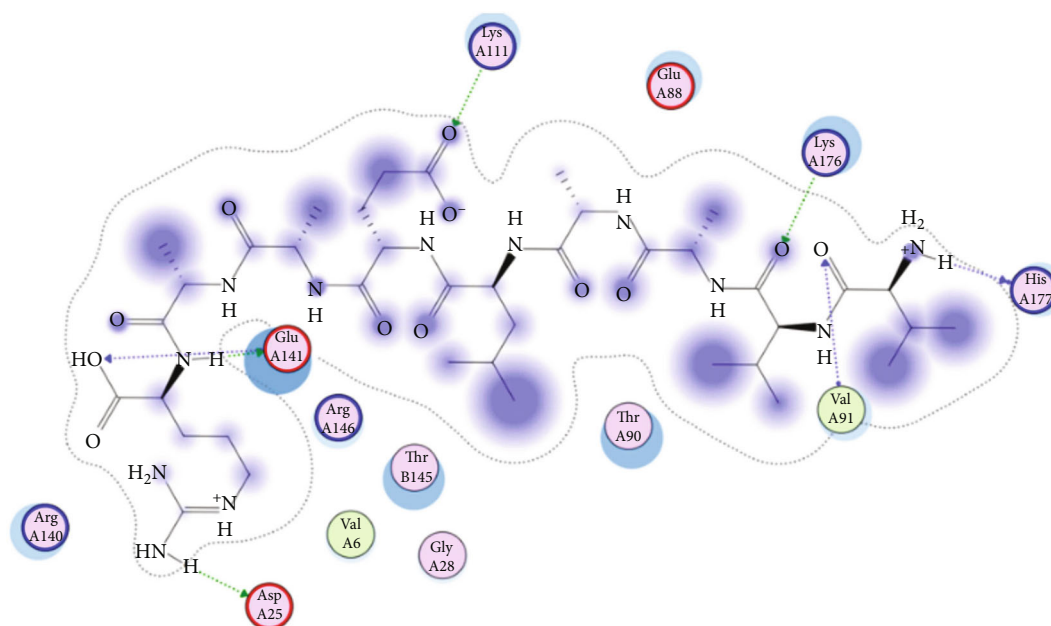


FIGURE 24: Illustration of the 2D interaction of the best docking poses of VVAALEAAR in the binding sites of HLA-DRB1\*01:01.

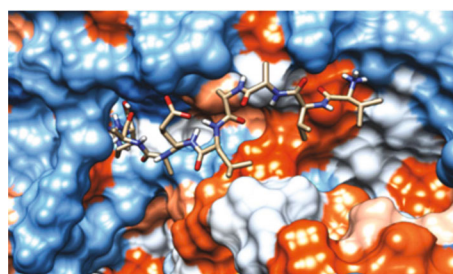


FIGURE 25: Illustration of the 2D interaction of the best docking poses of VVAALEAAR in the binding sites of HLA-DRB1\*01:01.

corresponding to their interaction with MHC II alleles; both had the affinity to interact with 9 MHC II alleles (see Table 5). Moreover, the predicted epitopes which have the high affinity to interact with MHC I, MHC II, and combined MHC I with MHC II international alleles were analyzed by population coverage resource in the IEDB [68]. The population coverage of the five most promising epitopes (AVHEALAPI, KYFKRMAAM, QTSNGGAAY, RMAAMNQWL, and YFKEHGEPL) for MHC I alleles was 92.54%, while for the three epitopes (IRGSIAAAH, LFSSHMLDL, and VVAALEAAR) that showed high affinity to MHC II alleles, it was 99.58% throughout the world according to the IEDB database as shown in Figures 5 and 6. It should be noted that the population coverage of the five most promising epitopes that exhibited binding affinity to both MHC I and MHC II alleles (IAPAYGIPV, AAFGNVHGV, VVAALEAAR, YIRSTIAPAY, and YQAGMVVLS) was 98.50% globally (see Figure 7). However, the molecular docking revealed that the epitopes QTSNGGAAY and LFSSHMLDL have high binding energy to MHC molecules HLA-A\*02:06 and HLA-DRB1\*01:01, respectively, which indicate favored affinity and stability in the epitope-molecule complex shown

in Table 7 and Figures 10–25. This study was limited by being strictly computational, and more in vitro and in vivo studies to prove the effectiveness of the proposed peptides are highly recommended.

## 5. In Conclusion

The epitope-based vaccines predicted by using immunoinformatics tools have remarkable advantages over the conventional vaccines in that they are more specific, less time consuming, safe, less allergic, and more antigenic. Further in vivo and in vitro experiments are needed to prove the effectiveness of the best candidate's epitopes QTSNGGAAY and LFSSHMLDL. To the best of our knowledge, this is the first study that has predicted B- and T-cell epitopes from the Fba1 protein by using in silico tools in order to design an effective epitope-based vaccine against *C. glabrata*.

## Data Availability

The data used to support the findings of this study are available from the corresponding author upon request.



## Conflicts of Interest

The authors declare that there are no conflicts of interest.

## Acknowledgments

The authors are grateful to Africa City of Technology, Khartoum, Sudan.

## References

- [1] D. Bitar, O. Lortholary, Y. le Strat et al., "Population-based analysis of invasive fungal infections, France, 2001-2010," *Emerging Infectious Diseases*, vol. 20, no. 7, pp. 1149–1155, 2014.
- [2] A. A. Cleveland, M. M. Farley, L. H. Harrison et al., "Changes in incidence and antifungal drug resistance in candidemia: results from population-based laboratory surveillance in Atlanta and Baltimore, 2008-2011," *Clinical Infectious Diseases*, vol. 55, no. 10, pp. 1352–1361, 2012.
- [3] B. J. Kullberg and M. C. Arendrup, "Invasive candidiasis," *The New England Journal of Medicine*, vol. 373, no. 15, pp. 1445–1456, 2015.
- [4] S. S. Magill, J. R. Edwards, W. Bamberg et al., "Multistate point-prevalence survey of health care-associated infections," *The New England Journal of Medicine*, vol. 370, no. 13, pp. 1198–1208, 2014.
- [5] B. Gonçalves, C. Ferreira, C. T. Alves, M. Henriques, J. Azeredo, and S. Silva, "Vulvovaginal candidiasis: epidemiology, microbiology and risk factors," *Critical Reviews in Microbiology*, vol. 42, no. 6, pp. 905–927, 2016.
- [6] J. Perlroth, B. Choi, and B. Spellberg, "Nosocomial fungal infections: epidemiology, diagnosis, and treatment," *Medical Mycology*, vol. 45, no. 4, pp. 321–346, 2007.
- [7] M. A. Pfaller and D. J. Diekema, "Epidemiology of invasive candidiasis: a persistent public health problem," *Clinical Microbiology Reviews*, vol. 20, no. 1, pp. 133–163, 2007.
- [8] N. Yapar, "Epidemiology and risk factors for invasive candidiasis," *Therapeutics and Clinical Risk Management*, vol. 10, pp. 95–105, 2014.
- [9] S. Silva, M. Negri, M. Henriques, R. Oliveira, D. W. Williams, and J. Azeredo, "Candida glabrata, Candida parapsilosis and Candida tropicalis: biology, epidemiology, pathogenicity and antifungal resistance," *FEMS Microbiology Reviews*, vol. 36, no. 2, pp. 288–305, 2012.
- [10] M. E. Brandt, "Candida and candidiasis," *Emerging Infectious Diseases*, vol. 8, no. 8, pp. 876–876, 2002.
- [11] G. P. Wormser and K. J. Ryan, "Medically important fungi: a guide to identification, 4th edition Davise H. Larone Washington, D.C.: American Society for Microbiology Press, 2002. 409 pp., illustrated. \$79.95 (cloth)," *Clinical Infectious Diseases*, vol. 37, no. 9, pp. 1281–1281, 2003.
- [12] L. Kasper, K. Seider, and B. Hube, "Intracellular survival of Candida glabrata in macrophages: immune evasion and persistence," *FEMS Yeast Research*, vol. 15, no. 5, p. fov042, 2015.
- [13] R. Atanasova, A. Angoulvant, M. Tefit et al., "A mouse model for Candida glabrata hematogenous disseminated infection starting from the gut: evaluation of strains with different adhesion properties," *PLoS One*, vol. 8, no. 7, article e69664, 2013.
- [14] B. Dujon, D. Sherman, G. Fischer et al., "Genome evolution in yeasts," *Nature*, vol. 430, no. 6995, pp. 35–44, 2004.
- [15] K. M. Ahmad, J. Kokošar, X. Guo, Z. Gu, O. P. Ishchuk, and J. Piškur, "Genome structure and dynamics of the yeast pathogen Candida glabrata," *FEMS Yeast Research*, vol. 14, no. 4, pp. 529–535, 2014.
- [16] E. López-Fuentes, G. Gutiérrez-Escobedo, B. Timmermans, P. Van Dijck, A. D. L. Peñas, and I. Castaño, "Candida glabrata's genome plasticity confers a unique pattern of expressed cell wall proteins," *Journal of Fungi*, vol. 4, no. 2, p. 67, 2018.
- [17] T. Gabaldón, T. Martin, M. Marcet-Houben et al., "Comparative genomics of emerging pathogens in the Candida glabrata clade," *BMC Genomics*, vol. 14, no. 1, p. 623, 2013.
- [18] P. W. J. de Groot, E. A. Kraneveld, Q. Y. Yin et al., "The cell wall of the human pathogen Candida glabrata: differential incorporation of novel adhesin-like wall proteins," *Eukaryotic Cell*, vol. 7, no. 11, pp. 1951–1964, 2008.
- [19] B. Timmermans, A. D. L. Peñas, I. Castaño, and P. Van Dijck, "Adhesins in Candida glabrata," *Journal of Fungi*, vol. 4, no. 2, p. 60, 2018.
- [20] NCBI, *Protein Database* <https://www.ncbi.nlm.nih.gov/protein>.
- [21] A. Nunez-Beltran, E. Lopez-Romero, and M. Cuellar-Cruz, "Identification of proteins involved in the adhesion of Candida species to different medical devices," *Microbial Pathogenesis*, vol. 107, pp. 293–303, 2017.
- [22] V. Cabezón, V. Vialás, A. Gil-Bona et al., "Apoptosis of Candida albicans during the interaction with murine macrophages: proteomics and cell-death marker monitoring," *Journal of Proteome Research*, vol. 15, no. 5, pp. 1418–1434, 2016.
- [23] M. D. Leach, D. A. Stead, E. Argo, D. M. MacCallum, and A. J. P. Brown, "Molecular and proteomic analyses highlight the importance of ubiquitination for the stress resistance, metabolic adaptation, morphogenetic regulation and virulence of Candida albicans," *Molecular Microbiology*, vol. 79, no. 6, pp. 1574–1593, 2011.
- [24] K. H. Lee, S. Y. Kim, J. H. Jung, and J. Kim, "Proteomic analysis of hyphae-specific proteins that are expressed differentially in cakem1/cakem1 mutant strains of Candida albicans," *Journal of Microbiology*, vol. 48, no. 3, pp. 365–371, 2010.
- [25] M. Martínez-Gomariz, P. Perumal, S. Mekala, C. Nombela, W. L. J. Chaffin, and C. Gil, "Proteomic analysis of cytoplasmic and surface proteins from yeast cells, hyphae, and biofilms of Candida albicans," *Proteomics*, vol. 9, no. 8, pp. 2230–2252, 2009.
- [26] C. L. Medrano-Díaz, A. Vega-González, E. Ruiz-Baca, A. Moreno, and M. Cuéllar-Cruz, "Moonlighting proteins induce protection in a mouse model against Candida species," *Microbial Pathogenesis*, vol. 124, pp. 21–29, 2018.
- [27] C. Compagno, B. M. Ranzi, and E. Martegani, "The promoter of Saccharomyces cerevisiae FBA1 gene contains a single positive upstream regulatory element," *FEBS Letters*, vol. 293, no. 1-2, pp. 97–100, 1991.
- [28] D. A. Fell, "Metabolic control analysis: a survey of its theoretical and experimental development," *The Biochemical Journal*, vol. 286, no. 2, pp. 313–330, 1992.
- [29] J. J. Marsh and H. G. Leberer, "Fructose-bisphosphate aldolases: an evolutionary history," *Trends in Biochemical Sciences*, vol. 17, no. 3, pp. 110–113, 1992.
- [30] H. G. Schwelberger, S. D. Kohlwein, and F. Paltauf, "Molecular cloning, primary structure and disruption of the structural gene of aldolase from Saccharomyces cerevisiae," *European Journal of Biochemistry*, vol. 180, no. 2, pp. 301–308, 1989.

- [31] X. Gao, S. Bao, X. Xing et al., "Fructose-1,6-bisphosphate aldolase of *Mycoplasma bovis* is a plasminogen-binding adhesin," *Microbial Pathogenesis*, vol. 124, pp. 230–237, 2018.
- [32] F. M. Klis, G. J. Sosinska, P. W. J. de Groot, and S. Brul, "Covalently linked cell wall proteins of *Candida albicans* and their role in fitness and virulence," *FEMS Yeast Research*, vol. 9, no. 7, pp. 1013–1028, 2009.
- [33] M. D. Ramirez-Quijas, E. Lopez-Romero, and M. Cuellar-Cruz, "Proteomic analysis of cell wall in four pathogenic species of *Candida* exposed to oxidative stress," *Microbial Pathogenesis*, vol. 87, pp. 1–12, 2015.
- [34] I. Serrano-Fujarte, E. Lopez-Romero, and M. Cuellar-Cruz, "Moonlight-like proteins of the cell wall protect sessile cells of *Candida* from oxidative stress," *Microbial Pathogenesis*, vol. 90, pp. 22–33, 2016.
- [35] A. Y. Jong, S. H. M. Chen, M. F. Stins, K. S. Kim, T. L. Tuan, and S. H. Huang, "Binding of *Candida albicans* enolase to plasmin(ogen) results in enhanced invasion of human brain microvascular endothelial cells," *Journal of Medical Microbiology*, vol. 52, no. 8, pp. 615–622, 2003.
- [36] A. Laín, N. Elguezabal, E. Amutio, I. F. de Larrinoa, M. D. Moragues, and J. Pontón, "Use of recombinant antigens for the diagnosis of invasive candidiasis," *Clinical & Developmental Immunology*, vol. 2008, article 721950, pp. 1–7, 2008.
- [37] S. Sandini, R. la Valle, S. Deaglio, F. Malavasi, A. Cassone, and F. de Bernardis, "A highly immunogenic recombinant and truncated protein of the secreted aspartic protease family (rSap2t) of *Candida albicans* as a mucosal anticandidal vaccine," *FEMS Immunology and Medical Microbiology*, vol. 62, no. 2, pp. 215–224, 2011.
- [38] A. Rodaki, T. Young, and A. J. Brown, "Effects of depleting the essential central metabolic enzyme fructose-1,6-bisphosphate aldolase on the growth and viability of *Candida albicans*: implications for antifungal drug target discovery," *Eukaryotic Cell*, vol. 5, no. 8, pp. 1371–1377, 2006.
- [39] S. H. I. R. I. N. E. L. H. A. I. K. GOLDMAN, S. H. A. H. A. R. DOTAN, A. M. I. R. TALIAS et al., "Streptococcus pneumoniae fructose-1,6-bisphosphate aldolase, a protein vaccine candidate, elicits Th1/Th2/Th17-type cytokine responses in mice," *International Journal of Molecular Medicine*, vol. 37, no. 4, pp. 1127–1138, 2016.
- [40] J. Huang, H. Zhu, J. Wang et al., "Fructose-1,6-bisphosphate aldolase is involved in *Mycoplasma bovis* colonization as a fibronectin-binding adhesin," *Research in Veterinary Science*, vol. 124, pp. 70–78, 2019.
- [41] S. Brunke and B. Hube, "Two unlike cousins: *Candida albicans* and *C. glabrata* infection strategies," *Cellular Microbiology*, vol. 15, no. 5, pp. 701–708, 2013.
- [42] K. R. Healey and D. S. Perlin, "Fungal resistance to echinocandins and the MDR phenomenon in *Candida glabrata*," *Journal Fungi*, vol. 4, no. 3, 2018.
- [43] L. S. Wilson, C. M. Reyes, M. Stolpman, J. Speckman, K. Allen, and J. Beney, "The direct cost and incidence of systemic fungal infections," *Value in Health*, vol. 5, no. 1, pp. 26–34, 2002.
- [44] C. Clerckx, D. Wilmes, S. Aydin, J. C. Yombi, E. Goffin, and J. Morelle, "*Candida glabrata* renal abscesses in a peritoneal dialysis patient," *Peritoneal Dialysis International*, vol. 32, no. 1, pp. 114–115, 2012.
- [45] G. A. Eschenauer, P. L. Carver, T. S. Patel et al., "Survival in patients with *Candida glabrata* bloodstream infection is associated with fluconazole dose," *Antimicrobial Agents and Chemotherapy*, vol. 62, no. 6, 2018.
- [46] Z. Zhu, Z. Huang, Z. Li, X. Li, C. du, and Y. Tian, "Multiple brain abscesses caused by infection with *Candida glabrata*: a case report," *Experimental and Therapeutic Medicine*, vol. 15, no. 3, pp. 2374–2380, 2018.
- [47] S. Nami, R. Mohammadi, M. Vakili, K. Khezripour, H. Mirzaei, and H. Morovati, "Fungal vaccines, mechanism of actions and immunology: a comprehensive review," *Biomedicine & Pharmacotherapy*, vol. 109, pp. 333–344, 2019.
- [48] H. Xin, "Effects of immune suppression in murine models of disseminated *Candida glabrata* and *Candida tropicalis* infection and utility of a synthetic peptide vaccine," *Medical Mycology*, vol. 57, no. 6, 2019.
- [49] IEDB, *Immune Epitope Database* <http://tools.iedb.org>.
- [50] R. Vita, J. A. Overton, J. A. Greenbaum et al., "The immune epitope database (IEDB) 3.0," *Nucleic Acids Research*, vol. 43, no. D1, pp. D405–D412, 2015.
- [51] L. Backert and O. Kohlbacher, "Immunoinformatics and epitope prediction in the age of genomic medicine," *Genome Medicine*, vol. 7, no. 1, p. 119, 2015.
- [52] A. A. Bahrami, Z. Payandeh, S. Khalili, A. Zakeri, and M. Bandehpour, "Immunoinformatics: in silico approaches and computational design of a multi-epitope, immunogenic protein," *International Reviews of Immunology*, vol. 38, no. 6, pp. 307–322, 2019.
- [53] Y. He, R. Rappuoli, A. S. De Groot, and R. T. Chen, "Vaccine informatics," *Journal of Biomedicine & Biotechnology*, vol. 2010, Article ID 765762, 2010.
- [54] T. A. Hall, "BioEdit: a user-friendly biological sequence alignment editor and analysis program for Windows 95/98/NT," in *Nucleic acids symposium series*, Information Retrieval Ltd., c1979-c2000, London, 1999.
- [55] P. Haste Andersen, "Prediction of residues in discontinuous B-cell epitopes using protein 3D structures," *Protein Science*, vol. 15, no. 11, pp. 2558–2567, 2006.
- [56] J. E. Larsen, O. Lund, and M. Nielsen, "Improved method for predicting linear B-cell epitopes," *Immunome Research*, vol. 2, no. 1, 2006.
- [57] J. V. Ponomarenko and P. E. Bourne, "Antibody-protein interactions: benchmark datasets and prediction tools evaluation," *BMC Structural Biology*, vol. 7, no. 1, p. 64, 2007.
- [58] E. A. Emini, J. V. Hughes, D. S. Perlow, and J. Boger, "Induction of hepatitis A virus-neutralizing antibody by a virus-specific synthetic peptide," *Journal of Virology*, vol. 55, no. 3, pp. 836–839, 1985.
- [59] A. S. Kolaskar and P. C. Tongaonkar, "A semi-empirical method for prediction of antigenic determinants on protein antigens," *FEBS Letters*, vol. 276, no. 1–2, pp. 172–174, 1990.
- [60] J. Ponomarenko, H.-H. Bui, W. Li et al., "ElliPro: a new structure-based tool for the prediction of antibody epitopes," *BMC Bioinformatics*, vol. 9, no. 1, p. 514, 2008.
- [61] M. Andreatta and M. Nielsen, "Gapped sequence alignment using artificial neural networks: application to the MHC class I system," *Bioinformatics*, vol. 32, no. 4, pp. 511–517, 2016.
- [62] S. Buus, S. L. Lauemøller, P. Worning et al., "Sensitive quantitative predictions of peptide-MHC binding by a 'Query by Committee' artificial neural network approach," *Tissue Antigens*, vol. 62, no. 5, pp. 378–384, 2003.
- [63] C. Lundegaard, K. Lamberth, M. Harndahl, S. Buus, O. Lund, and M. Nielsen, "NetMHC-3.0: accurate web accessible

- predictions of human, mouse and monkey MHC class I affinities for peptides of length 8-11," *Nucleic Acids Research*, vol. 36, 2008.
- [64] C. Lundegaard, O. Lund, and M. Nielsen, "Accurate approximation method for prediction of class I MHC affinities for peptides of length 8, 10 and 11 using prediction tools trained on 9mers," *Bioinformatics*, vol. 24, no. 11, pp. 1397-1398, 2008.
- [65] C. Lundegaard, M. Nielsen, and O. Lund, "The validity of predicted T-cell epitopes," *Trends in Biotechnology*, vol. 24, no. 12, pp. 537-538, 2006.
- [66] M. Nielsen, C. Lundegaard, P. Worning et al., "Reliable prediction of T-cell epitopes using neural networks with novel sequence representations," *Protein Science*, vol. 12, no. 5, pp. 1007-1017, 2003.
- [67] M. Nielsen and O. Lund, "NN-align. An artificial neural network-based alignment algorithm for MHC class II peptide binding prediction," *BMC Bioinformatics*, vol. 10, no. 1, 2009.
- [68] H. H. Bui, J. Sidney, K. Dinh, S. Southwood, M. J. Newman, and A. Sette, "Predicting population coverage of T-cell epitope-based diagnostics and vaccines," *BMC Bioinformatics*, vol. 7, no. 1, p. 153, 2006.
- [69] J. E. Chen, C. C. Huang, and T. E. Ferrin, "RRDistMaps: a UCSF Chimera tool for viewing and comparing protein distance maps," *Bioinformatics*, vol. 31, no. 9, pp. 1484-1486, 2015.
- [70] S. Hertig, T. D. Goddard, G. T. Johnson, and T. E. Ferrin, "Multidomain Assembler (MDA) generates models of large multidomain proteins," *Biophysical Journal*, vol. 108, no. 9, pp. 2097-2102, 2015.
- [71] M. Källberg, H. Wang, S. Wang et al., "Template-based protein structure modeling using the RaptorX web server," *Nature Protocols*, vol. 7, no. 8, pp. 1511-1522, 2012.
- [72] E. F. Pettersen, T. D. Goddard, C. C. Huang et al., "UCSF Chimera—a visualization system for exploratory research and analysis," *Journal of Computational Chemistry*, vol. 25, no. 13, pp. 1605-1612, 2004.
- [73] Z. Yang, K. Lasker, D. Schneidman-Duhovny et al., "UCSF Chimera, MODELLER, and IMP: an integrated modeling system," *Journal of Structural Biology*, vol. 179, no. 3, pp. 269-278, 2012.
- [74] E. Gasteiger, A. Gattiker, C. Hoogland, I. Ivanyi, R. D. Appel, and A. Bairoch, "ExPASy: the proteomics server for in-depth protein knowledge and analysis," *Nucleic Acids Research*, vol. 31, no. 13, pp. 3784-3788, 2003.
- [75] C. C. G. Inc, *Molecular Operating Environment (MOE)*, 2007, <http://www.chemcomp.com>.
- [76] D. S. BIOVIA, *Discovery Studio Visualizer 2.5 ed*, San Diego, Dassault Systèmes, 2009, <https://www.3dsbiovia.com/>.
- [77] Y. Shen, J. Maupetit, P. Derreumaux, and P. Tufféry, "Improved PEP-FOLD approach for peptide and miniprotein structure prediction," *Journal of Chemical Theory and Computation*, vol. 10, no. 10, pp. 4745-4758, 2014.
- [78] P. Thevenet, Y. Shen, J. Maupetit, F. Guyon, P. Derreumaux, and P. Tuffery, "PEP-FOLD: an updated de novo structure prediction server for both linear and disulfide bonded cyclic peptides," *Nucleic Acids Research*, vol. 40, no. W1, pp. W288-W293, 2012.
- [79] N. de Klerk, C. de Vogel, A. Fahal, A. van Belkum, and W. W. J. van de Sande, "Fructose-bisphosphate aldolase and pyruvate kinase, two novel immunogens in *Madurella mycetomatis*," *Medical Mycology*, vol. 50, no. 2, pp. 143-151, 2012.
- [80] M. Elhag, M. Abubaker, N. M. Ahmad, E. M. Haroon, R. M. Alaagib, and M. A. Hassan, "Immunoinformatics prediction of epitope based peptide vaccine against listeria monocytogenes fructose bisphosphate aldolase protein," *BioRxiv*, p. 649111, 2019.
- [81] M. Elhag, R. M. Alaagib, N. M. Ahmed et al., "Design of epitope-based peptide vaccine against pseudomonas aeruginosa fructose bisphosphate aldolase protein using immunoinformatics," *Journal of Immunology Research*, vol. 2020, pp. 1-11, 2020.
- [82] M. Elhag, R. M. Alaagib, E. M. Haroun, N. M. Ahmed, S. O. Abd Albagi, and M. A. Hassan, "Immunoinformatics prediction of epitope based peptide vaccine against schistosoma mansoni fructose bisphosphate aldolase protein," *BioRxiv*, 2019.
- [83] A. A. Mohammed, A. M. H. ALnaby, S. M. Sabeel et al., "Epitope-based peptide vaccine against fructose-bisphosphate aldolase of *Madurella mycetomatis* using immunoinformatics approaches," *Bioinform Biol Insights*, vol. 12, p. 117793221880970, 2018.
- [84] J. S. Testa and R. Philip, "Role of T-cell epitope-based vaccine in prophylactic and therapeutic applications," *Future Virol*, vol. 7, no. 11, pp. 1077-1088, 2012.
- [85] A. Idris and M. Hassan, "Immunoinformatics prediction and modelling of a cocktail of B- and T-cells epitopes from envelope glycoprotein and nucleocapsid proteins of Sin Nombre virus," *Immunome Research*, vol. 13, 2017.

## Research Article

# Clinical Features and Risk Factors of Active Tuberculosis in Patients with Behçet's Disease

Yaxu Liu <sup>1</sup>, Lifan Zhang,<sup>1,2,3</sup> Ziyue Zhou,<sup>1</sup> Luxi Sun,<sup>4</sup> Baotong Zhou,<sup>1,3</sup> Xiaoqing Liu <sup>1,2,3</sup> and Wenjie Zheng <sup>4</sup>

<sup>1</sup>Department of Infectious Diseases, Peking Union Medical College Hospital, Chinese Academy of Medical Sciences & Peking Union Medical College, Beijing 100730, China

<sup>2</sup>Peking Union Medical College Hospital, Chinese Academy of Medical Science, Clinical Epidemiology Unit, International Epidemiology Network, Beijing 100730, China

<sup>3</sup>Chinese Academy of Medical Sciences and Peking Union Medical College, Centre for Tuberculosis Research, Beijing 100730, China

<sup>4</sup>Department of Rheumatology, Peking Union Medical College Hospital, Chinese Academy of Medical Sciences & Peking Union Medical College, The Ministry of Education Key Laboratory, National Clinical Research Center for Dermatologic and Immunologic Diseases, Beijing 100730, China

Correspondence should be addressed to Xiaoqing Liu; liuxqpmch@126.com and Wenjie Zheng; wenjzheng@gmail.com

Received 29 July 2020; Revised 20 October 2020; Accepted 27 October 2020; Published 24 November 2020

Academic Editor: Roberta Antonia Diotti

Copyright © 2020 Yaxu Liu et al. This is an open access article distributed under the Creative Commons Attribution License, which permits unrestricted use, distribution, and reproduction in any medium, provided the original work is properly cited.

To investigate the clinical features and potential risk factors of active tuberculosis (ATB) in Behçet's disease (BD), we conducted a case-control study on hospitalized BD patients in our institute from 2010 to 2019. BD patients with ATB were enrolled as the case group. The control group was selected by random number sampling from the remaining BD patients, including those with latent tuberculosis infection, previous tuberculosis, or without tuberculosis. Finally, we reviewed 386 BD patients and identified 21 (5.4%) ATB cases, including four (19.0%) microbiologically confirmed and 17 (81.0%) clinically diagnosed. We found that BD patients with ATB were more prone to have systemic symptoms (fever, night sweating, and unexplained weight loss) and/or symptoms related to the infection site. Multivariate logistic regression analysis revealed that erythrocyte sedimentation rate (ESR) > 60 mm/h (OR = 13.710, 95% CI (1.101, 170.702)), increased IgG (OR = 1.226, 95% CI (1.001, 1.502)), and positive T-SPOT.TB (OR = 7.793, 95% CI (1.312, 48.464)), for 24-200 SFC/10<sup>6</sup>PBMC; OR = 17.705 95% CI (2.503, 125.260), for >200 SFC/10<sup>6</sup>PBMC) were potential risk factors for ATB in BD patients. Our study suggested that when BD patients have systemic symptoms with significantly elevated TB-SPOT, the diagnosis of ATB should be considered.

## 1. Introduction

Behçet's disease (BD) is a systemic vasculitis prevalent in the areas along the Ancient Silk Road such as Turkey, Iran, China, and Japan [1]. In China, the prevalence of BD is estimated to be 14 in 100 000 [2]. It has been noticed that BD is closely related to tuberculosis (TB) [3, 4], which is also prevalent in China [5].

TB infection may trigger the pathogenesis of BD [6, 7], and BD patients are at high risk of active tuberculosis (ATB) infection [8, 9]. The treatment of BD generally includes glucocorticoid, immunosuppressant, and biologic agents [10–12].

Once a BD patient is infected with ATB, the immunosuppressive therapy would be reduced or suspended [13], resulting in the BD deterioration and increased risk of developing immune reconstitution inflammatory syndrome [14]. If the ATB is not promptly diagnosed or properly treated, the intensive immunosuppressive therapy may lead to disseminated TB and severe consequences [15]. Thus, understanding the clinical features and risk factors of ATB in patients with BD is of great importance.

To date, related studies are very limited. Lin et al. reported the clinical features of ATB in 10 BD patients, but the BD sample size for the study was only 37, and the

statistical analysis was not conducted [16]. Liu compared the clinical features of 36 BD patients with ATB and 407 BD patients without TB. Liu discovered that ATB patients were more prone to fever, arthritis, thrombosis, and elevated IgG [17]. However, patients with latent tuberculosis infection (LTBI) or previous tuberculosis (PTB) were not included in the study. Moreover, to the best of our knowledge, there is no study investigating the risk factor of ATB in BD patients. Therefore, a case-control study was conducted to investigate the clinical features and explore the risk factors of ATB in BD patients.

## 2. Materials and Methods

**2.1. Participants.** Medical records of all hospitalized patients diagnosed with BD in Peking Union Medical College Hospital (PUMCH) from January 1, 2010, to June 30, 2019, were retrospectively reviewed. All patients fulfilled the 2013 International Criteria for Behçet's Disease (ICBD) [18]. Patients suspected of tuberculosis infection underwent careful examinations, including pathological examinations (culture and acid-fast staining of sputum and other available samples like pleural effusion), a biopsy of the suspected organs (colonoscopy of the colorectal lesions, the surgical sample of the vertebra), and immunological examinations (T-SPOT.TB test), for the evidence of tuberculosis infection as well as the exclusion of other common infections in BD like bacteria and CMV. The categorization of TB was based on the 2000 criteria [19] and those applied in previous studies [20, 21] (see Table S1 in the Supplementary Material online). Two experienced experts of infectious diseases were asked to review the cases and check the diagnosis of ATB independently. Only confirmed by both experts would the clinical diagnosis of ATB be accepted. All patients diagnosed with BD and ATB were enrolled as the case group. The remaining patients with BD were ranked according to the date of admission, and the random samples were chosen using random number tables as the control group.

**2.2. Data Collection.** The demographic features (age and sex), past medical history (the course and treatment of BD before hospitalization, previous infection of TB, etc.), current treatment (glucocorticoid dosage, immunosuppressant, etc.), BD systemic involvement, TB-related systemic symptoms (fever, cough, etc.), laboratory results (complete blood cell count, T-SPOT.TB, etc.), and comorbidities of the patients were collected and analyzed. The flowchart of the study was shown in Figure 1.

**2.3. Ethic Review.** This study complied with the Declaration of Helsinki and was approved by the Ethics Committee of PUMCH (ethics approval number: S-715). Informed consent was obtained from all patients for being included in the study.

**2.4. Statistical Analyses.** Continuous variables were examined by the Kolmogorov-Smirnov test, and those with normal distribution were expressed as mean  $\pm$  standard deviation (SD), while those without were described as median and interquartile range (IQR). Categorical variables were pre-

sented as numbers and percentages. Comparisons of continuous variables were performed using Student's *t*-test when they were in normal distribution, and Mann-Whitney *U*-test when they were not. Categorical data were compared using the Chi-squared test or Fisher's exact test.  $p < 0.05$  was considered to be statistically significant.

Variables with  $p < 0.1$  in the univariate analysis were considered candidate risk factors, and those with clinical significance were evaluated with stepwise binary logistic regression analysis (inclusion threshold  $p < 0.05$ , exclusion threshold  $p > 0.1$ ). The odds ratio (OR) of the risk factors and its 95% confidential interval (CI) were calculated. All statistical analyses were performed with SPSS 16.0 (SPSS Inc., USA).

## 3. Results

**3.1. General Data.** Three hundred eighty-six hospitalized patients were diagnosed with BD in PUMCH from January 2010 to June 2019. Twenty-one (5.4%) of them were confirmed with the diagnosis of ATB, including four microbiologically confirmed and 17 clinically diagnosed. The control group consisted of 69 patients, including 25 (36.2%) with LTBI or PTB and 44 (63.8%) without TB.

**3.2. Clinical Features of BD with ATB.** Four of the 21 ATB patients were microbiologically confirmed while 17 were clinically diagnosed (see Table S2 in the Supplementary Material online). Sixteen (76.2%) patients had pulmonary TB, four (19.0%) had extrapulmonary TB, and one patient's infection site could not be identified. Four patients (19.0%) had more than one organ involved. The involved organs other than the lung included the gastrointestinal tract (2, 9.5%), bones (2, 9.5%), lymph nodes (1, 4.8%), larynx (1, 4.8%), peritoneum (1, 4.8%), and pericardium (1, 4.8%).

Patients with ATB were more likely to develop systematic symptoms including fever (18, 85.7%), night sweating (8, 38.1%), and unexplained weight loss (13, 61.9%). Meanwhile, many ATB patients also had symptoms related to the site of infection. For example, pulmonary ATB patients had a productive cough; osteal ATB patients had bone pain and restricted range of motion; lymphatic ATB patients had lymphadenopathy and sinus formation; pharyngeal ATB patients had mucosal erosions, ulcers, and tubercles; and gastrointestinal ATB patients had abdominal pain, diarrhea, and/or constipation.

All ATB patients showed abnormalities in chest radiology, including nodules, cord, or patches, predominantly in the upper and medial lobes. Some other abnormalities can also be revealed by CT scan, such as lymph node enlargement with a low-density core in lymphatic ATB, vertebral damage in osteal ATB, and swelling of gastrointestinal walls in gastrointestinal ATB. The pericardial ATB patients also showed fibrinous pericardial effusion on echocardiogram.

All BD patients with ATB had clinical improvement after anti-TB treatment. Moreover, with intensive treatment of BD following the control of ATB, patients had achieved long-term stability of their disease condition during the follow-up period.

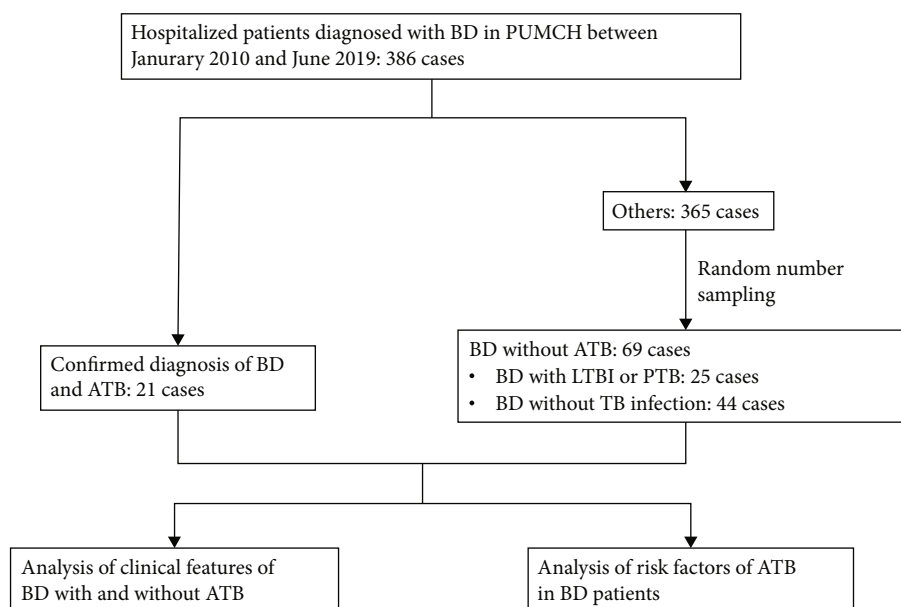


FIGURE 1: Flowchart of the study. BD: Behçet's disease; PUMCH: Peking Union Medical College Hospital; ATB: active tuberculosis; LTBI: latent tuberculosis infection; PTB: previous tuberculosis.

### 3.3. Clinical Comparison of BD Patients with and without ATB

**3.3.1. Past Medical History and Medication.** More ATB patients had evidence of previous TB infection (13 (61.90%) vs. 17 (24.64%),  $p = 0.002$ ). The duration of previous glucocorticoid use was shorter in the ATB group (0 (0, 3.5) month vs. 3 (0, 13) months,  $p = 0.028$ ) (Table 1). The case and control groups showed no difference in immunosuppressant or biologics treatment (Table 1) and comorbidities (diabetes mellitus: 4.76% vs. 7.25%,  $p = 1.00$ ; myelodysplastic syndrome: 4.76% vs. 7.25%,  $p = 1.00$ ; and others: 52.38% vs. 52.17%,  $p = 1.00$ ).

**3.3.2. Symptoms and Signs.** The systemic involvement of BD patients with and without ATB revealed no difference (Table 2), but more ATB patients had TB toxic symptoms like fever (85.7% vs. 49.3%,  $p = 0.003$ ), cough (38.1% vs. 7.2%,  $p = 0.002$ ), expectoration (33.3% vs. 4.3%,  $p = 0.001$ ), and night sweating (38.1% vs. 5.8%,  $p = 0.001$ ).

**3.3.3. Laboratory Tests.** ATB patients had increased level of erythrocyte sedimentation rate (ESR, 31 (22, 57) vs. 16 (6, 39) mm/h,  $p = 0.004$ ), hypersensitive C reactive protein (hsCRP, 28.32 (8.50, 63.83) vs 10.37 (1.61, 43.59) mg/L,  $p = 0.038$ ), immunoglobulin G (IgG, 12.55 (9.98, 15.61) vs. 9.6 (7.84, 13.13) g/L,  $p = 0.006$ ), complement 3 (C3,  $1.3048 \pm 0.23713$  vs.  $1.1664 \pm 0.24768$  g/L,  $p = 0.036$ ), and complement 4 (C4,  $0.2644 \pm 0.09852$  vs.  $0.2213 \pm 0.03997$  g/L,  $p = 0.039$ ), higher positive rate of T-SPOT.TB (17 (80.95%) vs. 19 (27.54%),  $p = 0.000$ ), and elevated SFC in T-SPOT.TB test (336 (92, 1084) SFC/ $10^6$ PBMC vs. 0 (0, 27) SFC/ $10^6$ PBMC,  $p = 0.000$ ) (Table 2). Complete blood cell count and the liver and kidney function tests revealed no significant difference.

**3.3.4. Risk Factors for ATB in BD Patients.** The result of logistic regression analysis is shown in Table 3. ESR > 60 mm/h (OR = 13.710, 95% CI (1.101, 170.702),  $p = 0.042$ ), increased IgG (OR = 1.226, 95% CI (1.001, 1.502),  $p = 0.049$ ), and positive T-SPOT.TB (OR = 7.793, 95% CI (1.312, 48.464),  $p = 0.024$ , for 24-200 SFC/ $10^6$ PBMC; OR = 17.705 (2.503, 125.260),  $p = 0.004$ , for >200 SFC/ $10^6$ PBMC) were found to be statistically significant.

## 4. Discussion

This study is the first well-designed case-control study investigating the clinical features of BD patients with ATB and exploring the potential risk factors of ATB in BD patients. We demonstrated that BD patients tend to develop pulmonary ATB and have multiple sites involved. Besides presenting with the symptoms related to the infection sites, ATB patients also had systemic symptoms, including fever, night sweating, and unexplained weight loss. Furthermore, logistic regression analysis indicates that ESR > 60 mm/h, increased IgG, and positive T-SPOT.TB are potential risk factors of ATB in BD patients.

Even with thorough examinations, most ATB patients in our study were clinically diagnosed and lacked the microbiological evidence, which is attributed to the high prevalence of TB in China and the complicated nature of the cases referred to our hospital. Microbiological examinations, including bacterial culture, acid-fast staining, and molecular tests, are currently the gold standard for ATB diagnosis. However, the sensitivity of these tests is not satisfactory [22]. In countries with heavy tuberculosis burden, culture- or smear-negative cases are not rare, sometimes even accounting for more than 70% of all ATB cases [20, 23, 24]. Other tests like acute inflammatory markers are not specific, while T-SPOT.TB cannot differentiate ATB from LTBI/PTB [25]. Thus, all

TABLE 1: Past medical history and medication of BD patients with and without ATB.

	BD with ATB ( <i>n</i> = 21)	BD without ATB ( <i>n</i> = 69)	<i>p</i>
Sex (male, %)	13 (61.90%)	35 (50.72%)	0.369
Age ( <i>M</i> ± <i>SD</i> )	36.19 ± 12.46	38.58 ± 12.68	0.450
Past medical history			
Previous contact with ATB patients (%)	3 (14.29%)	2 (2.90%)	0.081
Previous prophylactic treatment of TB (%)	1 (4.76%)	3 (4.35%)	1.000
Evidence of PTB <sup>a</sup> (%)	13 (61.90%)	17 (24.64%)	0.002
Previous treatment of BD			
Glucocorticoid			
Maximal dosage (mg/d, median, IQR) <sup>b</sup>	0 (0, 50)	25 (0, 60)	0.093
Duration (months, median, IQR)	0 (0, 3.5)	3 (0, 13)	0.028
Biologics			
Infliximab (%)	2 (9.52%)	2 (2.90%)	0.231
Other TNF- $\alpha$ inhibitors (%)	2 (9.52%)	3 (4.35%)	0.587
Immunosuppressant			
CTX (%)	5 (23.81%)	11 (15.94%)	0.515
CsA (%)	0 (0%)	10 (14.49%)	0.109
MTX (%)	1 (4.76%)	3 (4.35%)	1.000
FK506 (%)	1 (4.76%)	2 (2.90%)	0.554
AZA (%)	2 (9.52%)	5 (7.25%)	0.663
Current treatment of BD <sup>c</sup>			
Glucocorticoid dosage (mg/d, median, IQR) <sup>b</sup>	0 (0, 15)	5 (0, 32.5)	0.177
Biologics			
Infliximab (%)	0 (0%)	2 (2.90%)	1.000
Other TNF- $\alpha$ inhibitor (%)	1 (4.76%)	0 (0%)	0.233
Immunosuppressant			
CTX (%)	1 (4.76%)	11 (15.94%)	0.281
CsA (%)	1 (4.76%)	7 (10.14%)	0.675
MTX (%)	0 (0%)	0 (0%)	—
FK506 (%)	1 (4.76%)	1 (1.45%)	0.414
AZA (%)	1 (4.76%)	1 (1.45%)	0.414

<sup>a</sup>Evidence of PTB includes past history of TB infection and radiological features indicating PTB in chest CT. <sup>b</sup>All forms of glucocorticoid were converted to the equivalent dosage of prednisone. <sup>c</sup>Current use of immunosuppressant and biologics indicates continuous use of the drug for 3 months before hospitalization, and the dosage of glucocorticoid records the maximal dose of glucocorticoid within 2 weeks before hospitalization. TNF- $\alpha$ : tumor necrosis factor- $\alpha$ ; CTX: cyclophosphamide; CsA: ciclosporin A; MTX: methotrexate; FK506: tacrolimus; AZA: azathioprine; LEF: leflunomide; MMF: mycophenolate mofetil.

patients who were highly suspected of ATB but had negative results in microbiological examinations would receive diagnostic anti-TB treatment for 3 months, and their responses to the treatment were documented to help the clinical diagnosis of ATB. Only by being confirmed by two infectious disease experts would the clinical diagnosis of ATB be accepted. In this way, we believe the clinical diagnosis of ATB in our study is reliable. Besides, our study enrolled BD patients with LTBI, PTB, and non-TB as the control group. Compared with previous case reports of patients mostly culture confirmed [26, 27] and the case-control studies lacking LTBI/PTB patients in the control group [17], our study population is closer to the actual clinical situation.

Generally, patients with ATB are more likely to experience the symptoms related to the site of infection. Therefore, TB infection should be suspected when a BD patient pre-

sented with the manifestations rarely occurring in BD, such as productive cough, bone pain, restricted range of motion, and lymphadenopathy. Severe systemic symptoms (fever, night sweating, and unexplained weight loss) are also important clues of ATB. It is challenging to identify active TB in BD patients when they presented with manifestations shared by BD and ATB, such as erythema nodosa, pericarditis, and gastrointestinal ulcers predominant at the ileocecal junction. Laboratory tests can be helpful in this situation. Patients with markedly elevated ESR, hsCRP, IgG, and/or positive T-SPOT.TB should be considered to have ATB, which is consistent with previous case reports [28] and studies [17, 29]. The involvement of lungs in BD generally presents as pulmonary artery thrombosis or aneurysm [30, 31], which could be easily differentiated from tuberculosis by chest CT, while the pulmonary parenchymal involvement in BD is rare. Empiric

TABLE 2: Clinical presentation and laboratory results of BD patients with and without ATB.

	BD with ATB ( <i>n</i> = 21)	BD without ATB ( <i>n</i> = 69)	<i>p</i>
Systemic involvement of BD			
Oral ulceration (%)	19 (90.5%)	68 (98.6%)	0.135
Genital ulceration (%)	18 (85.7%)	49 (71.0%)	0.176
Erythema nodosa (%)	12 (57.1%)	30 (43.5%)	0.272
Ocular lesions (%)	4 (19.0%)	25 (36.2%)	0.140
Vascular manifestations (%)	4 (19.0%)	25 (36.2%)	0.140
Gastrointestinal involvement (%)	6 (28.6%)	24 (34.8%)	0.597
CNS involvement (%)	3 (14.3%)	15 (21.7%)	0.548
Symptoms related to TB infection			
Fever (%)	18 (85.7%)	34 (49.3%)	0.003
Cough (%)	8 (38.1%)	5 (7.2%)	0.002
Expectoration (%)	7 (33.3%)	3 (4.3%)	0.001
Night sweating (%)	8 (38.1%)	4 (5.8%)	0.001
Weight loss (%)	13 (61.9%)	28 (40.6%)	0.086
Laboratory tests			
ESR (mm/h, median, IQR)	31 (22, 57)	16 (6, 39)	0.004
hsCRP (mg/L, median, IQR)	28.32 (8.50, 63.83)	10.37 (1.61, 43.59)	0.038
IgG (g/L, median, IQR)	12.55 (9.98, 15.61)	9.6 (7.84, 13.13)	0.006
IgA (g/L, median, IQR)	2.78 (1.75, 3.66)	2.28 (1.59, 3.04)	0.286
IgM (g/L, median, IQR)	0.91 (0.71, 1.74)	0.93 (0.71, 1.33)	0.575
Positive T-SPOT.TB (%)	17 (80.95%) ( <i>n</i> = 19)	19 (27.54%) ( <i>n</i> = 66)	0.000
T-SPOT.TB value (SFC/10 <sup>6</sup> PBMC, median, IQR)	336 (92, 1084)	0 (0, 27)	0.000

ESR: erythrocyte sedimentation rate; hsCRP: hypersensitive C reactive protein; IgG: immunoglobulin G; IgA: immunoglobulin A; IgM: immunoglobulin M; SFC: spot-forming cells; PBMC: peripheral blood mononuclear cells.

TABLE 3: Potential risk factors for ATB in BD patients.

	<i>b</i>	SE( <i>b</i> )	Wald	<i>p</i>	OR (95% CI)
ESR (mm/h)					
0-20			4.658	0.097	
20-60	1.719	0.965	3.178	0.075	5.581 (0.843, 36.960)
>60	2.618	1.287	4.141	0.042	13.710 (1.101, 170.702)
IgG (g/L)					
	0.204	0.104	3.876	0.049	1.226 (1.001, 1.502)
T-SPOT.TB (SFC/10 <sup>6</sup> PBMC)					
<24			9.266	0.010	
24-200	2.076	0.921	5.084	0.024	7.793 (1.312, 48.464)
>200	2.874	0.998	8.288	0.004	17.705 (2.503, 125.260)

OR: odds ratio; CI: confidential interval.

anti-TB treatment can be considered for patients with the abovementioned clues of ATB. Meanwhile, the response to anti-TB therapy could help the clinical diagnosis or exclusion of ATB.

ESR > 60 mm/h, increased IgG, and positive T-SPOT.TB were found to be potential risk factors for ATB in patients with BD by logistic regression analysis. ESR was reported to be markedly [27] or slightly [32] increased in ATB patients, and increased IgG in ATB patients had also been reported in Wang's case report [28] and Liu's case-control study [17]. However, prospective cohort studies are needed to understand whether the increase of these nonspecific inflam-

matory markers is the cause or the result of ATB. T-SPOT.TB is an interferon-gamma release assay (IGRA) based on the MTB-specific T cell response [25]. The logistic analysis revealed a higher OR value as spot forming cells (SFC) of T-SPOT.TB increases. Even though T-SPOT.TB could not differentiate LTBI and ATB [25], many studies had shown more robust T cell immune response in ATB patients [20, 33], supporting that positive or markedly increased T-SPOT.TB can be a potential risk factor of ATB in patients with BD.

Notably, our study revealed a smaller dosage and shorter glucocorticoid treatment duration in ATB patients, which is different from previous studies [34]. This may be due to the retrospective design of our study, when patients not excluded for ATB may have avoided using glucocorticoids during the previous treatment. TNF- $\alpha$  inhibitor use, though identified as a risk factor of ATB in previous studies [9], revealed no significant difference between cases and controls in our study. On the one hand, this might be related to the limited sample number in this study; on the other hand, this could be attributed to the thorough screening and proper prophylaxis of patients using TNF- $\alpha$  inhibitors, according to the guidelines [11, 13, 35, 36] published in the 2000s.

We acknowledge some limitations in our study. First, our sample size was relatively small, and most ATB cases were diagnosed according to clinical criteria rather than culture confirmed, which might introduce a risk of bias. Second,



our center is a national referral center for complicated and critical cases, which might induce a potential selection bias, and the extension of the conclusion must be drawn carefully. Third, the risk factors identified in this case-control study are still required to be confirmed by prospective cohort studies in the future. Finally, most (81.0%) of the ATB cases in this study were clinically diagnosed without microbiological evidence. Even though the clinical diagnosis was carefully reviewed and seemed to be plausible in a country with high prevalence of tuberculosis, the diagnosis without a gold standard might introduce a high risk of bias.

## 5. Conclusion

The diagnosis of ATB should be considered when BD patients presented with systemic symptoms like fever, night sweating, and unexplained weight loss, as well as rare presentations of BD such as productive cough, lymphadenopathy, and bone pain. Significantly elevated ESR, hsCRP, IgG, and positive T-SPOT.TB supports the diagnosis of ATB. Furthermore, the markedly increased SFC in T-SPOT.TB indicates a high risk factor of ATB in BD patients.

## Data Availability

The clinical data used to support the findings of this study are included in the article.

## Conflicts of Interest

The authors declare that there is no conflict of interest regarding the publication of this paper.

## Acknowledgments

This work was supported by the National Science and Technology Major Project of the People's Republic of China (grant number 2017ZX10201302), CAMS Initiative for Innovative Medicine (grant number 2016-I2M-1-013), the CAMS Innovation Fund for Medical Sciences (grant number 2019-I2M-2-005), National Natural Science Foundation of China (grant number 81871299), National Key Research and Development Program: 'Precise Medical Research' (grant number 2016YFC0906201).

## Supplementary Materials

The supplementary materials include two tables. Table S1: The diagnostic criteria for different TB infection statuses. Table S2: the detailed information of 21 BD patients diagnosed with ATB. (*Supplementary materials*)

## References

- [1] F. Davatchi, C. Chams-Davatchi, H. Shams et al., "Behcet's disease: epidemiology, clinical manifestations, and diagnosis," *Expert Review of Clinical Immunology*, vol. 13, no. 1, pp. 57–65, 2016.
- [2] J. N. Kim, S. G. Kwak, J. Y. Choe, and S. K. Kim, "The prevalence of Behcet's disease in Korea: data from Health Insurance Review and Assessment Service from 2011 to 2015," *Clinical and Experimental Rheumatology*, vol. 108, no. 6, pp. 38–42, 2017.
- [3] P. R. Botha and C. F. N. Koegelenberg, "Risk Factors for Tuberculosis in Patients Receiving Tumour Necrosis Factor- $\alpha$  Blockers: What Do We Really Know?," *Respiration*, vol. 90, no. 3, pp. 185–186, 2015.
- [4] Y. Zhou and Z. Lv, "The relationship between Behcet disease and tuberculosis infection," *Clin Focus*, vol. 24, no. 19, pp. 1742–1744, 2009.
- [5] *WHO tuberculosis report*, 2019, 2019 [Available from: [https://www.who.int/tb/publications/global\\_report/en/](https://www.who.int/tb/publications/global_report/en/)].
- [6] H. Direskeneli, "Innate and Adaptive Responses to Heat Shock Proteins in Behcet's Disease," *Genetics Research International*, vol. 2013, Article ID 249157, 6 pages, 2013.
- [7] L. Zhang, Y. Xu, Y. Peng, B. Yan, and Y. Liu, "Behcet's disease-like syndrome secondary to microbial infection: a case report and review of the literature," *International Journal of Clinical and Experimental Pathology*, vol. 8, no. 10, pp. 13619–13624, 2015.
- [8] S. Borekci, E. Atahan, D. Demir Yilmaz et al., "Factors affecting the tuberculosis risk in patients receiving anti-tumor necrosis Factor- $\alpha$  treatment," *Respiration*, vol. 90, no. 3, pp. 191–198, 2015.
- [9] B. Kisacik, O. N. Pamuk, A. M. Onat et al., "Characteristics predicting tuberculosis risk under tumor necrosis factor- $\alpha$  inhibitors: report from a large multicenter cohort with high background prevalence," *The Journal of Rheumatology*, vol. 43, no. 3, pp. 524–529, 2016.
- [10] T. Hisamatsu, F. Ueno, T. Matsumoto et al., "The 2nd edition of consensus statements for the diagnosis and management of intestinal Behcet's disease: indication of anti-TNF $\alpha$  monoclonal antibodies," *Journal of Gastroenterology*, vol. 49, no. 1, pp. 156–162, 2014.
- [11] G. Hatemi, A. Silman, D. Bang et al., "EULAR recommendations for the management of Behcet disease," *Annals of the Rheumatic Diseases*, vol. 67, no. 12, pp. 1656–1662, 2008.
- [12] G. Hatemi, R. Christensen, D. Bang et al., "2018 update of the EULAR recommendations for the management of Behcet's syndrome," *Annals of the Rheumatic Diseases*, vol. 77, no. 6, pp. 808–818, 2018.
- [13] British Thoracic Society Standards of Care Committee, "BTS recommendations for assessing risk and for managing Mycobacterium tuberculosis infection and disease in patients due to start anti-TNF- treatment," *Thorax*, vol. 60, no. 10, pp. 800–805, 2005.
- [14] C. C. Dobler, "Biologic Agents and Tuberculosis," *Microbiology Spectrum*, vol. 4, no. 6, 2016.
- [15] Y. Kobashi, M. Fukuda, K. Yoshida, and M. Oka, "An indeterminate QuantiFERON TB-2G response for miliary tuberculosis, due to severe pancytopenia," *Journal of Infection and Chemotherapy*, vol. 13, no. 6, pp. 414–417, 2007.
- [16] Y. Lin, G. Yin, and Y. Shu, "Analysis of 10 cases of Behcet disease with tuberculosis infection," *West Chin Med J*, vol. 23, no. 1, pp. 125–126, 2008.
- [17] L. Yuanyuan, "Analysis of the clinical features of Behcet disease related to tuberculosis infection," *J Clin Inter Med*, vol. 9, no. 35, pp. 615–617, 2018.
- [18] International Team for the Revision of the International Criteria for Behcet's Disease, "The International Criteria for Behcet's Disease (ICBD): a collaborative study of 27 countries on

- the sensitivity and specificity of the new criteria," *J Eur Acad Dermatol Venereol*, vol. 28, no. 3, pp. 338–347, 2014.
- [19] "Diagnostic Standards and Classification of Tuberculosis in Adults and Children. This official statement of the American Thoracic Society and the Centers for Disease Control and Prevention was adopted by the ATS Board of Directors, July 1999. This statement was endorsed by the Council of the Infectious Disease Society of America, September 1999," *American Journal of Respiratory and Critical Care Medicine*, vol. 161, no. 4, pp. 1376–1395, 2000.
- [20] X. Wu, P. Chen, W. Wei et al., "Diagnostic value of the interferon- $\gamma$  release assay for tuberculosis infection in patients with Behçet's disease," *BMC Infectious Diseases*, vol. 19, no. 1, p. 323, 2019.
- [21] H. S. Whitworth, A. Badhan, A. A. Boakye et al., "Clinical utility of existing and second-generation interferon- $\gamma$  release assays for diagnostic evaluation of tuberculosis: an observational cohort study," *The Lancet Infectious Diseases*, vol. 19, no. 2, pp. 193–202, 2019.
- [22] M. Zhang, D. Li, Z. D. Hu, and Y. L. Huang, "The diagnostic utility of pleural markers for tuberculosis pleural effusion," *Annals of translational medicine.*, vol. 8, no. 9, p. 607, 2020.
- [23] G. J. Fei, L. F. Zhang, and H. J. Shu, "Values of different laboratory diagnostic approaches for tuberculous peritonitis," *Zhongguo Yi Xue Ke Xue Yuan Xue Bao*, vol. 40, no. 4, pp. 534–538, 2018.
- [24] I. Afsar, M. Gunes, H. Er, and A. G. Sener, "Comparison of culture, microscopic smear and molecular methods in diagnosis of tuberculosis," *Revista Española de Quimioterapia*, vol. 31, no. 5, pp. 435–438, 2018.
- [25] M. Pai, C. M. Denking, S. V. Kik et al., "Gamma interferon release assays for detection of Mycobacterium tuberculosis infection," *Clinical Microbiology Reviews*, vol. 27, no. 1, pp. 3–20, 2014.
- [26] J. L. De Oliveira, D. A. De Souza Rangel, R. A. Cordeiro et al., "Tuberculous lymphadenopathy mimicking disease activity in a patient with Behçet's disease," *Adv Rheumatol.*, vol. 58, 2018.
- [27] İ. Gönen, "Disseminated Tuberculosis During the Course of Behçet's Disease: A Case Report," *Turkish Journal of Rheumatology*, vol. 27, no. 1, pp. 70–73, 2012.
- [28] M. Wang, "A case report of Behcet syndrome with osteoarticular tuberculosis," *J New Med.*, vol. 24, no. 12, pp. 637–638, 1993.
- [29] S. Liu, J. Ren, X. Wu et al., "Preliminary Case-control Study to Evaluate Diagnostic Values of C-Reactive Protein and Erythrocyte Sedimentation Rate in Differentiating Active Crohn's Disease From Intestinal Lymphoma, Intestinal Tuberculosis and Behcet's Syndrome," *The American Journal of the Medical Sciences*, vol. 346, no. 6, pp. 467–472, 2013.
- [30] L. L. Zhuang, H. M. Liu, G. M. Li et al., "Dural sinus thrombosis and giant pulmonary artery aneurysm in paediatric Behçet's disease," *Clinical and Experimental Rheumatology*, vol. 38, no. 3, pp. 558–566, 2020.
- [31] Y. Korogi, N. Tanaka, H. Yoshifuji, J. Tazaki, T. Kubo, and K. Tanizawa, "Complete occlusion of right pulmonary artery in Behçet disease," *Respirology case reports.*, vol. 8, no. 6, article e00594, 2020.
- [32] A. Iliopoulos, S. Kedikoglou, S. Laxanis, S. Kourouklis, and E. Katsaros, "A case of tuberculous meningoencephalitis in a patient with Behçet's disease," *Clinical Rheumatology*, vol. 25, no. 1, pp. 121–122, 2006.
- [33] S. Wang, J. Wu, J. Chen et al., "Evaluation of Mycobacterium tuberculosis-specific antibody responses for the discrimination of active and latent tuberculosis infection," *International Journal of Infectious Diseases*, vol. 70, pp. 1–9, 2018.
- [34] W. Long, F. Cai, X. Wang, N. Zheng, and R. Wu, "High risk of activation of latent tuberculosis infection in rheumatic disease patients," *Infectious Diseases*, vol. 52, no. 2, pp. 80–86, 2020.
- [35] N. Miyasaka, T. Takeuchi, and K. Eguchi, "Guidelines for the proper use of etanercept in Japan," *Modern Rheumatology*, vol. 16, no. 2, pp. 63–67, 2014.
- [36] J. J. Cush, "Biological drug use: US perspectives on indications and monitoring," *Annals of the Rheumatic Diseases*, vol. 64, Suppl\_4, pp. iv18–iv23, 2005.

## Review Article

# Elucidating the Pivotal Immunomodulatory and Anti-Inflammatory Potentials of Chloroquine and Hydroxychloroquine

Seidu A. Richard <sup>1</sup>, Sylvanus Kampo,<sup>2</sup> Maite Esquijarosa Hechavarria,<sup>2</sup> Marian Sackey,<sup>3</sup> Alexis D. B. Buunaaim,<sup>4</sup> Eugene Dogkotenge Kuugbee,<sup>5</sup> and Thomas Winsum Anabah<sup>6</sup>

<sup>1</sup>Department of Medicine, Princefield University, P. O. Box MA128, Ho, Ghana West Africa

<sup>2</sup>Department of Anesthesia and Critical Care, School of Medicine, University of Health and Allied Sciences, Ho, Ghana

<sup>3</sup>Department of Pharmacy, Ho Teaching Hospital, P.O. Box MA374, Ho, Ghana West Africa

<sup>4</sup>Department of Surgery, School of Medicine and Health Science, University for Development Studies, Tamale, Ghana

<sup>5</sup>Department of Clinical Microbiology, School of Medicine and Health Science, University for Development Studies, Tamale, Ghana

<sup>6</sup>Department of Clinical Medicine, Habana Medical Services, Tamale, Ghana

Correspondence should be addressed to Seidu A. Richard; [gbepoo@gmail.com](mailto:gbepoo@gmail.com)

Received 30 May 2020; Accepted 3 August 2020; Published 25 September 2020

Academic Editor: Roberta Antonia Diotti

Copyright © 2020 Seidu A. Richard et al. This is an open access article distributed under the Creative Commons Attribution License, which permits unrestricted use, distribution, and reproduction in any medium, provided the original work is properly cited.

Chloroquine (CQ) and hydroxychloroquine (HCQ) are derivatives of 4-aminoquinoline compounds with over 60 years of safe clinical usage. CQ and HCQ are able to inhibit the production of cytokines such as interleukin- (IL-) 1, IL-2, IL-6, IL-17, and IL-22. Also, CQ and HCQ inhibit the production of interferon- (IFN-)  $\alpha$  and IFN- $\gamma$  and/or tumor necrotizing factor- (TNF-)  $\alpha$ . Furthermore, CQ blocks the production of prostaglandins (PGs) in the intact cell by inhibiting substrate accessibility of arachidonic acid necessary for the production of PGs. Moreover, CQ affects the stability between T-helper cell (Th) 1 and Th2 cytokine secretion by augmenting IL-10 production in peripheral blood mononuclear cells (PBMCs). Additionally, CQ is capable of blocking lipopolysaccharide- (LPS-) triggered stimulation of extracellular signal-modulated extracellular signal-regulated kinases 1/2 in human PBMCs. HCQ at clinical levels effectively blocks CpG-triggered class-switched memory B-cells from differentiating into plasmablasts as well as producing IgG. Also, HCQ inhibits cytokine generation from all the B-cell subsets. IgM memory B-cells exhibits the utmost cytokine production. Nevertheless, CQ triggers the production of reactive oxygen species. A rare, but serious, side effect of CQ or HCQ in nondiabetic patients is hypoglycaemia. Thus, in critically ill patients, CQ and HCQ are most likely to deplete all the energy stores of the body leaving the patient very weak and sicker. We advocate that, during clinical usage of CQ and HCQ in critically ill patients, it is very essential to strengthen the CQ or HCQ with glucose infusion. CQ and HCQ are thus potential inhibitors of the COVID-19 cytokine storm.

## 1. Introduction

Chloroquine (CQ) and hydroxychloroquine (HCQ) are derivatives of 4-aminoquinoline compounds with over 60 years of safe clinical use in the treatment of malaria and, recently, the treatment of inflammatory disorders [1, 2]. CQ and HCQ have proven to be an effective and safe treatment option for autoimmune diseases like rheumatoid arthritis (RA) as well as systemic lupus erythematosus (SLE) [1, 3]. Also, in recent years, CQ and HCQ have gained special attention because of the nonexistence of effective and

efficient antiviral medications against new emerging viruses such as human immunodeficiency virus (HIV), dengue virus, chikungunya virus, and Ebola virus [4–6]. These compounds are readily available, cost effective, highly tolerated by the body, and elicit very critical immunomodulatory activities [4]. The structure and mechanism of action of CQ and HCQ are exactly the same except for an extra hydroxy moiety in one terminal in HCQ [7, 8].

After oral ingestion, CQ and HCQ are absolutely and rapidly absorbed into the blood stream [2]. The proteins in both compounds are bound in plasma and partly

metabolized through the cytochrome P450 (CYP) enzymes in the liver [2]. CQ undergoes hepatic modifications via the N-dealkylation pathway into two functional metabolites such as desethyl-CQ and bisdesethyl-CQ. In human liver microsomes, CYP2C8 and CYP3A4/5 are the key enzymes accountable for the CQ N-desethylation to desethyl-CQ [2, 9]. On the other hand, HCQ is metabolized into one main metabolite, N-desethyl-HCQ, by CYP enzymes CYP2D6, CYP2C8, CYP3A4, and CYP3A5 via the N-desethylation pathway. *In vivo* studies have demonstrated a correlation between blood N-desethyl-HCQ levels and effectiveness of HCQ [2, 10].

CQ and HCQ amass in tissues with elevated levels in the liver, brain, heart, muscle, and skin than the blood after prolonged usage [2, 11, 12]. Therefore, it was speculated that tissue levels may be more associated with their effectiveness than blood levels [2, 13]. Studies have demonstrated that the buildup of CQ and HCQ in lymphocytes as well as macrophages resulted in anti-inflammatory activities in diverse viral diseases depicted with the overproduction of tumor necrosis factor- $\alpha$  (TNF- $\alpha$ ) by the alveolar macrophages [14, 15]. Also, CQ precisely blocked TNF, interleukin- (IL-) 6, and prostaglandin (PG) E release without modulating the expression of IL-1 by normal macrophages [16].

CQ and HCQ are capable of modulating immune players like toll-like receptors (TLRs), T-cells, B-cells, interferons (IFNs), mitogen-activated protein kinase (MAPK), chemokines, and generation of reactive oxygen species (ROS) [17–22]. This review therefore explicitly explores the key immune and inflammatory players modulated by CQ and HCQ. Most of the articles reviewed were indexed in PubMed with strict inclusion criteria being *in vitro* and *in vivo* up- or downregulation of these immune and inflammatory biomarkers in different disease conditions.

## 2. Mechanism of Action and Dosage

CQ and HCQ easily penetrate the lipid bilayer due to their small lipophilic nature after oral or intramuscular administration [23, 24]. Inside the cell, these diprotic weak bases diffuse across a pH gradient into acidic subcellular compartments like endolysosomes where they become diprotonated at lower pH [23, 25]. The diprotonated CQ and HCQ accumulates inside endolysosomes up to 10,000-fold elevations as compared to their extracellular levels leading to curatively accessible intracellular levels in the millimolar range [23, 24, 26]. These drugs inhibited protein synthesis and processing, as well as degradation via mechanisms involving alkalization of endosomes and lysosomes [23]. Nevertheless, extra actions of the drugs seem to be independent of lysosomotropism [23, 27].

Also, these drugs are capable of interrelating with DNA resulting in the modification of its super helical structure, as well as inhibition of DNA synthesis at extreme concentrations [23, 27]. Furthermore, studies have shown that they are capable of inhibiting inositol 1,4,5-triphosphate signaling as well as protein phosphorylation [23, 28]. Qu et al. demonstrated that the total ROS and mitochondrial (mt) ROS levels in QBC939 cells were obviously augmented while mitochon-

drial membrane potentials were obviously diminished after CQ treatment [29]. CQ and CHQ are capable of neutralizing the cellular acidic compartments containing lysosomes as well as endosomes [30–32]. They have been implicated in the modification and the intracellular trafficking of newly synthesized proteins [30–32]. HCQ can regulate human inflammatory macrophage polarization through the downregulation of M1 contrary to the upregulation of M2 macrophages [33, 34].

CQ was capable of inhibiting the function of lysosomes, leading to a widespread blockage of autophagy [29]. It was established that oxidized proteins cannot be damaged by molecular chaperone-mediated autophagy in lysosomes, which are inhibited by CQ [29]. Thus, CQ is likely to have a robust blockade effect on the antioxidant capacity and cell-death-stimulatory properties [29, 35]. Studies have demonstrated that CQ triggered a bitter taste receptor (TAS2R) leading to an upsurge in intracellular  $\text{Ca}^{2+}$  via the  $\text{G}\beta\gamma$ -PLC $\beta$ -IP3-IP3R signaling pathway in the airway smooth muscle [36–38]. It was also established that the upsurge in  $\text{Ca}^{2+}$  was probably mediated in the CQ-triggered glucose transporter 4 (GLUT4) trafficking to the plasma membrane [36].

The plasma concentration of CQ peaked half an hour after administration while the plasma concentration of HCQ peaked within 3–4 hours after administration [39, 40]. A study revealed that the action of CQ and HCQ in the blockade of TNF- $\alpha$ , IL-1 $\beta$ , and IL-6 synthesis operated via diverse approaches and their therapeutic doses were capable of suppressing the production of TNF- $\alpha$ , IL-1 $\beta$ , and IL-6 in patients [30]. The intracellular concentrations of HCQ in mononuclear cells from patients on a 3-month course of standard dose of 400 mg daily was similar to that in mononuclear cells incubated *in vitro* with 100  $\mu\text{M}$  CQ or HCQ for 1 hour [26, 30]. CQ and HCQ have long terminal as well as elimination half-lives of 22 and 20–60 days, respectively [39, 40]. Nevertheless, the excretion HCQ in the urine persists up to 3 months from the time of the last dose [39].

CQ and HCQ are mostly in tablet formula for oral usage as CQ phosphate 500 mg which is equivalent to 300 mg CQ base and HCQ sulfate 200 mg which is equivalent to 155 mg HCQ base active drug per tablet, respectively [39]. It is advocated that, in autoimmune diseases like rheumatoid arthritis and systemic lupus erythematosus, the doses of CQ and HCQ should not exceed 500 mg/day and 400 mg/day, respectively [39]. Nevertheless, in acute malaria, doses as high as 2000 mg CQ and HCQ have been used [39, 40]. We are of the view that these drugs may target the protozoan cells with less affinity for normal body cells in malaria, thus reducing the adverse effects of the drugs due to high concentrations in the protozoan cells and lesser concentration in the normal body cells.

In viral as well as autoimmune diseases, the drugs may target only the normal body cells, thereby increasing adverse effects with doses exceeding 500 mg/day for CQ and 400 mg/day for HCQ. Complications like retinopathy and QTc prolongation with consequential possibility of ventricular arrhythmias have been associated with CQ and HCQ [39]. CQ has higher possibilities of retinopathy than HCQ though

short-term dosing of both medicines has no such complication [39, 41].

### 3. Toll-Like Receptor (TLR)

The key mechanism of action of HCQ is the blockade of nucleic acid-sensing toll-like receptors (TLRs) [17]. The inhibitory effect of nucleic acid-sensing TLRs occurs as a result of reduction in endosomal pH or direct binding of nucleic acid machineries to the TLRs [17–19]. In both *in vitro* and *in vivo* experimental prototypes, CQ inhibited proinflammatory cytokine secretion triggered by microbial TLR ligands via downregulating TLR-9 and TLR-4 mRNA secretion, inhibiting NF- $\kappa$ B as well as activated protein-1 (AP-1) stimulation, interfering with endosome maturation, and blockade of nucleic acid binding to TLR-7, TLR-8, and TLR-9 (Table 1) [42, 43]. Studies have shown that CQ was capable of triggering endosomal acidification and fusion, thus blocking the stimulation and facilitation of the virus via endocytic TLR-3, TLR-7, TLR-8, and TLR-9 (Table 1) in HIV patients [20, 21, 44]. Also, CQ was capable of inhibiting TLR-7 downregulatory signaling pathways resulting in the blockade of transcription factors like interferon regulatory factor- (IRF-) 7, which modulates the production of IFN- $\alpha$ , an effective CD8 T-cell immune stimulator [20–22].

Plasmacytoid dendritic cells (pDC), which identify pathogens via TLR-7 and TLR-9, are an essential component of the innate and adaptive immune systems [22]. TLRs are intracellular, and thus, their ligands involve cellular uptake as well as endosomal maturation to trigger NF- $\kappa$ B and MAPK-mediated signals via the MyD88-dependent pathway. These TLR signals result in pDC stimulation or maturation and in the generation of proinflammatory cytokines as well as huge quantities of IFNs- $\alpha/\beta$  [22]. Martinson et al. demonstrated that CQ blocked pDC stimulation or maturation, upregulation of the MyD88 pathway signaling molecules like IRF-7 and IL-1 receptor-associated kinase 4 (IRAK-4), IFN- $\alpha$  generation, indoleamine 2,3-dioxygenase (IDO) synthesis, and programmed death-ligand 1 (PDL-1) secretion. The precise association between these markers and CQ or HCQ in viral disease still needs further studies [22].

### 4. Interferons

IFNs have been implicated in several immune responses as triggers and modulators as well as effectors of both innate and adaptive immune systems during viral infections [45, 46]. IFNs have the capability of inhibiting viral replication and are often the most conspicuous cytokines produced during viral infections [45, 46]. Studies have shown that the concentrations of IFN and IFN-inducible chemokines/cytokines like macrophage inflammatory protein-1 (MIP-1) and monocyte chemotactic protein-1 (MCP-1) as well as interferon-inducible protein-10 (IP-10) are associated with disease burden [47–49]. These chemokines or cytokines are measured by the different disease activity indices, the erythrocyte sedimentation rate, and anti-dsDNA antibody titers [47–49].

Cytokine and TCR-triggered IFN- $\gamma$  secretion was via separate signal transduction pathways comprising of transcription factors such as nuclear factor of activated T-cells (NFATs), signal transducer and activator of transcriptions (STATs), and nuclear factor kappa-light-chain-enhancer of activated B-cells (NF- $\kappa$ B) [45]. This resulted in the stimulation as well as the triggering of several intrinsic antiviral factors like RNA-activated protein kinase (PKR), the 2-5A system, Mx proteins, and many apoptotic pathways [45]. Studies have shown that human IFN- $\alpha$  and IFN- $\gamma$  bound to receptors and entered cells via receptor-mediated endocytosis through coated pits as well as endosomes [50, 51]. Studies have indicated that IFN acted from outside the cell membrane to attain antiviral state [50, 52, 53]. Studies have further proven that the antiviral activity was triggered when IFNs bind to an insoluble matrix and the nonactivity of IFN microinjected directly into cells [50, 54, 55].

Type I IFN offers effective innate immune machinery against a verity of viruses, but it may also stimulate pathogenic immune response, thus leading to huge loss of stimulated CD4<sup>+</sup> T-cells. Branca et al. reported that CQ induced the production of the 2',5'-A synthetase [56]. Nevertheless, Chelbi-Alix and Thang found out that the presence of CQ during IFN treatment does not affect the triggering of the 2',5'-A synthetase but impairs the IFN-dependent inhibition of virus growth [50]. Studies have demonstrated that CQ and HCQ inhibited the production of IFN- $\alpha$  and IFN- $\gamma$  and/or TNF- $\alpha$  (Table 1) [50]. Studies using different cell populations have demonstrated that HCQ inhibited proinflammatory cytokines, like TNF- $\alpha$ , IFN- $\gamma$ , IL-1 $\alpha$ , and IL-6 (Table 1) [50, 57–59]. Also, HCQ inhibited the production of IFN- $\alpha$  (Table 1) in pDCs *in vitro*, either after stimulation by DNA-containing immune complexes or upon activation with TLR-9 agonists [60]. The explicit pathways via which CQ and HCQ trigger the release or inhibit the release of IFNs still need further studies since current evidence is paradoxical.

### 5. Interleukins

Several studies have persistently shown an inhibition of the production of cytokines such as IL-1, IL-2, IL-6, IL-17, and IL-22 (Table 1) by CQ and HCQ [30, 61]. In RA patients, IL-1 was primarily produced by monocytes and macrophages in the synovial tissue and was strongly implicated in joint destruction [30, 62]. Studies have demonstrated that a huge quantity of IL-1 $\beta$  perhaps in the form of pro-IL-1 $\beta$  was retained in cells and the concentration of cell-associated IL-1 $\beta$  was reduced by CQ (Table 1) [30, 63]. This study further revealed that the blockade of IL-1 $\beta$  production stimulated by weak-base amines occurred via the inhibition of pro-IL-1 $\beta$  rather than via reduced IL-1 $\beta$  mRNA [30]. Studies have demonstrated that CQ was capable of inhibiting the release of IL-1 $\beta$  via a pathway involving endolysosome-associated vesicles in lipopolysaccharide- (LPS-) stimulated monocytes [30, 64].

CQ was capable of inhibiting IL-2 generation and IL-2 mRNA stimulation as well as the alteration of IL-2 receptiveness of T-cell clones [65]. Studies have shown that IL-2 generation by  $\alpha$ CD3 MoAb-triggered T-cells was possibly

TABLE 1: Shows the explicit effect of CQ or HCQ on various immune/inflammatory factors.

Immune/inflammatory factors	Type	Effect of CQ/HCQ	Citation
Toll-like receptors (TLRs)	TLR-3	Inhibition	[20, 21, 44]
	TLR-7	Inhibition	[20, 21, 42–44]
	TLR-8	Inhibition	[20, 21, 42–44]
	TLR-9	Inhibition	[20, 21, 44]
Interferons (IFNs)	IFN- $\alpha$	Inhibition	[50, 57–59]
	IFN- $\beta$	Inconclusive	No data
	IFN- $\gamma$	Inhibition	[50, 57–59]
Interleukins	IL-1	Inhibition	[30, 61–63]
	IL-2	Inhibition	[30, 61, 65, 67, 68]
	IL-6	Inhibition	[16, 23, 30, 33, 58, 61, 70–72]
	IL-10	Facilitator	[1, 81]
	IL-17	Inhibition	[30, 57, 61]
	IL-22	Inhibition	[30, 57, 61]
T-cells	Th1	Stability	[1, 81]
	Th2	Stability	[1, 81]
	Th17	Inconclusive	No data
B-cells	CD4 <sup>+</sup>	Inconclusive	[20, 82–85]
	All B-cell subsets	Inhibition	[17, 93–95]
Prostaglandins (PGs)	PGs	Inhibition	[98, 99]
Tumor necrosis factor (TNF)	TNF- $\alpha$	Inhibition	[16, 23, 30, 58, 71, 72, 109]
Extracellular signal-regulated kinases (ERK)	1/2	Inhibition	[23, 30, 110, 116]
Chemokines	CXCL8	Facilitator	[1]
Reactive oxygen species (ROS)	—	Facilitator	[1, 29]
Glucose	—	Facilitator	[36, 131, 132, 134, 136, 137]

modulated in an autocrine fashion [65–67]. It was affirmed that  $\alpha$ CD3 MoAb triggers the generation of IL-2, and IL-2 stimulated T-cell proliferation via the interrelation of IL-2 with high affinity IL-2R [65]. Nevertheless, CQ did not affect secretory levels of the IL-2R p55 chain, but it is possible that it might influence some other component of the IL-2 receptor (IL-2R) complex [65, 68]. It was established that the interrelation between IL-2 and its receptor resulted in augmentation of IL-2 generation during CQ administration [65, 67]. Also, blockade of IL-2 generation as well as blockade of T-cell proliferation led to either rescindment of the triggering signal or blockade of IL-2 receptiveness [65]. Landewe et al. demonstrated that CQ partly blocks the internalization and completely inhibited the intracellular degradation of IL-2 (Table 1) [65].

IL-6 is a pleiotropic cytokine produced by macrophages and T-cells as well as synovial fibroblasts in inflammatory joint tissues [30, 69]. IL-6 facilitates synovitis by triggering antibody production due to its influence on B-cell maturation. It also triggered T-cells as well as stimulated the proliferation of synovial fibroblasts [30, 70]. CQ was capable of inhibiting IL-6 synthesis (Table 1) in LPS-stimulated mouse macrophages as well as human monocytes, though the mode of blockage was dissimilar in mouse and human cells [16, 30, 58, 71]. Studies with human peripheral blood mononuclear cells (PBMCs) demonstrated that CQ decreased LPS-induced secretion of IL-1 $\beta$  as well as IL-6 mRNA [23, 30, 72]. Yu et al. found that the role of HCQ in decreasing plasma IL-6 (Table 1) concentrations was highly coherent with the length of its administration, and once the medicine was

halted, plasma IL-6 concentrations reverted to the control concentrations [33]. They demonstrated that HCQ was capable of mimicking the influential properties of anti-IL-6 antibody by significantly decreasing the concentrations of IL-6 in the critically ill COVID-19 patients [33].

Jang et al. observed a decreased in IL-1 $\beta$  and IL-6 (Table 1) release after treatment of PBMCs and monocytes or macrophages with CQ [30]. CQ blocked IL-1 $\beta$  and IL-6 generation via reduction of their mRNA levels, resulting in reduction in mRNA stability rather than alteration of transcriptional activity [30]. They indicated further that CQ regulated some steps involved in the synthesis as well as metabolism of IL-1 $\beta$  and IL-6 mRNA [30]. These steps included transcription of IL-1 $\beta$  and IL-6 genes, the processing of prime transcripts in the nucleus, the transport of processed mRNA to the cytosol, and the degradation of mRNA [30]. In their nuclear run-on analysis, transcriptional behaviors of the IL-1 $\beta$  and IL-6 genes in LPS-stimulated monocytes or macrophages were not considerably transformed by CQ, signifying that CQ did not influence the synthesis of key transcripts of these cytokines [30].

Cruz da Silva et al. demonstrated a blockade of IL-17 and IL-22 (Table 1) supernatant levels by HCQ. They indicated that HCQ reduced helper T-cell (Th) 17 cytokine levels in the PBMCs from healthy individuals and SLE or RA patients [57]. It was established that IL-17 augmented the immune reaction by augmenting target organ inflammation as well as damage. Also, IL-17 enhances antibody production by B-cells, a significant immune player in SLE [73]. The exact mechanism via which HCQ decreased IL-6 and IL-17 as well as IL-22 concentrations is still a matter of debate. Nevertheless, one potential explanation is that the reduction occurred via decreasing Th17 cells through a reduction in antigen presentation [57].

## 6. T-Cells

Helper T-cells (Th) are phenotypically heterogeneous in nature [57, 74]. They are categorized based on the cytokines they generated via the innate immune system during the process of Th-cell differentiation. Th1, Th2, Th17, and regulatory T-cells (Treg) are 4 principal lineages described [57, 74]. In periphery, Treg cells are capable of triggering self-reactive lymphocytes via cell contact and expression of anti-inflammatory cytokines as well as alteration of proficient antigen presenting cells, such as DCs [75–78]. Studies have shown that adoptive transfer of Treg cells decreased inflammatory diseases, like human graft versus host disease, experimental arthritis, experimental autoimmune hepatitis, experimental diabetes, and experimental autoimmune encephalomyelitis [75]. Therefore, Treg cells are suitable for the decrease of chronic inflammation perceived in most autoimmune diseases [75].

The stimulation of T-cells occurred via the triggering of T-cell receptors [65]. It was well established that stimulated T-cells triggered IL-2 mRNA resulting in the production of IL-2 protein [65]. The expressed IL-2 in turn triggered T-cell proliferation via binding to IL-2R present on activated T-cells [65]. Landewe et al. indicated that the inhibition of

T-cell proliferation by CQ means that CQ stimulated the alteration of receptor-mediated endocytosis [65]. Studies have shown that HCQ is capable of inhibiting Treg cell-induced upregulation of CD69 [79, 80]. Nevertheless, HCQ failed to elicit inhibitory effect during evaluation of multiple proximal Treg cell-mediated signaling events such as Treg cell-induced protein tyrosine-kinase stimulation, inositol phosphate generation, and MAPK stimulation [79]. CQ affected the stability between Th1 and Th2 cytokine secretion by augmenting IL-10 production in PBMC [1, 81].

Several studies have demonstrated that HCQ in human immunodeficiency virus/acquired immunodeficiency syndrome (HIV/AIDS) patients stabilized CD4 T-cell counts or elevation (Table 1) when used in combination with hydroxyurea as well as didanosine [20, 82–85]. Piconi et al. demonstrated that 6-month HCQ therapy in combination with antiretroviral therapy (ART) was associated with reduced immune stimulation as well as augmented CD4<sup>+</sup> T-cell frequency [86]. Routy et al. demonstrated contrary findings compared to the Piconi et al. findings (Table 1) [20]. Routy et al. detected reduced secretion of the maturation marker CD83 on pDCs after CQ therapy, which they assumed possibly contributed to a reduction in DC-mediated inflammation [20].

A study revealed that both untreated and CQ-treated animals suffered a deep loss of CD4<sup>+</sup> T-cells during the acute phase of infection [87]. Nevertheless, the ability to regenerate peripheral CD4<sup>+</sup> T-cells was obviously enhanced initially and subsequently hindered by CQ therapy in the long term [87]. CQ therapy during chronic simian immune deficiency virus infection exhibited a decrease in immune stimulation as well as an enhanced recovery of CD4<sup>+</sup> T-cells, but this did not influence virus levels [87, 88]. The precise pathways via which CQ and HCQ influence CD4<sup>+</sup> T-cells still need further studies since current evidence is inconsistent.

## 7. B-Cells

Clusters of differentiation (CD) 19<sup>+</sup> B-cells are categorized into 3 functionally definite subsets: immunoglobulin (Ig) D<sup>+</sup>CD27<sup>-</sup> naïve B-cells, IgD<sup>+</sup>CD27<sup>+</sup> IgM memory B-cells, and IgD<sup>-</sup>CD27<sup>+</sup> class-switched memory B-cells [3, 17]. Class-switched memory B-cells proliferate in the peripheral blood as well as inflammatory tissues of patients with extremely vigorous RA or SLE and are linked to the worsening of these autoimmune diseases [17, 89–91]. There are 5 classes of immunoglobulins generated by antibody-producing cells during disease process. IgG is the most effective inflammation facilitator, due to its robust antigen-binding affinity and complement-activation as well as opsonic capability [17, 92]. Thus, IgGs produced by self-reactive B-cells are presumed to perform pathogenic autoantibody functions [17].

Studies have shown that HCQ inhibited extreme autoimmune responses as well as exerts therapeutic effects by blocking the ligation of TLRs with nucleic acids [17, 93–95]. It was established that nucleic acid-sensing TLRs are secreted by human B-cells [17, 93, 94]. These TLR ligations activated B-cells to regulate inflammatory responses via antibody and

cytokine production, as well as antigen presentation [17, 93–95]. Torigoe et al. showed that HCQ at clinical levels effectively blocked CpG-triggered class-switched memory B-cells from differentiating into plasmablasts as well as producing IgG [17]. Also, HCQ also inhibited cytokine generation from all the B-cell subsets (Table 1) [17]. IgM memory B-cells exhibited the utmost cytokine production [17].

Torigoe et al. found that TLR-9 secretion was predominantly elevated in resting B-cells and CpG activation more effectively triggered B-cells to proliferate as well as differentiate into plasmablasts compared to loxoribine activation [17]. They indicated that the extremely secreted TLR-9 could sensitively identify dsDNA-containing antigens and were extremely capable of facilitating the inflammatory responses of B-cells in infection prevention as well as autoimmune diseases [17]. Studies have demonstrated that CQ decreased the survival of CpG-activated B-cells and suppressed the secretion of coactivators as well as blocked the facilitatory effect of IL-10 production (Table 1) [17, 96, 97]. Cepika et al. also affirmed that IgM memory B-cells exhibited the utmost effective cytokine-generating capability as compared to class-switched memory B-cells and naïve B-cells and HCQ competently blocked all the three B-cell subsets from producing inflammatory cytokines (Table 1) [96].

## 8. Prostaglandins

Prostaglandins (PGs) are produced in numerous types of tissue injury as well as acute and chronic inflammation [98, 99]. The levels of exogenous PGs produced during inflammatory response often reproduced as well as augmented the cardinal signs of inflammation such as edema, erythema, and hyperalgesia [98, 99]. Floman demonstrated that CQ blocked the production of PGs (Table 1) in the intact cell by inhibiting substrate accessibility of arachidonic acid necessary for the production of PGs [98]. Floman further indicated that CQ may decrease arachidonic acid accessibility via the blockade of phospholipase A2 activity [98]. *In vitro* studies using a murine hemorrhagic shock model were inconclusive on the inhibitory effect of CQ on cytokines as well as PG synthesis and the lowering of Kupffer cell function like antigen presentation and I $\alpha$  secretion [16, 100]. Contrarily, CQ and HCQ inhibited IL-1, IL-2, IL-6, IL-17, and IL-22 as well as PGs (Table 1) [61, 98, 99].

## 9. Tumor Necrotizing Factor

Tumor necrosis factor (TNF) is a pleiotropic cytokine that partakes in crucial regulatory roles in immune and inflammatory responses via cell surface receptors [59, 101]. Studies have identified p55 and p75 as the 2 distinctive categories of TNF receptors (TNF-R) amongst members of the TNF-R superfamily [59, 102]. It was affirmed that the p55 TNF-R was secreted universally on the surface of almost all cell types, whereas the p75 TNF-R was secreted predominantly in hematopoietic cells as well as endothelial cells [59]. It was established that both TNF-R possess four common cysteine-rich extracellular domains via which they bind TNF with high affinity [59]. Also, the cytoplasmic regions

on both receptors are different and transmit distinctive but interrelating signals. These receptors have been implicated in the stimulation of nuclear factor beta (NF- $\kappa$ B) as well as TNF-mediated apoptosis [59, 101, 103].

Studies revealed that p55 TNF-R intermediated in TNF signals in lethal endotoxaemia as well as nonspecific immunity to infection, whereas p75 TNF-R inhibits TNF-mediated inflammatory responses during gene knockout [59, 104, 105]. It was well established that CQ triggered downregulation of cell surface p75 TNF-R in human peripheral blood monocytes incubated with phorbol 12-myristate 13-acetate and/or BB-3103 [59, 105]. Nevertheless, in resting monocytes, the blockade effect of CQ was not observed, probably because resting monocytes exhibited low levels of TNF-R secretion [59]. It was further affirmed that cell surface p75 TNF-R considerably increased when receptor shedding was inhibited by BB-3103 but was partially blocked by CQ [59]. CQ also reduced the surface secretion of TNF-R in inactivated cells in a similar degree as was seen in the protein expression blocker monensin and brefeldin A [59]. Thus, CQ inhibited soluble TNF-R generation by blocking the intracellular trafficking of these molecules to the cell surface, instead of inhibiting cleavage of TNF-R on the cell surface [59].

Studies have demonstrated that TNF- $\alpha$  was crucial for the development of both the innate as well as the adaptive immune response [23, 106]. It was affirmed that neutralization of TNF- $\alpha$  with mAbs or soluble TNF- $\alpha$  receptors resulted in enhanced clinical outcomes in certain infectious and autoimmune diseases [23, 107]. TNF- $\alpha$  was capable of modulating posttranslations at the transcriptional level. It was established that, after translation, the 26 kDa membrane-bound pro-TNF- $\alpha$  was cleaved at the cell surface by a matrix metalloproteinase, TNF- $\alpha$  converting enzyme (ADAM-17), freeing a soluble 17 kDa form of the cytokine [23, 108]. It was proven that secretion of the antigen-presenting process occurred in parallel with an augmented TNF secretion by Kupffer cells as well as obvious augmentation of circulating TNF levels 2 hours after hemorrhage [16].

Monocytes and macrophages are the main source of TNF- $\alpha$  during RA pathogenesis [23, 30, 107, 109]. CQ was capable of inhibiting TNF- $\alpha$  synthesis (Table 1) in LPS-activated mouse macrophages as well as human monocytes, though the blockade route was dissimilar in the mouse and human cells [16, 30, 58, 71]. CQ blocked TNF- $\alpha$  synthesis via inhibiting the conversion of cell-mediated TNF- $\alpha$  precursor to the soluble mature form, rather than blocking the stimulation of TNF- $\alpha$  mRNA or synthesis of TNF- $\alpha$  precursor (Table 1) [30, 109]. Studies with human PBMCs revealed that CQ decreased LPS-triggered secretion of TNF- $\alpha$ , as well as cell-related TNF- $\alpha$  [23, 30, 72]. Jang et al. demonstrated that CQ blocked TNF- $\alpha$  secretion (Table 1) but did not alter the level of TNF- $\alpha$  mRNA or the synthesis of TNF- $\alpha$  precursor [30]. They indicated that blockade of TNF- $\alpha$  synthesis by CQ occurred at a posttranslational step rather than a transcriptional step [30]. Also, the blockade effect of CQ on TNF- $\alpha$  synthesis occurred at a step in the processing of pro-TNF- $\alpha$  as well as the release of mature proteins [30].



## 10. Mitogen-Activated Protein Kinase

The extracellular signal-regulated kinases (ERK) 1/2 are meticulously necessitated for TNF transcription in some human and murine macrophage populations, whereas p38 and the c-Jun N-terminal kinase (JNK) are meticulously necessitated for posttranscriptional modulation of TNF synthesis [110–113]. It was well affirmed that ERK was stimulated via a serine-threonine kinase cascade activated by Raf phosphorylation of the ERK activating kinases like MAP/ERK kinases (MEK) 1/2 [110]. Furthermore, Raf stimulation was activated via recruitment of this protein to the membrane by the protooncogene Ras resulting in Raf phosphorylation [110, 114]. Nevertheless, the phosphorylation of Raf at Ser259 led to inactivation of this enzyme [110, 115]. Therefore, phosphorylation at different domains led to an up- or downregulation of this signaling pathway [110]. The Raf-MEK-ERK signaling was very essential in a wide range of macrophage inflammatory activities [110].

Weber et al. demonstrated that CQ precisely inhibited the stimulation of ERK-MAP kinase proteins (Table 1) which are obligatory for prime LPS-triggered TNF secretion in human mononuclear phagocytes and murine macrophage cell line AMJ2C-8 [23, 110, 116]. CQ was also capable of blocking LPS-triggered stimulation of extracellular signal-modulated ERK1/2 in human PBMCs (Table 1) [30]. Moreover, the secretion of the TNF- $\alpha$  promoter-driven reporter gene in human monocytic THP-1 cells revealed that CQ inhibited the transcription of the TNF- $\alpha$  gene via blockade of LPS-triggered stimulation of the ERK1/2 signaling pathway [30, 110]. Further *in vitro* and *in vivo* studies on this pathway and CQ are still warranted.

## 11. Chemokines

Chemokines are a group of molecules implicated in the trafficking of leukocytes in normal immune surveillance as well as recruitment of inflammatory cells in host defense [1, 117, 118]. They comprise over 40 members, which are categorized into four classes based on the locations of fundamental cysteine residues such as C, CC, CXC, and CX3C [1]. CQ was capable of stimulating the mRNA and protein levels of chemokines like CCL2 and CXCL8 in human astroglial cells [1]. The stimulation of these chemokine mRNAs was detected at 3 hours, optimum at 16 hours, and persisted up to 24 hours after CQ therapy [1]. It was speculated that the upsurge in mRNA secretory levels of these proinflammatory chemokines was as a result of either transcriptional stimulation or stabilization of mRNA by CQ [1].

It was affirmed that CQ therapy resulted in stimulation of CXCL8 promoter activities (Table 1), which means that transcriptional stimulation was partially accountable for mRNA secretion of chemokines [1]. It was established that CQ triggered stimulation of the NF- $\kappa$ B transcription factor, and blockade of NF- $\kappa$ B stimulation inhibited CQ-triggered chemokine secretion in astroglial cells [1]. This strongly indicates that stimulation of chemokines was mediated at the transcriptional level [1].

Studies have demonstrated that leukocytes and neutrophils as well as eosinophils secreted CXCL10 during inflammation [119, 120]. Also, monocytes, epithelia, endothelial, and stromal cells as well as keratinocytes are expressed in response to IFN- $\gamma$  during inflammation [119, 121, 122]. Th1 cells generated IFN- $\gamma$ , which stimulates the CXCL10 production by diverse cell types [119]. CXCL10 in turn attracted and recruited Th1 cells, signifying the occurrence of a positive feedback loop between IFN- $\gamma$ -producing Th1 cells and resident cells producing CXCL10 [119, 123]. Further studies on the effects of CQ or HCQ on the positive feedback loop between IFN- $\gamma$  producing Th1 cells and resident cells producing CXCL10 in viral diseases are warranted.

## 12. Reactive Oxygen Species

Cells produce reactive oxygen species (ROS) via metabolism and respiratory burst, as well as the respiratory chain [29]. Cells clear ROS through peroxisomes, superoxide dismutase, and the nicotinamide adenine dinucleotide phosphate-(NADPH-) dependent reduction system, as well as the autophagy-lysosome pathway resulting in the regulation of reduction-oxidation (REDOX) balance in cells [29, 124]. Several extracellular stimuli have been implicated in the stimulation of the transient upsurge in intracellular ROS levels [1, 125]. Also, inhibition of intracellular ROS led to a substantial blockade of stimulant-dependent signaling in mammalian cells [1, 125]. In the REDOX balance adjustment process, the principal source of mitochondrial (mt) ROS was oxidative respiration. Studies have demonstrated that disruption of mitochondrial functions was capable of augmenting mtROS generation as well as triggering cell death [29, 124, 126].

Park et al. demonstrated that ROS generated by CQ facilitated the stimulation of NF- $\kappa$ B following the secretion of chemokines in human astroglial cells (Table 1) [1]. Nevertheless, they observed that CQ did not trigger an upsurge of intracellular ROS in human monocytic U937 cells and murine microglial BV-2 as well as macrophage RAW 264.7 cells. They indicated that disparities in the immunomodulatory effect of CQ between monocytes, microglia, and astroglial cells seem to be determined at the level of ROS production following the stimulation of NF- $\kappa$ B [1]. It was affirmed that CQ-triggered production of ROS was annulled by diphenyl iodonium, signifying the probability that non-phagocytic NADPH oxidase partook in the production of ROS during CQ therapy [1]. Qu et al. demonstrated that the overall ROS and mtROS levels in QBC939 cells were augmented severely after CQ administration (Table 1) while mitochondrial membrane potentials were severely reduced [29]. They concluded that CQ was capable of triggering an upsurge in ROS level (Table 1), specifically mtROS, in QBC939 cells which resulted in the loss of mitochondrial membrane potentials [29].

## 13. Glucose Metabolism

Glucose uptake is primarily reliant on GLUT4 which translocates extracellular glucose via the cell membrane into the cell

[36, 127]. Therefore, GLUT4 is very critical for sustenance whole-body glucose homeostasis [36, 127]. It was well established that GLUT4 was predominantly located in intracellular GLUT4-storage vesicles (GLUT4-SVs) [127]. Studies have shown that insulin triggered fast translocation of GLUT4SVs from the trans-Golgi network and/or endosomes to the plasma membrane [36, 128]. The fusion of GLUT4-SVs with the plasma membrane led to augmented glucose uptake [128]. Further studies have demonstrated that this step was upregulated via insulin receptor or insulin receptor substrate-1 (IRS-1), protein kinase B (PKB/Akt), phosphatidylinositol 3 kinase (PI3-K), and atypical protein kinase C (aPKC) as well as cytosolic  $Ca^{2+}$  [129, 130].

Studies revealed that CQ facilitated cellular glucose uptake via the stimulation of GLUT4 trafficking to, and fusion with (Table 1), the cellular plasma membrane via augmentation of cellular  $Ca^{2+}$  uptake [36, 131, 132]. Another study demonstrated that CQ was an effective stimulator of the insulin-responsive protein like PKB/Akt and considerably augmented glycogen synthesis via the phosphorylation of glycogen synthase kinase 3 $\beta$  (GSK-3 $\beta$ ), which made it an attractive potential antidiabetic drug [36, 133]. It was further established that the antidiabetic mechanism of CQ analogues involved reductions in insulin clearance as well as degradation rates and an upsurge in the expression of C-peptide [134, 135].

CQ and HCQ are well-tolerated therapeutic options for type II diabetic mellitus [134]. Glycated hemoglobin reduced considerably when HCQ was combined with insulin for the treatment of diabetes mellitus, compared with patients receiving placebo, and the insulin dose had to be lowered by 30% in the HCQ group [134, 136]. We anticipate that, in critically ill patients, CQ and HCQ are likely to deplete all the energy stores of the body leaving the patient very weak and sicker. A study revealed that a rare, but serious, side effect of CQ or HCQ in nondiabetic patients is hypoglycaemia (Table 1) [132, 137]. Thus, during clinical usage of CQ or HCQ in critically ill patients, it is very essential to strengthen the CQ or HCQ with glucose infusion.

## 14. Conclusion

CQ and HCQ are able to inhibit the production of cytokines such as IL-1, IL-2, IL-6, IL-17, and IL-22. Also, CQ blocked TNF- $\alpha$  synthesis via inhibiting the conversion of cell-mediated TNF- $\alpha$  precursor to the soluble mature form, rather than blocking the stimulation of TNF- $\alpha$  mRNA or synthesis of TNF- $\alpha$  precursor. Furthermore, CQ was also capable of inhibiting IL-2 generation and IL-2 mRNA stimulation as well as the alteration of IL-2 receptiveness of T-cell clones. Similarly, HCQ also inhibits cytokine generation from all the B-cell subsets. IgM memory B-cells exhibit the utmost cytokine production. Nevertheless, CQ is capable of producing ROS via a facilitated stimulation of NF- $\kappa$ B and following secretion of chemokines in human astroglial cells. A rare, but serious, side effect of CQ or HCQ in nondiabetic patients is hypoglycaemia. We advocate that, in critically ill patients, CQ and HCQ are more likely to deplete all the energy stores of body leaving the patient very weak and

sicker. Thus, during clinical usage of CQ or HCQ in critically ill patients, it is very essential to strengthen the CQ or HCQ with glucose infusion. CQ and HCQ are thus potential inhibitors of the COVID-19 cytokine storm.

## Abbreviations

AP-1:	Activated protein-1
aPKC:	Atypical protein kinase C
CD:	Cluster of differentiation
CQ:	Chloroquine
CYP:	Cytochrome P450
ERK1/2:	Extracellular signal-regulated kinases
GLUT4:	Glucose transporter 4
GLUT4SVs:	GLUT4 storage vesicles
HIV:	Human immunodeficiency virus
HCQ:	Hydroxychloroquine
IL:	Interleukin
IL-2R:	IL-2 receptor
IRF:	Interferon regulatory factor
IFN:	Interferon
IRS-1:	Insulin receptor substrate-1
JNK:	c-Jun N-terminal kinase
MAPK:	Mitogen-activated protein kinase
mt:	Mitochondrial
NFATs:	Nuclear factor of activated T-cells
NF- $\kappa$ B:	Nuclear factor kappa-light-chain-enhancer of activated B-cells
NADPH:	Nicotinamide adenine dinucleotide phosphate
PI3-K:	Phosphatidylinositol 3 kinase
pDC:	Plasmacytoid dendritic cells
PGs:	Prostaglandins
PKR:	Protein kinase
PBMCs:	Peripheral blood mononuclear cells
ROS:	Reactive oxygen species
RA:	Rheumatoid arthritis
REDOX:	Reduction-oxidation
Treg:	Regulatory T-cells
SLE:	Systemic lupus erythematosus
STATs:	Signal transducer and activator of transcriptions
Th:	T-helper cell
TNF:	Tumor necrotizing factor
TLRs:	Toll-like receptors.

## Conflicts of Interest

The authors declare that they have no conflicts of interest.

## Authors' Contributions

All authors contributed toward the literature search, drafting, and critical revision of the paper and agree to be accountable for all aspects of the work.

## References

- [1] J. Park, K. Choi, E. Jeong, D. Kwon, E. N. Benveniste, and C. Choi, "Reactive oxygen species mediate chloroquine-

- induced expression of chemokines by human astroglial cells," *Glia*, vol. 47, no. 1, pp. 9–20, 2004.
- [2] D. Plantone and T. Koudriavtseva, "Current and future use of chloroquine and hydroxychloroquine in infectious, immune, neoplastic, and neurological diseases: a mini-review," *Clinical Drug Investigation*, vol. 38, no. 8, pp. 653–671, 2018.
  - [3] C. Vasquez, M. A. Franco, and J. Angel, "Rapid proliferation and differentiation of a subset of circulating IgM memory B cells to a CpG/cytokine stimulus in vitro," *PLOS ONE*, vol. 10, no. 10, article e0139718, 2015.
  - [4] S. D'Alessandro, D. Scaccabarozzi, L. Signorini et al., "The use of antimalarial drugs against viral infection," *Microorganisms*, vol. 8, no. 1, p. 85, 2020.
  - [5] F. Touret and X. de Lamballerie, "Of chloroquine and COVID-19," *Antiviral Research*, vol. 177, article 104762, 2020.
  - [6] A. M. Hashem, B. S. Alghamdi, A. A. Algaissi et al., "Therapeutic use of chloroquine and hydroxychloroquine in COVID-19 and other viral infections: a narrative review," *Travel Medicine and Infectious Disease*, vol. 35, article 101735, 2020.
  - [7] A. K. Singh, A. Singh, A. Shaikh, R. Singh, and A. Misra, "Chloroquine and hydroxychloroquine in the treatment of COVID-19 with or without diabetes: a systematic search and a narrative review with a special reference to India and other developing countries," *Diabetes & Metabolic Syndrome: Clinical Research & Reviews*, vol. 14, no. 3, pp. 241–246, 2020.
  - [8] D. J. Browning, "Pharmacology of chloroquine and hydroxychloroquine," in *Hydroxychloroquine and Chloroquine Retinopathy*, pp. 35–63, Springer, New York, NY, 2014.
  - [9] K.-A. Kim, J.-Y. Park, J.-S. Lee, and S. Lim, "Cytochrome P450 2C8 and CYP3A4/5 are involved in chloroquine metabolism in human liver microsomes," *Archives of Pharmacal Research*, vol. 26, no. 8, pp. 631–637, 2003.
  - [10] T. Munster, J. P. Gibbs, D. Shen et al., "Hydroxychloroquine concentration–response relationships in patients with rheumatoid arthritis," *Arthritis & Rheumatism*, vol. 46, no. 6, pp. 1460–1469, 2002.
  - [11] A. H. Mackenzie, "Dose refinements in long-term therapy of rheumatoid arthritis with antimalarials," *The American Journal of Medicine*, vol. 75, no. 1, pp. 40–45, 1983.
  - [12] E. W. McChesney, "Animal toxicity and pharmacokinetics of hydroxychloroquine sulfate," *The American Journal of Medicine*, vol. 75, no. 1, pp. 11–18, 1983.
  - [13] L. Durcan, W. A. Clarke, L. S. Magder, and M. Petri, "Hydroxychloroquine blood levels in systemic lupus erythematosus: clarifying dosing controversies and improving adherence," *The Journal of Rheumatology*, vol. 42, no. 11, pp. 2092–2097, 2015.
  - [14] A. Savarino, J. R. Boelaert, A. Cassone, G. Majori, and R. Cauda, "Effects of chloroquine on viral infections: an old drug against today's diseases," *The Lancet Infectious Diseases*, vol. 3, no. 11, pp. 722–727, 2003.
  - [15] R. Baughman, E. E. Lower, and R. M. du Bois, "Sarcoidosis," *Lancet*, vol. 361, no. 9363, pp. 1111–1118, 2003.
  - [16] W. Ertel, M. H. Morrison, A. Ayala, and I. Chaudry, "Chloroquine attenuates hemorrhagic shock-induced suppression of Kupffer cell antigen presentation and major histocompatibility complex class II antigen expression through blockade of tumor necrosis factor and prostaglandin release," *Blood*, vol. 78, no. 7, pp. 1781–1788, 1991.
  - [17] M. Torigoe, K. Sakata, A. Ishii, S. Iwata, S. Nakayamada, and Y. Tanaka, "Hydroxychloroquine efficiently suppresses inflammatory responses of human class-switched memory B cells via toll-like receptor 9 inhibition," *Clinical Immunology*, vol. 195, pp. 1–7, 2018.
  - [18] A. Kužnik, M. Benčina, U. Švajger, M. Jeras, B. Rozman, and R. Jerala, "Mechanism of endosomal TLR inhibition by anti-malarial drugs and imidazoquinolines," *The Journal of Immunology*, vol. 186, no. 8, pp. 4794–4804, 2011.
  - [19] R. I. Fox, "Mechanism of action of hydroxychloroquine as an antirheumatic drug," *Seminars in Arthritis and Rheumatism*, vol. 23, no. 2, pp. 82–91, 1993.
  - [20] J. P. Routy, J. Angel, M. Patel et al., "Assessment of chloroquine as a modulator of immune activation to improve CD4 recovery in immune nonresponding HIV-infected patients receiving antiretroviral therapy," *HIV Medicine*, vol. 16, no. 1, pp. 48–56, 2015.
  - [21] M. Ries, K. Pritschet, and B. Schmidt, "Blocking type I interferon production: a new therapeutic option to reduce the HIV-1-induced immune activation," *Clinical and Developmental Immunology*, vol. 2012, Article ID 534929, 9 pages, 2012.
  - [22] J. A. Martinson, C. J. Montoya, X. Usuga, R. Ronquillo, A. L. Landay, and S. N. Desai, "Chloroquine modulates HIV-1-induced plasmacytoid dendritic cell alpha interferon: implication for T-cell activation," *Antimicrobial Agents and Chemotherapy*, vol. 54, no. 2, pp. 871–881, 2010.
  - [23] S. M. Weber and S. M. Levitz, "Chloroquine interferes with lipopolysaccharide-induced TNF- $\alpha$  gene expression by a nonlysosomal mechanism," *The Journal of Immunology*, vol. 165, no. 3, pp. 1534–1540, 2000.
  - [24] P. M. O'Neill, P. G. Bray, S. R. Hawley, S. A. Ward, and B. K. Park, "4-Aminoquinolines—Past, present, and future; A chemical perspective," *Pharmacology & Therapeutics*, vol. 77, no. 1, pp. 29–58, 1998.
  - [25] H. H. van Es, H. Renkema, H. Aerts, and E. Schurr, "Enhanced lysosomal acidification leads to increased chloroquine accumulation in CHO cells expressing the pfmdr1 gene," *Molecular and Biochemical Parasitology*, vol. 68, no. 2, pp. 209–219, 1994.
  - [26] J. French, N. Hurst, M. O'Donnell, and W. Betts, "Uptake of chloroquine and hydroxychloroquine by human blood leucocytes in vitro: relation to cellular concentrations during anti-rheumatic therapy," *Annals of the Rheumatic Diseases*, vol. 46, no. 1, pp. 42–45, 1987.
  - [27] H. Bröll, "Effect of chloroquine diphosphate on the superhelix structure of DNA and protein synthesis in synovial cells in chronic polyarthritis," *Wiener Klinische Wochenschrift*, vol. 95, no. 24, pp. 877–880, 1983.
  - [28] H. Kalisz, G. Pohlig, and H. Holzer, "Inhibition of protein phosphorylation by chloroquine," *Archives of Microbiology*, vol. 147, no. 3, pp. 235–239, 1987.
  - [29] X. Qu, J. Sheng, L. Shen et al., "Autophagy inhibitor chloroquine increases sensitivity to cisplatin in QBC939 cholangiocarcinoma cells by mitochondrial ROS," *PLOS ONE*, vol. 12, no. 3, article e0173712, 2017.
  - [30] C.-H. Jang, J.-H. Choi, M.-S. Byun, and D.-M. Jue, "Chloroquine inhibits production of TNF- $\alpha$ , IL-1 $\beta$  and IL-6 from lipopolysaccharide-stimulated human monocytes/macrophages by different modes," *Rheumatology*, vol. 45, no. 6, pp. 703–710, 2006.

- [31] F. R. Maxfield, "Weak bases and ionophores rapidly and reversibly raise the pH of endocytic vesicles in cultured mouse fibroblasts," *The Journal of Cell Biology*, vol. 95, no. 2, pp. 676–681, 1982.
- [32] P. O. Seglen, "[59] Inhibitors of lysosomal function," in *Methods in enzymology*, vol. 96, pp. 737–764, 1983.
- [33] B. Yu, C. Li, P. Chen et al., "Low dose of hydroxychloroquine reduces fatality of critically ill patients with COVID-19," *Science China Life Sciences*, vol. 1, 2020.
- [34] H. Shiratori, C. Feinweber, S. Luckhardt et al., "An in vitro test system for compounds that modulate human inflammatory macrophage polarization," *European Journal of Pharmacology*, vol. 833, pp. 328–338, 2018.
- [35] R. Kiffin, C. Christian, E. Knecht, and A. M. Cuervo, "Activation of chaperone-mediated autophagy during oxidative stress," *Molecular Biology of the Cell*, vol. 15, no. 11, pp. 4829–4840, 2004.
- [36] Q. Zhou, X. Yang, M. Xiong et al., "Chloroquine increases glucose uptake via enhancing GLUT4 translocation and fusion with the plasma membrane in L6 cells," *Cellular Physiology and Biochemistry*, vol. 38, no. 5, pp. 2030–2040, 2016.
- [37] C.-H. Zhang, L. M. Lifshitz, K. F. Uy, M. Ikebe, K. E. Fogarty, and R. ZhuGe, "Correction: The cellular and molecular basis of bitter tastant-induced bronchodilation," *PLOS Biology*, vol. 11, no. 3, 2013.
- [38] D. A. Deshpande, W. C. Wang, E. L. McIlmoyle et al., "Bitter taste receptors on airway smooth muscle bronchodilate by localized calcium signaling and reverse obstruction," *Nature Medicine*, vol. 16, no. 11, pp. 1299–1304, 2010.
- [39] K. A. Pastick, E. C. Okafor, F. Wang et al., "Review: Hydroxychloroquine and chloroquine for treatment of SARS-CoV-2 (COVID-19)," *Open Forum Infectious Diseases*, vol. 7, no. 4, 2020.
- [40] J. Ducharme and R. Farinotti, "Clinical pharmacokinetics and metabolism of chloroquine," *Clinical Pharmacokinetics*, vol. 31, no. 4, pp. 257–274, 1996.
- [41] M. F. Marmor, U. Kellner, T. Y. Lai, R. B. Melles, W. F. Mieler, and American Academy of Ophthalmology, "Recommendations on screening for chloroquine and hydroxychloroquine retinopathy (2016 revision)," *Ophthalmology*, vol. 123, no. 6, pp. 1386–1394, 2016.
- [42] J. M. Jacobson, S. E. Bosinger, M. Kang et al., "The effect of chloroquine on immune activation and interferon signatures associated with HIV-1," *AIDS Research and Human Retroviruses*, vol. 32, no. 7, pp. 636–647, 2016.
- [43] M. Rutz, J. Metzger, T. Gellert et al., "Toll-like receptor 9 binds single-stranded CpG-DNA in a sequence- and pH-dependent manner," *European Journal of Immunology*, vol. 34, no. 9, pp. 2541–2550, 2004.
- [44] H. Yasuda, A. Leelahavanichkul, S. Tsunoda et al., "Chloroquine and inhibition of toll-like receptor 9 protect from sepsis-induced acute kidney injury," *American Journal of Physiology-Renal Physiology*, vol. 294, no. 5, pp. F1050–F1058, 2008.
- [45] L. Malmgaard, "Induction and regulation of IFNs during viral infections," *Journal of Interferon & Cytokine Research*, vol. 24, no. 8, pp. 439–454, 2004.
- [46] G. C. Sen, "Viruses and interferons," *Annual Review of Microbiology*, vol. 55, no. 1, pp. 255–281, 2001.
- [47] R. Willis, A. M. Seif, G. McGwin et al., "Effect of hydroxychloroquine treatment on pro-inflammatory cytokines and disease activity in SLE patients: data from LUMINA (LXXV), a multiethnic US cohort," *Lupus*, vol. 21, no. 8, pp. 830–835, 2012.
- [48] J. W. Bauer, E. C. Baechler, M. Petri et al., "Elevated serum levels of interferon-regulated chemokines are biomarkers for active human systemic lupus erythematosus," *PLOS Medicine*, vol. 3, no. 12, article e491, 2006.
- [49] J. W. Bauer, M. Petri, F. M. Batliwalla et al., "Interferon-regulated chemokines as biomarkers of systemic lupus erythematosus disease activity: a validation study," *Arthritis & Rheumatism*, vol. 60, no. 10, pp. 3098–3107, 2009.
- [50] M. Chelbi-Alix and M. N. Thang, "Chloroquine impairs the interferon-induced antiviral state without affecting the 2',5'-oligoadenylate synthetase," *Journal of Biological Chemistry*, vol. 260, no. 13, pp. 7960–7964, 1985.
- [51] K. C. Zoon, H. Arnheiter, D. Z. Nedden, D. J. Fitzgerald, and M. C. Willingham, "Human interferon alpha enters cells by receptor-mediated endocytosis," *Virology*, vol. 130, no. 1, pp. 195–203, 1983.
- [52] H. Ankel, C. Chany, B. Galliot, M. Chevalier, and M. Robert, "Antiviral Effect of Interferon Covalently Bound to Sepharose," *Proceedings of the National Academy of Sciences*, vol. 70, no. 8, pp. 2360–2363, 1973.
- [53] C. Chany and I. Cerutti, "Enhancement of antiviral protection against encephalomyocarditis virus by a combination of isoprinosine and interferon," *Archives of Virology*, vol. 55, no. 3, pp. 225–231, 1977.
- [54] Y. Higashi and Y. Sokawa, "Microinjection of Interferon and 2',5'-Oligoadenylate into Mouse L Cells and Their Effects on Virus Growth," *The Journal of Biochemistry*, vol. 91, no. 6, pp. 2021–2028, 1982.
- [55] G. Huez, M. Silhol, and B. Lebleu, "Microinjected interferon does not promote an antiviral response in Hela cells," *Biochemical and Biophysical Research Communications*, vol. 110, no. 1, pp. 155–160, 1983.
- [56] A. Branca, C. R. Faltynek, S. B. D'Alessandro, and C. Baglioni, "Interaction of interferon with cellular receptors. Internalization and degradation of cell-bound interferon," *Journal of biological chemistry*, vol. 257, no. 22, pp. 13291–13296, 1982.
- [57] J. C. Silva, H. A. Mariz, L. F. Rocha Jr et al., "Hydroxychloroquine decreases Th17-related cytokines in systemic lupus erythematosus and rheumatoid arthritis patients," *Clinics*, vol. 68, no. 6, pp. 766–771, 2013.
- [58] B. Dijkmans and C. Verweij, "Chloroquine and hydroxychloroquine equally affect tumor necrosis factor-alpha, interleukin 6, and interferon-gamma production by peripheral blood mononuclear cells," *The Journal of rheumatology*, vol. 24, no. 1, pp. 55–60, 1997.
- [59] J. Y. Jeong, J. W. Choi, K. I. Jeon, and D. M. Jue, "Chloroquine decreases cell-surface expression of tumour necrosis factor receptors in human histiocytic U-937 cells," *Immunology*, vol. 105, no. 1, pp. 83–91, 2002.
- [60] K. Sacre, L. A. Criswell, and J. M. McCune, "Hydroxychloroquine is associated with impaired interferon-alpha and tumor necrosis factor-alpha production by plasmacytoid dendritic cells in systemic lupus erythematosus," *Arthritis Research & Therapy*, vol. 14, no. 3, 2012.
- [61] N. Costedoat-Chalumeau, B. Dunogué, N. Morel, V. Le Guern, and G. Guettrot-Imbert, "Hydroxychloroquine: a multifaceted treatment in lupus," *La Presse Médicale*, vol. 43, no. 6, pp. e167–e180, 2014.

- [62] W. P. Arend and J. M. Dayer, "Inhibition of the production and effects of interleukins-1 and tumor necrosis factor  $\alpha$  in rheumatoid arthritis," *Arthritis & Rheumatism*, vol. 38, no. 2, pp. 151–160, 1995.
- [63] K. Matsushima, M. Taguchi, E. Kovacs, H. Young, and J. Oppenheim, "Intracellular localization of human monocyte associated interleukin 1 (IL 1) activity and release of biologically active IL 1 from monocytes by trypsin and plasmin," *The Journal of Immunology*, vol. 136, no. 8, pp. 2883–2891, 1986.
- [64] C. Andrei, C. Dazzi, L. Lotti, M. R. Torrisi, G. Chimini, and A. Rubartelli, "The secretory route of the leaderless protein interleukin 1 $\beta$  involves exocytosis of endolysosome-related vesicles," *Molecular Biology of the Cell*, vol. 10, no. 5, pp. 1463–1475, 1999.
- [65] R. B. M. Landewe, A. M. M. Miltenburg, M. J. A. Verdonk et al., "Chloroquine inhibits T cell proliferation by interfering with IL-2 production and responsiveness," *Clinical & Experimental Immunology*, vol. 102, no. 1, pp. 144–151, 1995.
- [66] S. C. Meuer, R. E. Hussey, D. A. Cantrell et al., "Triggering of the T3-Ti antigen-receptor complex results in clonal T-cell proliferation through an interleukin 2-dependent autocrine pathway," *Proceedings of the National Academy of Sciences*, vol. 81, no. 5, pp. 1509–1513, 1984.
- [67] D. Cantrell, M. Collins, and M. Crumpton, "Autocrine regulation of T-lymphocyte proliferation: differential induction of IL-2 and IL-2 receptor," *Immunology*, vol. 65, no. 3, pp. 343–349, 1988.
- [68] S. D. Voss, T. P. Leary, P. M. Sondel, and R. J. Robb, "Identification of a direct interaction between interleukin 2 and the p64 interleukin 2 receptor gamma chain," *Proceedings of the National Academy of Sciences*, vol. 90, no. 6, pp. 2428–2432, 1993.
- [69] M. Field, C. Chu, M. Feldmann, and R. Maini, "Interleukin-6 localisation in the synovial membrane in rheumatoid arthritis," *Rheumatology International*, vol. 11, no. 2, pp. 45–50, 1991.
- [70] S. Akira, T. Taga, and T. Kishimoto, "Interleukin-6 in biology and medicine," in *Advances in immunology*, vol. 54, pp. 1–78, 1993.
- [71] S. Picot, F. Peyron, A. Donadille, J. Vuillez, G. Barbe, and P. Ambroise-Thomas, "Chloroquine-induced inhibition of the production of TNF, but not of IL-6, is affected by disruption of iron metabolism," *Immunology*, vol. 80, no. 1, pp. 127–133, 1993.
- [72] I. Karres, J.-P. Kremer, I. Dietl, U. Steckholzer, M. Jochum, and W. Ertel, "Chloroquine inhibits proinflammatory cytokine release into human whole blood," *American Journal of Physiology-Regulatory, Integrative and Comparative Physiology*, vol. 274, no. 4, pp. R1058–R1064, 1998.
- [73] J. C. Crispin and G. C. Tsokos, "Interleukin-17-producing T cells in lupus," *Current Opinion in Rheumatology*, vol. 22, no. 5, pp. 499–503, 2010.
- [74] M. S. Maddur, P. Miossec, S. V. Kaveri, and J. Bayry, "Th17 cells: biology, pathogenesis of autoimmune and inflammatory diseases, and therapeutic strategies," *The American Journal of Pathology*, vol. 181, no. 1, pp. 8–18, 2012.
- [75] R. Thomé, A. S. Moraes, A. L. Bombeiro et al., "Chloroquine treatment enhances regulatory T cells and reduces the severity of experimental autoimmune encephalomyelitis," *PLOS ONE*, vol. 8, no. 6, article e65913, 2013.
- [76] S. Sakaguchi, "Naturally arising CD4+ regulatory T cells for immunologic self-tolerance and negative control of immune responses," *Annual Review of Immunology*, vol. 22, no. 1, pp. 531–562, 2004.
- [77] S. Sakaguchi, T. Yamaguchi, T. Nomura, and M. Ono, "Regulatory T cells and immune tolerance," *Cell*, vol. 133, no. 5, pp. 775–787, 2008.
- [78] T. Takahashi and S. Sakaguchi, "Naturally arising CD25+ CD4+ regulatory T cells in maintaining immunologic self-tolerance and preventing autoimmune disease," *Current Molecular Medicine*, vol. 3, no. 8, pp. 693–706, 2003.
- [79] F. D. Goldman, A. L. Gilman, C. Hollenback, R. M. Kato, B. A. Premack, and D. J. Rawlings, "Hydroxychloroquine inhibits calcium signals in T cells: a new mechanism to explain its immunomodulatory properties," *Blood*, vol. 95, no. 11, pp. 3460–3466, 2000.
- [80] A. Gilman, F. Beams, M. Tefft, and A. Mazumder, "The effect of hydroxychloroquine on alloreactivity and its potential use for graft-versus-host disease," *Bone Marrow Transplantation*, vol. 17, no. 6, pp. 1069–1075, 1996.
- [81] E. Hugosson, A. Björkman, and M. Troye-Blomberg, "Chloroquine enhances the number of IL-10 producing cells and the expression of B7-2 and ICAM-1 in in vitro-cultured PBMC," *Scandinavian Journal of Immunology*, vol. 55, no. 4, pp. 399–408, 2002.
- [82] N. I. Paton, R. L. Goodall, D. T. Dunn et al., "Effects of hydroxychloroquine on immune activation and disease progression among HIV-infected patients not receiving antiretroviral therapy: a randomized controlled trial," *Journal of the American Medical Association*, vol. 308, no. 4, pp. 353–361, 2012.
- [83] N. Paton and J. Aboulhab, "Hydroxychloroquine, hydroxyurea and didanosine as initial therapy for HIV-infected patients with low viral load: safety, efficacy and resistance profile after 144 weeks," *HIV Medicine*, vol. 6, no. 1, pp. 13–20, 2005.
- [84] K. Sperber, G. Chiang, H. Chen et al., "Comparison of hydroxychloroquine with zidovudine in asymptomatic patients infected with human immunodeficiency virus type 1," *Clinical Therapeutics*, vol. 19, no. 5, pp. 913–923, 1997.
- [85] K. Sperber, M. Louie, T. Kraus et al., "Hydroxychloroquine treatment of patients with human immunodeficiency virus type 1," *Clinical Therapeutics*, vol. 17, no. 4, pp. 622–636, 1995.
- [86] S. Piconi, S. Parisotto, G. Rizzardini et al., "Hydroxychloroquine drastically reduces immune activation in HIV-infected, antiretroviral therapy-treated immunologic nonresponders," *Blood*, vol. 118, no. 12, pp. 3263–3272, 2011.
- [87] M. Vaccari, C. Fenizia, Z.-M. Ma et al., "Transient increase of interferon-stimulated genes and no clinical benefit by chloroquine treatment during acute simian immunodeficiency virus infection of macaques," *AIDS Research and Human Retroviruses*, vol. 30, no. 4, pp. 355–362, 2014.
- [88] M. Ma, L. Wang, J. Yang et al., "Age-related impaired Th1 responses to PRV vaccine in vivo in aged pigs," *Molecular Immunology*, vol. 52, no. 3-4, pp. 217–223, 2012.
- [89] S. Iwata, K. Saito, M. Tokunaga et al., "Phenotypic changes of lymphocytes in patients with systemic lupus erythematosus who are in longterm remission after B cell depletion therapy with rituximab," *The Journal of Rheumatology*, vol. 38, no. 4, pp. 633–641, 2011.
- [90] B. Moller, D. Aeberli, S. Egli et al., "Class-switched B cells display response to therapeutic B-cell depletion in

- rheumatoid arthritis," *Arthritis Research & Therapy*, vol. 11, no. 3, 2009.
- [91] M. Torigoe, S. Iwata, S. Nakayamada et al., "Metabolic reprogramming commits differentiation of human CD27+ IgD+ B cells to plasmablasts or CD27- IgD- cells," *The Journal of Immunology*, vol. 199, no. 2, pp. 425-434, 2017.
- [92] H. W. Schroeder Jr. and L. Cavacini, "Structure and function of immunoglobulins," *Journal of Allergy and Clinical Immunology*, vol. 125, no. 2, pp. S41-S52, 2010.
- [93] D. J. Rawlings, M. A. Schwartz, S. W. Jackson, and A. Meyer-Bahlburg, "Integration of B cell responses through toll-like receptors and antigen receptors," *Nature Reviews Immunology*, vol. 12, no. 4, pp. 282-294, 2012.
- [94] E. A. Leadbetter, I. R. Rifkin, A. M. Hohlbaum, B. C. Beaudette, M. J. Shlomchik, and A. Marshak-Rothstein, "Chromatin-IgG complexes activate B cells by dual engagement of IgM and toll-like receptors," *Nature*, vol. 416, no. 6881, pp. 603-607, 2002.
- [95] E. Bourke, D. Bosisio, J. Golay, N. Polentarutti, and A. Mantovani, "The toll-like receptor repertoire of human B lymphocytes: inducible and selective expression of TLR9 and TLR10 in normal and transformed cells," *Blood*, vol. 102, no. 3, pp. 956-963, 2003.
- [96] A.-M. Cepika, D. Soldo Jureša, J. Morović Vergles et al., "Decrease in circulating DNA, IL-10 and BAFF levels in newly-diagnosed SLE patients after corticosteroid and chloroquine treatment," *Cellular Immunology*, vol. 276, no. 1-2, pp. 196-203, 2012.
- [97] A.-K. Yi, D. W. Peckham, R. F. Ashman, and A. M. Krieg, "CpG DNA rescues B cells from apoptosis by activating NF $\kappa$ B and preventing mitochondrial membrane potential disruption via a chloroquine-sensitive pathway," *International Immunology*, vol. 11, no. 12, pp. 2015-2024, 1999.
- [98] Y. Floman, "Prostaglandin e production by cultured inflamed rat synovium; stimulation by colchicine and inhibition by chloroquine," *Prostaglandins and Medicine*, vol. 1, no. 1, pp. 39-48, 1978.
- [99] Y. Floman, E. Okon, and U. Zor, "The role of prostaglandins in experimental arthritis in the rat," *Clinical Orthopaedics and Related Research*, vol. 125, no. 125, pp. 214-220, 1977.
- [100] K. Authi and J. Traynor, "Effects of antimalarial drugs on phospholipase A2 [proceedings]," *British Journal of Pharmacology*, vol. 66, no. 3, 1979.
- [101] B. B. Aggarwal, "Tumor necrosis factors: developments during the last decade," *European Cytokine Network*, vol. 7, no. 2, pp. 93-124, 1996.
- [102] P. W. Gray, K. Barrett, D. Chantry, M. Turner, and M. Feldmann, "Cloning of human tumor necrosis factor (TNF) receptor cDNA and expression of recombinant soluble TNF-binding protein," *Proceedings of the National Academy of Sciences*, vol. 87, no. 19, pp. 7380-7384, 1990.
- [103] H. Hohmann, M. Brockhaus, P. Baeuerle, R. Remy, R. Kolbeck, and A. Van Loon, "Expression of the types A and B tumor necrosis factor (TNF) receptors is independently regulated, and both receptors mediate activation of the transcription factor NF-kappa B. TNF alpha is not needed for induction of a biological effect via TNF receptors," *Journal of Biological Chemistry*, vol. 265, no. 36, pp. 22409-22417, 1990.
- [104] J. Rothe, W. Lesslauer, H. Löttscher et al., "Mice lacking the tumour necrosis factor receptor 1 are resistant to IMF-mediated toxicity but highly susceptible to infection by *Listeria monocytogenes*," *Nature*, vol. 364, no. 6440, pp. 798-802, 1993.
- [105] J. J. Peschon, D. S. Torrance, K. L. Stocking et al., "TNF receptor-deficient mice reveal divergent roles for p55 and p75 in several models of inflammation," *The Journal of Immunology*, vol. 160, no. 2, pp. 943-952, 1998.
- [106] G. B. Huffnagle, G. B. Toews, M. D. Burdick et al., "Afferent phase production of TNF-alpha is required for the development of protective T cell immunity to *Cryptococcus neoformans*," *The Journal of Immunology*, vol. 157, no. 10, pp. 4529-4536, 1996.
- [107] L. W. Moreland, S. W. Baumgartner, M. H. Schiff et al., "Treatment of rheumatoid arthritis with a recombinant human tumor necrosis factor receptor (p75)-Fc fusion protein," *New England Journal of Medicine*, vol. 337, no. 3, pp. 141-147, 1997.
- [108] R. A. Black, C. T. Rauch, C. J. Kozlosky et al., "A metalloproteinase disintegrin that releases tumour-necrosis factor- $\alpha$  from cells," *Nature*, vol. 385, no. 6618, pp. 729-733, 1997.
- [109] J.-Y. Jeong and D.-M. Jue, "Chloroquine inhibits processing of tumor necrosis factor in lipopolysaccharide-stimulated RAW 264.7 macrophages," *The Journal of Immunology*, vol. 158, no. 10, pp. 4901-4907, 1997.
- [110] S. M. Weber, J.-M. Chen, and S. M. Levitz, "Inhibition of mitogen-activated protein kinase signaling by chloroquine," *The Journal of Immunology*, vol. 168, no. 10, pp. 5303-5309, 2002.
- [111] T. van der Bruggen, S. Nijenhuis, E. van Raaij, J. Verhoef, and B. Sweder van Asbeck, "Lipopolysaccharide-induced tumor necrosis factor alpha production by human monocytes involves the raf-1/MEK1-MEK2/ERK1-ERK2 pathway," *Infection and Immunity*, vol. 67, no. 8, pp. 3824-3829, 1999.
- [112] T. K. Means, R. P. Pavlovich, D. Roca, M. W. Vermeulen, and M. J. Fenton, "Activation of TNF- $\alpha$  transcription utilizes distinct MAP kinase pathways in different macrophage populations," *Journal of Leukocyte Biology*, vol. 67, no. 6, pp. 885-893, 2000.
- [113] J. L. Swantek, M. H. Cobb, and T. D. Geppert, "Jun N-terminal kinase/stress-activated protein kinase (JNK/SAPK) is required for lipopolysaccharide stimulation of tumor necrosis factor alpha (TNF-alpha) translation: glucocorticoids inhibit TNF-alpha translation by blocking JNK/SAPK," *Molecular and Cellular Biology*, vol. 17, no. 11, pp. 6274-6282, 1997.
- [114] R. Marais, Y. Light, H. Paterson, and C. Marshall, "Ras recruits Raf-1 to the plasma membrane for activation by tyrosine phosphorylation," *The EMBO Journal*, vol. 14, no. 13, pp. 3136-3145, 1995.
- [115] S. Zimmermann and K. Moelling, "Phosphorylation and regulation of Raf by Akt (protein kinase B)," *Science*, vol. 286, no. 5445, pp. 1741-1744, 1999.
- [116] A. B. Carter, M. M. Monick, and G. W. Hunninghake, "Both Erk and p38 kinases are necessary for cytokine gene transcription," *American Journal of Respiratory Cell and Molecular Biology*, vol. 20, no. 4, pp. 751-758, 1999.
- [117] W. J. Streit, J. R. Condeelis, and J. K. Harrison, "Chemokines and Alzheimer's disease," *Neurobiology of Aging*, vol. 22, no. 6, pp. 909-913, 2001.
- [118] A. Bajetto, R. Bonavia, S. Barbero, T. Florio, and G. Schettini, "Chemokines and their receptors in the central nervous

- system,” *Frontiers in Neuroendocrinology*, vol. 22, no. 3, pp. 147–184, 2001.
- [119] M. Liu, S. Guo, J. M. Hibbert et al., “CXCL10/IP-10 in infectious diseases pathogenesis and potential therapeutic implications,” *Cytokine & Growth Factor Reviews*, vol. 22, no. 3, pp. 121–130, 2011.
- [120] K. D. Dyer, C. M. Percopo, E. R. Fischer, S. J. Gabryszewski, and H. F. Rosenberg, “Pneumoviruses infect eosinophils and elicit MyD88-dependent release of chemoattractant cytokines and interleukin-6,” *Blood*, vol. 114, no. 13, pp. 2649–2656, 2009.
- [121] A. D. Luster and J. V. Ravetch, “Biochemical characterization of a gamma interferon-inducible cytokine (IP-10),” *The Journal of Experimental Medicine*, vol. 166, no. 4, pp. 1084–1097, 1987.
- [122] B. K. K. Lo, M. Yu, D. Zloty, B. Cowan, J. Shapiro, and K. J. McElwee, “CXCR3/ligands are significantly involved in the tumorigenesis of basal cell carcinomas,” *The American Journal of Pathology*, vol. 176, no. 5, pp. 2435–2446, 2010.
- [123] J. D. Campbell, V. Gangur, F. E. R. Simons, and K. T. Hay-Glass, “Allergic humans are hypo-responsive to CXCR3 chemokines in a Th1 immunity-promoting loop,” *The FASEB Journal*, vol. 18, no. 2, pp. 1–19, 2003.
- [124] M. P. Murphy, “How mitochondria produce reactive oxygen species,” *Biochemical Journal*, vol. 417, no. 1, pp. 1–13, 2009.
- [125] S. G. Rhee, “Redox signaling: hydrogen peroxide as intracellular messenger,” *Experimental & Molecular Medicine*, vol. 31, no. 2, pp. 53–59, 1999.
- [126] J. Gutierrez, S. W. Ballinger, V. M. Darley-Usmar, and A. Landar, “Free radicals, mitochondria, and oxidized lipids,” *Circulation Research*, vol. 99, no. 9, pp. 924–932, 2006.
- [127] Y. Minokoshi, C. R. Kahn, and B. B. Kahn, “Tissue-specific ablation of the GLUT4 glucose transporter or the insulin receptor challenges assumptions about insulin action and glucose homeostasis,” *Journal of Biological Chemistry*, vol. 278, no. 36, pp. 33609–33612, 2003.
- [128] A. Klip, “The many ways to regulate glucose transporter 4,” *Applied Physiology, Nutrition, and Metabolism*, vol. 34, no. 3, pp. 481–487, 2009.
- [129] F. S. Thong, C. B. Dugani, and A. Klip, “Turning signals on and off: GLUT4 traffic in the insulin-signaling highway,” *Physiology*, vol. 20, no. 4, pp. 271–284, 2005.
- [130] Q. Li, X. Zhu, S. Ishikura et al., “Ca<sup>2+</sup> signals promote GLUT4 exocytosis and reduce its endocytosis in muscle cells,” *American Journal of Physiology-Endocrinology and Metabolism*, vol. 307, no. 2, pp. E209–E224, 2014.
- [131] K. Kotani, O. D. Peroni, Y. Minokoshi, O. Boss, and B. B. Kahn, “GLUT4 glucose transporter deficiency increases hepatic lipid production and peripheral lipid utilization,” *Journal of Clinical Investigation*, vol. 114, no. 11, pp. 1666–1675, 2004.
- [132] M. Blignaut, Y. Espach, M. van Vuuren, K. Dhanabalan, and B. Huisamen, “Revisiting the cardiotoxic effect of chloroquine,” *Cardiovascular Drugs and Therapy*, vol. 33, no. 1, pp. 1–11, 2019.
- [133] A. E. Stenbit, T.-S. Tsao, J. Li et al., “GLUT4 heterozygous knockout mice develop muscle insulin resistance and diabetes,” *Nature Medicine*, vol. 3, no. 10, pp. 1096–1101, 1997.
- [134] M. A. A. Al-Bari, “Chloroquine analogues in drug discovery: new directions of uses, mechanisms of actions and toxic manifestations from malaria to multifarious diseases,” *Journal of Antimicrobial Chemotherapy*, vol. 70, no. 6, pp. 1608–1621, 2015.
- [135] S. Kalia and J. P. Dutz, “New concepts in antimalarial use and mode of action in dermatology,” *Dermatologic Therapy*, vol. 20, no. 4, pp. 160–174, 2007.
- [136] A. Pareek, N. Chandurkar, N. Thomas et al., “Efficacy and safety of hydroxychloroquine in the treatment of type 2 diabetes mellitus: a double blind, randomized comparison with pioglitazone,” *Current Medical Research and Opinion*, vol. 30, no. 7, pp. 1257–1266, 2014.
- [137] M. C. M. Wasko, C. K. McClure, S. F. Kelsey, K. Huber, T. Orchard, and F. G. Toledo, “Antidiabetogenic effects of hydroxychloroquine on insulin sensitivity and beta cell function: a randomised trial,” *Diabetologia*, vol. 58, no. 10, pp. 2336–2343, 2015.

## Research Article

# Comprehensive Screening of Mouse T-Cell Epitopes in Human Herpesvirus 6B Glycoprotein H/L/Q1/Q2 Tetramer Complex

**Mie Okutani,<sup>1,2</sup> Akiko Kawabata,<sup>3</sup> Mitsuhiro Nishimura,<sup>3</sup> Satoshi Nagamata,<sup>3,4</sup> Soichiro Kuwabara,<sup>1,2</sup> Yasunari Haseda,<sup>2</sup> Lisa Munakata,<sup>5</sup> Ryo Suzuki,<sup>5</sup> Yasuko Mori,<sup>3</sup> and Taiki Aoshi<sup>2,6</sup>**

<sup>1</sup>BIKEN Center for Innovative Vaccine Research and Development, The Research Foundation for Microbial Diseases of Osaka University, 3-1 Yamadaoka, Suita, Osaka 565-0871, Japan

<sup>2</sup>Vaccine Dynamics Project, BIKEN Innovative Vaccine Research Alliance Laboratories, Research Institute for Microbial Diseases, Osaka University, 3-1 Yamadaoka, Suita, Osaka 565-0871, Japan

<sup>3</sup>Division of Clinical Virology, Center for Infectious Diseases, Kobe University Graduate School of Medicine, 7-5-2 Kusunoki-cho, Chuo-ku, Kobe, Hyogo 650-0017, Japan

<sup>4</sup>Department of Obstetrics and Gynecology, Kobe University Graduate School of Medicine, 7-5-2 Kusunoki-cho, Chuo-ku, Kobe, Hyogo 650-0017, Japan

<sup>5</sup>Laboratory of Drug and Gene Delivery Research, Faculty of Pharma-Science, Teikyo University, 2-11-1 Kaga, Itabashi-ku, Tokyo 173-8605, Japan

<sup>6</sup>Department of Cellular Immunology, Research Institute for Microbial Diseases, Osaka University, 3-1 Yamadaoka, Suita, Osaka 565-0871, Japan

Correspondence should be addressed to Taiki Aoshi; [aoshi@biken.osaka-u.ac.jp](mailto:aoshi@biken.osaka-u.ac.jp)

Received 4 May 2020; Revised 30 June 2020; Accepted 2 July 2020; Published 26 July 2020

Academic Editor: Roberta Antonia Diotti

Copyright © 2020 Mie Okutani et al. This is an open access article distributed under the Creative Commons Attribution License, which permits unrestricted use, distribution, and reproduction in any medium, provided the original work is properly cited.

Human herpesvirus 6 (HHV-6) infects over 90% of people. The HHV-6 subtype, HHV-6B in particular, is often associated with exanthem subitum in early childhood. Exanthem subitum is usually self-limiting and good prognosis disease; however, some infants primarily infected with HHV-6B develop encephalitis/encephalopathy, and half of the patients developed encephalopathy reported to have neurological sequelae. Furthermore, after primary infection, HHV-6B remains in a latent state and sometimes reactivated in immunosuppressed patients, causing life-threatening severe encephalopathy. However, effective immunotherapies or vaccines for controlling HHV-6B infection and reactivation have not yet been established. Recently, we have found that the HHV-6B tetrameric glycoprotein (g) complex, gH/gL/gQ1/gQ2 is a promising vaccine candidate, and currently under preclinical development. To confirm our vaccine candidate protein complex induce detectable T-cell responses, in this study, we comprehensively screened CD4<sup>+</sup> and CD8<sup>+</sup> T-cell epitopes in the gH/gL/gQ1/gQ2 tetrameric complex protein in mice immunisation model. Both BALB/c and C57BL/6 mice were immunised with the tetrameric complex protein or plasmid DNA encoding gH, gL, gQ1, and gQ2, and then restimulated with 162 20-mer peptides covering the whole gH/gL/gQ1/gQ2 sequences; multiple CD4<sup>+</sup> and CD8<sup>+</sup> T-cell-stimulating peptides were identified in both BALB/c and C57BL/6 mice. Our study demonstrates that gH/gL/gQ1/gQ2 tetramer-targeted vaccination has potential to induce T-cell responses in two different strains of mice and supports the future development and application of T-cell-inducing vaccine and immunotherapies against HHV-6B.

## 1. Introduction

Human herpesvirus 6 (HHV-6) belongs to the  $\beta$ -herpesvirus subfamily and infects over 90% of people globally [1]. HHV-6 can be classified into two groups, variant A (HHV-6A) and

variant B (HHV-6B), by their epidemiology and pathology [2, 3]. Although both HHV-6A and HHV-6B have been shown to be involved in human diseases [4, 5], HHV-6B infection is clearly associated with exanthem subitum in early childhood [1, 6]. Exanthem subitum is a self-limited disease



with a good prognosis; however, it is relatively highly associated with febrile seizure. Although it is rare, some infants develop encephalitis/encephalopathy associated with HHV-6B infection. About half of children with encephalitis or encephalopathy are reported to have neurological sequelae in Japan [7]. Furthermore, after primary infection, HHV-6B remains in a latent state and is sometimes reactivated in immunosuppressed patients with severe encephalopathy [8–10]. However, there is no specific drug, no vaccines, and no cellular immunotherapy for controlling HHV-6B infection and reactivation has been established.

HHV-6B glycoprotein (g) H/gL/gQ1/gQ2 tetrameric complex has been shown to bind human CD134 (also called OX40) and be expressed on activated T lymphocytes [11]. gQ1 and gQ2 subunits were shown to be sufficient for CD134 binding, and a region in gQ1 was required for its function [12]. Regarding gH and gL subunits, a number of studies in other herpesviruses have shown that gH and gL subunits are involved in penetration and cell-to-cell spread [13, 14]. The gQ1 and gQ2 nucleotide sequences are shared only 70% between HHV-6A and HHV-6B, while the gH and gL genes are mostly conserved (approximately 90%) between these two variants; in fact, the gH and gL sequences are also conserved even among other herpesvirus families [15–18]. Monoclonal antibodies (MAbs) against HHV-6B gH and gQ1 were found to specifically neutralise virus infection [19, 20]. Recently, we have found HHV-6B gH/gL/gQ1/gQ2 tetrameric complex is one of the most attractive vaccine targets for controlling HHV-6B infection (Wang et al. manuscript submitted).

In a previous study, we identified that HHV-6B gQ1 protein-induced CD4<sup>+</sup> and CD8<sup>+</sup> T-cell responses by immunising BALB/c mice using DNA vaccination [21]. In this study, we more comprehensively screened T-cell responses against gH/gL/gQ1/gQ2 complex of HHV-6B by using a library of 162 peptides covering the whole gH/gL/gQ1/gQ2 protein sequences by using two strains of mice (BALB/c and C57BL/6) with two immunisation methods. These methods were intradermal protein injection of gH/gL/gQ1/gQ2 complex together with CpG adjuvant (protein vaccination), and intravenous injection of the corresponding plasmid DNA formulated with polyethylenimine (PEI) (DNA vaccination). The results revealed the successful identification of multiple CD4<sup>+</sup> T-cell and CD8<sup>+</sup> T-cell epitopes in both BALB/c and C57BL/6 mice, suggesting that vaccination targeting the gH/gL/gQ1/gQ2 complex can induce detectable T-cell responses irrespective of the strain of mice. Our results support the future application of gH/gL/gQ1/gQ2 complex for T-cell-inducing vaccines and immunotherapies against HHV-6B. The difference in T-cell responses between the two strains of mice and between the two vaccine systems is also discussed.

## 2. Results

*2.1. Detection of CD4<sup>+</sup> and CD8<sup>+</sup> T-Cell Response Induction upon Immunisation with the Tetrameric Complex Protein.* First, we performed immunisation with the gH/gL/gQ1/gQ2

tetrameric protein complex together with our developed CpG adjuvant named D35/DOTAP [22], which efficiently induces both MHC Class I and Class II immune responses against a variety of antigens including OVA, influenza HA split vaccine, and LLO91-99 peptide (Supplementary Figure 1). To identify CD4<sup>+</sup> or CD8<sup>+</sup> T-cell responses against gH/gL/gQ1/gQ2 tetrameric protein, gH/gL/gQ1/gQ2 tetrameric protein-immunised splenocytes from six mice were pooled and appropriately prepared (CD4<sup>+</sup> or CD8<sup>+</sup> T-cell-depleted, and undepleted whole splenocytes). Then, they were stimulated in vitro with each of 162 peptides covering all gH/gL/gQ1/gQ2 sequences and IFN- $\gamma$  production was measured by ELISA. Due to both the variation of interexperimental IFN- $\gamma$  production differences and some T-cell responses against cryptic T-cell epitopes [23] were not always consistently detected, we repeated this experiment three times. We also utilized Z-scoring normalization method [24] to merge and better visualize IFN- $\gamma$  production data against 162 peptides from these three independent experiments. Of note, in our previous study, gQ1-expressing plasmid vaccination induced at least one CD4<sup>+</sup> T-cell response and one CD8<sup>+</sup> T-cell response in gQ1 protein in BALB/c mice [21], so we also expected that immunisation with gH/gL/gQ1/gQ2 tetrameric protein complex with CpG adjuvant would also induce at least one CD4<sup>+</sup> T-cell response and one CD8<sup>+</sup> T-cell response.

Our results revealed IFN- $\gamma$  production in whole splenocytes against a total of 12 peptides out of the library of 162 peptides covering the gH/gL/gQ1/gQ2 tetrameric proteins (see Supplementary Table 1) in BALB/c mice (Figure 1(a)). These 12 responses were consistently observed from our three independent experiments and indicated as black bars in Figure 1. Among them, a total of 9 peptides, namely, No. 46 (gH), No. 74 (gL), No. 79 (gL), No. 112 (gQ1), No. 133 (gQ1), No. 134 (gQ1), No. 139 (gQ1), No. 147 (gQ2), and No. 155 (gQ2) peptides, were confirmed to induce CD4<sup>+</sup> T-cell responses because these responses still remained after CD8<sup>+</sup> T-cell depletion (Figure 1(b)). Our previously identified CD4 T-cell epitope containing the 20-mer peptide AGLLMVNNIFTVQARYSKQN [21] was also included as No. 139 in this study's result. Other CD4<sup>+</sup> T-cell responses against No. 65 (gH), No. 80 (gL), No. 113 (gQ1), No. 141 (gQ1), and No. 153 (gQ2) emerged only after CD8<sup>+</sup> T-cell depletion, suggesting that they are relatively weak T-cell-stimulating peptides or that a relatively small population of CD4<sup>+</sup> T cells responds to these peptides (Figure 1(b)), because after CD8<sup>+</sup> T-cell depletion, we used the CD8<sup>+</sup> cell-depleted cells containing the same cell number of nondepleted cells for stimulation meaning that relative CD4<sup>+</sup> T-cell frequency was increased after CD8<sup>+</sup> cell depletion. Upon including peptides detected in two out of three independent experiments (indicated as gray bars in Figure 1), the overall responses of whole splenocytes (Figure 1(a)) and of CD4<sup>+</sup> T cells (Figure 1(b)) generally overlapped. In contrast and unexpectedly, no consistent CD8<sup>+</sup> T-cell responses were detected (Figure 1(c)). Notably, responses against No. 157 (gQ2) were only observed with whole splenocytes but disappeared after CD4<sup>+</sup> or CD8<sup>+</sup> T-cell depletion.

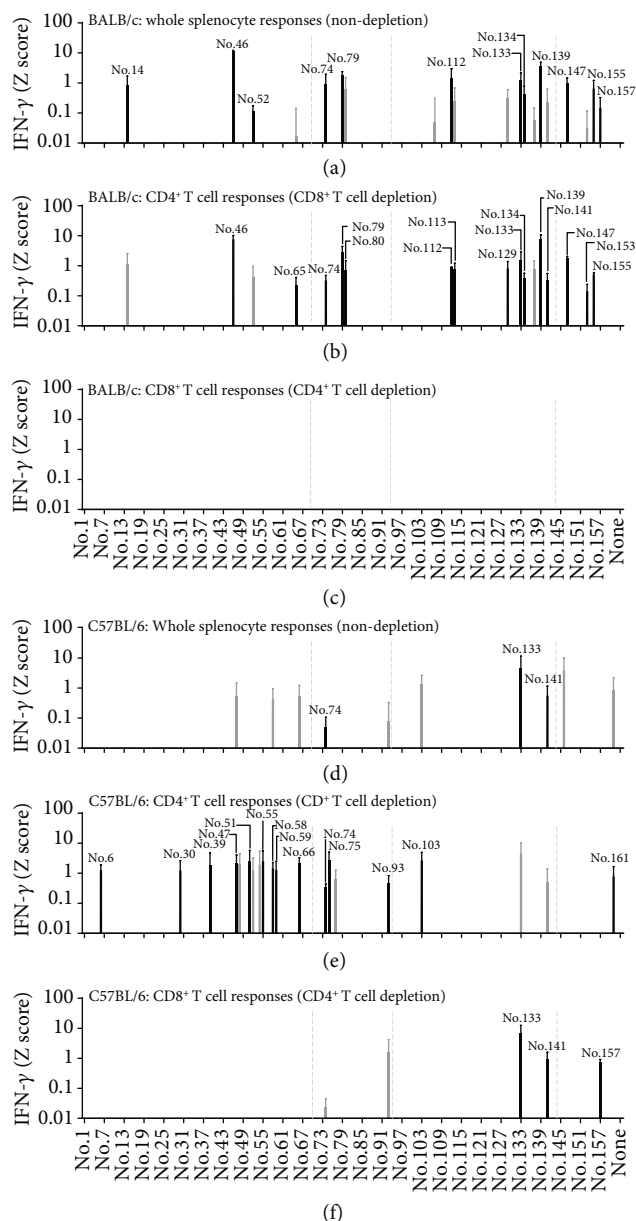


FIGURE 1: T-cell responses of mice immunised with the tetrameric protein complex plus CpG adjuvant. Undepleted whole splenocytes (a, d), CD8<sup>+</sup> T-cell-depleted splenocytes (b, e), and CD4<sup>+</sup> T-cell-depleted splenocytes (c, f) of BALB/c (a-c) and C57BL/6 (d-f) mice that had been immunised with HHV-6B gH/gL/gQ1/gQ2 tetrameric protein complex plus CpG adjuvant were tested for reactivity to a library of 162 peptides after 20 h of stimulation by IFN-γ ELISA. The quantity of IFN-γ (pg/mL) of each peptide was transformed to a Z score ( $Z = (x - \text{mean})/\text{SD}$ , where  $x$  is the quantity of IFN-γ for each peptide). Individual peptide samples with a Z score exceeding 0.01 were considered positive. Black bars indicate that the response was detected as positive in all three independent experiments, and gray bars indicate that there was positivity in two out of three independent experiments. T-cell responses detected as positive in only one experiment are not shown. Data are shown as the mean Z score  $\pm$  SD of three independent experiments. The gray dot lines indicate the boundaries of gH, gL, gQ1, and gQ2.

In C57BL/6 mice, consistent (meaning three times out of three independent experiments) IFN-γ production was only seen against No. 74 (gL), No. 133 (gQ1), and No. 141 (gQ1) (Figure 1(d)). After CD8<sup>+</sup> T-cell depletion, many weak but consistently detectable CD4<sup>+</sup> T-cell responses were raised (Figure 1(e)). Unlike in BALB/c mice, CD8<sup>+</sup> T-cell responses were consistently detected against No. 133 (gQ1), No. 141 (gQ1), and No. 157 (gQ2) by the protein vaccination in C57BL/6 mice, suggesting that protein immunisation with CpG adjuvant potentiated CD8<sup>+</sup> T-cell responses as expected, at least in C57BL/6 mice.

**2.2. T-Cell Response Induction upon Immunisation with DNA Vaccine.** Because protein vaccination with CpG adjuvant in BALB/c mice unexpectedly induced no detectable CD8<sup>+</sup> T-cell responses (Figure 1(c)), we also attempted plasmid DNA vaccination to more comprehensively screen T-cell responses against the gH/gL/gQ1/gQ2 tetrameric complex antigen. Mice were immunised with plasmids expressing each of gH, gL, gQ1, and gQ2, or a gH/gL/gQ1/gQ2 plasmid mixture, and then whole splenocytes from 2 mice per group were pooled and stimulated with the corresponding library peptides for each immunised plasmid (gH: No. 1–69, gL: No. 70–93, gQ1: No. 94–144, and gQ2: No. 145–162); subsequently, IFN-γ production was assayed by ELISA. This experiment was also performed three times independently, and the results were visualized similarly as Figure 1. IFN-γ production was consistently detected against No. 13, No. 46 (gH), No. 107, No. 112, No. 113, No. 115, and No. 139 (gQ1) peptides when BALB/c mice were immunised with single gH or gQ1 plasmid (Figure 2(a)). Interestingly, immunisation with gH/gL/gQ1/gQ2 plasmid mixture induced consistent T-cell responses only against two peptides, namely, No. 46 (gH) and No. 157 (gQ2) (Figure 2(b)), but not against other peptides, which induced such responses upon single plasmid immunisation, such as No. 13, No. 107, No. 112, No. 113, No. 115, and No. 139 (Figure 2(a)). T-cell responses against No. 157 peptide were only detected upon immunisation with gH/gL/gQ1/gQ2 plasmid mixture (Figure 2(b)). Immunisation with the single gQ2 plasmid did not induce any detectable T-cell responses against No. 157 peptide throughout three independent experiments (Figure 2(a)).

In C57BL/6 mice, immunisation with each single plasmid gH, gL, gQ1, or gQ2 induced no consistent T-cell responses against the peptide library (Figure 3(a)); the gray bars indicate only two times detection from three independent experiments. On the other hand, immunisation with the plasmid mixture induced weak but consistent T-cell responses against No. 6 (gH), No. 75, No. 89 (gL), No. 133, and No. 141 (gQ1) peptides (Figure 3(b)). Notably, in both BALB/c and C57BL/6 mice, no T-cell responses were seen upon immunisation with gQ2 single plasmid, but detectable responses such as against No. 157 peptide in gQ2 were seen after immunisation with the plasmid mixture, suggesting that the gQ2-encoding plasmid was successfully expressed and worked as a DNA vaccine in vivo.

**2.3. CD4<sup>+</sup> and CD8<sup>+</sup> T-Cell Response Induction upon Immunisation with DNA Vaccine.** To determine whether

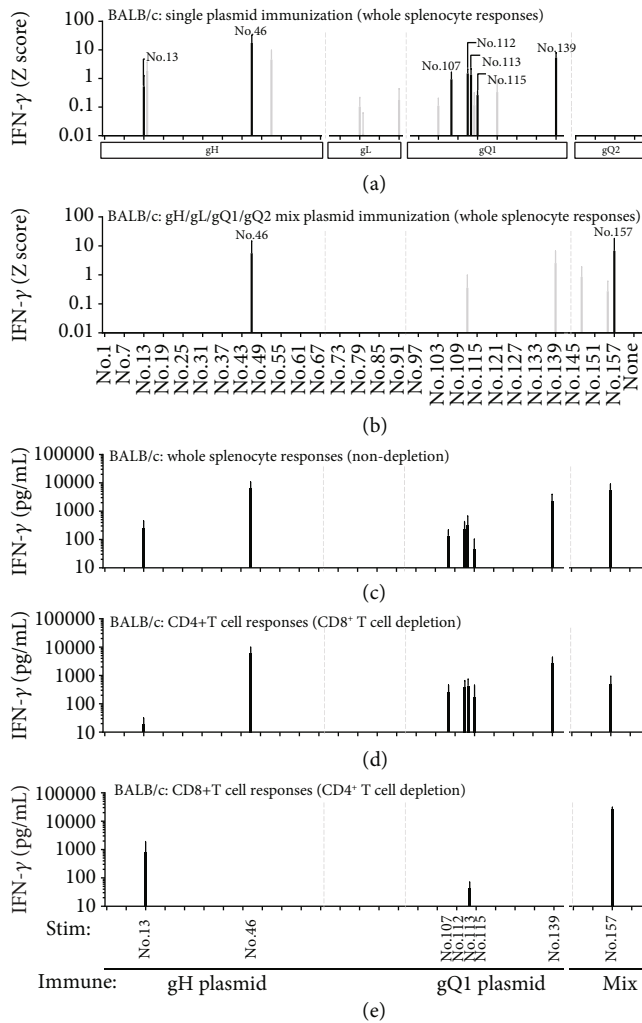


FIGURE 2: T-cell responses of immunised BALB/c mice upon vaccination with expression plasmid DNA. Undepleted whole splenocytes immunised with each expression plasmid for gH, gL, gQ1, and gQ2 (a), or a mixture of them (b) were tested for the corresponding library peptides (gH: No. 1–69, gL: No. 70–93, gQ1: No. 94–144, and gQ2: No. 145–162). After 20 h of stimulation, the quantity of IFN- $\gamma$  (pg/mL) for each peptide was measured by ELISA and transformed to a Z score ( $Z = x - \text{mean}/\text{SD}$ , where  $x$  is the quantity of IFN- $\gamma$  for each peptide). Individual peptide samples with a Z score exceeding 0.01 were considered as positive. Black bar indicates three detections, and gray bar indicates two detections out of three independent experiments. Data are shown as the mean Z score  $\pm$  SD of three independent experiments. Consistently detected peptides shown by black bars in (a) and (b) were chosen and another independent experiment was performed. Undepleted whole splenocytes (c), CD8<sup>+</sup> T-cell-depleted splenocytes (d), and CD4<sup>+</sup> T-cell-depleted splenocytes (e) were tested for reactivity to the chosen peptides. After 20 h of stimulation, the production of IFN- $\gamma$  was measured by ELISA. Data are presented in pg/mL and shown as mean  $\pm$  SD. The gray dot lines indicate the boundaries of gH, gL, gQ1, and gQ2.

the DNA vaccination induced responses were from CD4<sup>+</sup> or CD8<sup>+</sup> T cells, the splenocytes after DNA vaccination were CD4<sup>+</sup> or CD8<sup>+</sup> T-cell-depleted and then stimulated with the selected peptides that had induced consistent T-cell

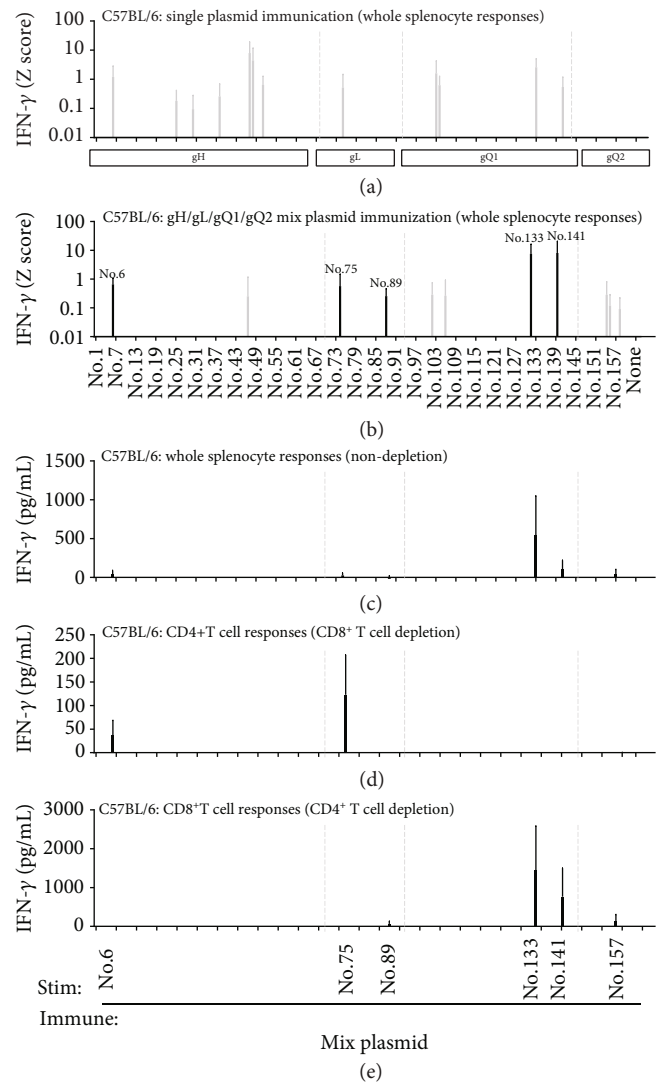


FIGURE 3: T-cell responses of C57BL/6 mice upon immunisation with expression plasmid DNA. Undepleted whole splenocytes immunised with each expression plasmid for gH, gL, gQ1, and gQ2 (a), and a mixture of them (b) were tested for the corresponding library peptides (gH: No. 1–69, gL: No. 70–93, gQ1: No. 94–144, and gQ2: No. 145–162). After 20 h of stimulation, the quantity of IFN- $\gamma$  (pg/mL) of each peptide was measured by ELISA and transformed into a Z score ( $Z = x - \text{mean}/\text{SD}$ , where  $x$  is the quantity of IFN- $\gamma$  for each peptide). Individual peptide samples with a Z score exceeding 0.01 were considered positive. Black bar indicates three, and gray bar indicates two detections out of three independent experiments. Data are shown as mean Z score  $\pm$  SD of three independent experiments. Consistently detected peptides as shown by black bars in (a) and (b) were chosen and another independent experiment was performed. Undepleted whole splenocytes (c), CD8<sup>+</sup> T-cell-depleted splenocytes (d), and CD4<sup>+</sup> T-cell-depleted splenocytes (e) were tested for reactivity to the chosen peptides. After 20 h of stimulation, the production of IFN- $\gamma$  was measured by ELISA. Data are presented in pg/mL and shown as mean  $\pm$  SD. The gray dot lines indicate the boundaries of gH, gL, gQ1, and gQ2.

TABLE 1: CD8<sup>+</sup> T-cell short epitope peptide prediction in BALB/c mice.

Peptide no. (glycoprotein)	Length (aa)	Amino acid sequence* <sup>1</sup>	Estimated scores for restriction molecules* <sup>2</sup>			%rank		
			BIMAS			NetMHC		
			D <sup>d</sup>	K <sup>d</sup>	L <sup>d</sup>	D <sup>d</sup>	K <sup>d</sup>	L <sup>d</sup>
No. 13 (gH)	20	IVYSLNLYPSHGIYYIRVVE						
	10	<u>LYPSHGIYYI</u>	<b>10</b>	<b>2880</b>	1.95	0.8	<b>4</b>	1.9
	9	LNLYPSHGI	0.5	80	1	27	10	37
	9	VYSLNLYPS	0.1	60	1	60	9.5	20
	9	<u>LYPSHGIYY</u>	2	60	3	<b>0.7</b>	17	13
	8	LYPSHGIY	2	60	—	3	18	35
	9	<u>YPSHGIYYI</u>	0.5	57.6	<b>39</b>	3.5	13	<b>0.17</b>
	8	NLYPSHGI	0.5	57.6	—	36	17	32
	10	SLNLYPSHGI	0.6	40	1	55	18	55
	9	HGIYYIRVV	6	20	2	7.5	33	50
	8	HGIYYIRV	6	20	—	12	55	37
No. 113 (gQ1)* <sup>3</sup>	20	RLKPLTAMTAIAFCPMTSKL						
	9	<b>AFCPMTSKL</b>	1	1382.4	5	37	0.8	23
No. 157 (gQ2)	20	NGPRYLQMETFISDLFRYEC						
	9	<u>RYLQMETFI</u>	0.3	<b>5760</b>	1	11	<b>0.01</b>	5
	8	<u>RYLQMETF</u>	0.18	144	—	9.5	0.8	16
	10	<u>RYLQMETFIS</u>	0.12	100	1	28	0.12	31
	10	LQMETFISDL	1.2	96	5	55	16	<b>2.5</b>
	9	TFISDLFRY	0.1	57.6	2	45	26	37
	9	QMETFISDL	1	48	1.5	60	12	4.5
	8	<u>YLQMETFI</u>	1.5	40	—	29	0.05	12
	10	TFISDLFRYE	0.01	6.912	0.1	55	33	75
	8	TFISDLFR	0.01	5.76	—	80	48	80
	8	<u>NGPRYLQM</u>	<b>120</b>	5	—	<b>0.08</b>	75	37
10	GPRYLQMETF	0.36	1	<b>90</b>	1	75	8.5	

\*<sup>1</sup> Underlined peptides were synthesised and used for experiments. Bold type peptides indicate determined short CD8<sup>+</sup> T-cell epitope. \*<sup>2</sup> No binding score. \*<sup>3</sup> AFCPMTSKL in No.113 was previously reported as the peptide including CD8<sup>+</sup> T-cell epitope (Nagamata et al., 2019).

responses upon single or mixed plasmid immunisation as shown in Figures 2(a) and 2(b). In BALB/c mice, IFN- $\gamma$  responses were detected against all eight examined peptides shown by the black bars in Figures 2(a) and 2(b), with particularly strong IFN- $\gamma$  production for No. 46, No. 139, and No. 157 (Figure 2(c)). After CD8<sup>+</sup> T-cell depletion, CD4<sup>+</sup> T-cell responses were detected for No. 46, No. 107, No. 112, No. 113, No. 115, No. 139, and No. 157 peptides (Figure 2(d)). After CD4<sup>+</sup> T-cell depletion, CD8<sup>+</sup> T-cell responses were detected for No. 13, No. 113, and No. 157 (Figure 2(e)). Notably, No. 113 peptide contains AFCPMTSKL, which we previously identified as a 9-mer H2K<sup>d</sup>-restricted CD8<sup>+</sup> T-cell epitope in BALB/c mice [21]; this demonstrated that gQ1 plasmid immunisation reproducibly induced similar CD8<sup>+</sup> T-cell responses in BALB/c mice.

In C57BL/6 mice, similarly, whole splenocytes immunised with a mixture of four plasmids responded to No. 133 and No. 141 among the five examined peptides shown by the black bar in Figure 3(b) (Figure 3(c)). CD4<sup>+</sup> T-cell responses were detected against No. 6 (gH) and No. 75 (gL) peptides after CD8<sup>+</sup> T-cell depletion (Figure 3(d)). CD8<sup>+</sup> T-

cell responses were detected against No. 89, No. 133, No. 141, and No. 157 after CD4<sup>+</sup> T-cell depletion; although, No. 89 and No. 157 were barely detectable (Figure 3(e)). From these results, we selected No. 13 and No. 157 peptides as new CD8<sup>+</sup> T-cell-responsive peptides for BALB/c mice (Figure 2(e)) and No. 133, No. 141, and No. 157 peptides for C57BL/6 mice (Figure 3(e)), for more detailed CD8<sup>+</sup> T-cell epitope examination.

**2.4. Determination of CD8<sup>+</sup> T-Cell Short Epitope Peptides in BALB/c Mice.** To determine short CD8<sup>+</sup> T-cell epitopes, several CD8<sup>+</sup> T-cell short epitope candidates within the two peptides No. 13 and No. 157 were predicted using two computer programmes: BIMAS HLA Peptide Binding Prediction ([https://www.bimas.cit.nih.gov/molbio/hla\\_bind/](https://www.bimas.cit.nih.gov/molbio/hla_bind/)) and NetMHC 4.0 (<http://www.cbs.dtu.dk/services/NetMHC/>) (Table 1). Three short peptides within No. 13 and five short peptides within No. 157 that exhibited a high score or low % rank were synthesised (shown by the underline in Table 1). Undepleted whole splenocytes of BALB/c mice immunised with gH plasmid, gQ1 plasmid, or gH/gL/gQ1/gQ2 plasmid

mixture were stimulated with these peptides. LYPSHGIYIYI or YPSHGIYIYI within No. 13 (gH) (Figure 4(a)) and RYLQMETFI within No. 157 (gQ2) (Figure 4(c)) provoked strong IFN- $\gamma$  production among these candidate peptides, indicating that LYPSHGIYIYI/YPSHGIYIYI in gH and RYLQMETFI in gQ2 are the CD8<sup>+</sup> T-cell short epitopes in BALB/c mice. For No. 133 peptide, we had already performed similar experiments and reported that No. 113 (gQ1) contained AFCPMTSKL, an H2K<sup>d</sup>-restricted CD8<sup>+</sup> T-cell short epitope [21]. We confirmed that gQ1 plasmid immunisation with the PEI method also induced AFCPMTSKL-reactive T cells (Figure 4(b)).

To determine the restricted MHC I molecule of these responses, single MHC I-expressing cells such as BW5147-H2K<sup>d</sup>, -H2D<sup>d</sup>, and -H2L<sup>d</sup> cells were pulsed with the short epitope peptide LYPSHGIYIYI or YPSHGIYIYI within No. 13 (gH) and RYLQMETFI within No. 157 (gQ2); then, they were used for the stimulation. Unexpectedly, all sets of BW5147-H2d-expressing cells pulsed with either LYPSHGIYIYI or YPSHGIYIYI within No. 13 (gH) resulted in no IFN- $\gamma$  responses (Figure 4(d)). On the other hand, RYLQMETFI within No. 157 (gQ2) induced the strongest IFN- $\gamma$  production in an H2K<sup>d</sup>-restricted manner (Figure 4(f)). To further investigate the failure of the short peptide-pulsed approach with No. 13 (gH) peptide (Figure 4(d)), we established internally gH-expressing BW5147-H2K<sup>d</sup>, -H2D<sup>d</sup>, and -H2L<sup>d</sup> cells, and then used them for stimulation. In this approach, we successfully detected IFN- $\gamma$  production by BW5147-H2K<sup>d</sup>-gH cells (Figure 4(e)). Taken together, these results suggested that LYPSHGIYIYI or YPSHGIYIYI within No. 13 (gH) was restricted by H2K<sup>d</sup>, and RYLQMETFI within No. 157 (gQ2) was also restricted by H2K<sup>d</sup>.

**2.5. Determination of CD8<sup>+</sup> T-Cell Short Epitope Peptides in C57BL/6 Mice.** Since No. 133, No. 141 (gQ1), and No. 157 (gQ2) were found to induce CD8<sup>+</sup> T-cell responses in C57BL/6 mice after both protein (Figure 1(f)) and plasmid immunisation (Figure 2(e)), several CD8<sup>+</sup> T-cell short epitope candidates within these peptides were also predicted in the same way as mentioned above (Table 2). Three short peptides from No. 133, four short peptides from No. 141, and five short peptides from No. 157 associated with a high score or a low % rank were synthesised (shown by the underline in Table 2). Undepleted splenocytes from C57BL/6 mice immunised with protein were stimulated with these peptides. TSIRNIDPA within No. 133 (gQ1) induced IFN- $\gamma$  production above the background level (Figure 4(g)), while no other epitope candidate peptides within No. 141 (gQ1) and No. 157 (gQ2) induced any discriminating responses (Figure 4(g)). In the MHC class I restriction determination, BW5147-H2D<sup>b</sup> pulsed with TSIRNIDPA induced slightly stronger IFN- $\gamma$  production compared with BW5147-H2K<sup>b</sup> pulsed with TSIRNIDPA (Figure 4(h)). We also performed similar experiments using C57BL/6 mouse splenocytes immunised with a mixture of plasmids (Supplementary Figure 2A); however, even with CD4<sup>+</sup> T-cell depletion, the results for both short peptides were not convincingly clear (Supplementary Figure 2B). Our results obtained in C57BL/6 mice did not provide a definitive answer regarding the restricted MHC I

molecule of TSIRNIDPA. The responses to other short peptides in No. 141 (gQ1) and No. 157 (gQ2) were not confirmed. Taking the obtained findings together, we concluded that at least TSIRNIDPA in gQ1 is a CD8<sup>+</sup> T-cell short epitope in C57BL/6 mice.

**2.6. CD8<sup>+</sup> T-Cell Response Induction by 20-Mer Peptide Vaccination.** In gH/gL/gQ1/gQ2 tetrameric complex, thus far, we have identified three confirmed H2K<sup>d</sup>-restricted CD8<sup>+</sup> T-cell epitopes in BALB/c mice and three potential CD8<sup>+</sup> T-cell-stimulating 20-mer peptides in C57BL/6 mice. To determine whether these CD8<sup>+</sup> T-cell epitope containing 20-mer peptides with CpG adjuvant (instead of whole protein or plasmid vaccination) could induce detectable CD8<sup>+</sup> T-cell responses, we immunised BALB/c mice with No. 13, No. 113, or No. 157 peptides (20-mers), which included LYPSHGIYIYI, AFCPMTSKL, and RYLQMETFI CD8<sup>+</sup> T-cell epitopes, and C57BL/6 mice with No. 133, No. 141, or No. 157. In BALB/c mice, No. 157 peptide vaccination induced a detectable CD8<sup>+</sup> T-cell response against RYLQMETFI (Figure 5(c)), while No. 13 and No. 113 peptide vaccination did not (Figures 5(a) and 5(b)). In C57BL/6 mice, No. 133 peptide vaccination induced a very weak CD8<sup>+</sup> T-cell response against TSIRNIDPA (Figure 5(e)), but No. 141 and No. 157 peptide vaccination did not induce any detectable CD8<sup>+</sup> T-cell responses (Figures 5(f) and 5(g)). Peptide vaccination induced RYLQMETFI/H2K<sup>d</sup> responses in BALB/c mice (Figure 5(d)), and No. 133 peptide vaccination similarly induced CD8<sup>+</sup> T-cell responses against TSIRNIDPA peptide (Figure 5(e)). However, again, the restricted MHC I molecules were still not clarified for TSIRNIDPA peptide (Figure 5(h)), potentially due to the weak binding to the corresponding MHC molecule and the resultant weak immune induction against this peptide in C57BL/6 mice.

### 3. Discussion

In this study, we identified multiple CD8<sup>+</sup> and CD4<sup>+</sup> T-cell-responding epitopes or 20-mer peptides in the HHV-6B gH/gL/gQ1/gQ2 tetrameric complex by using two different immunisation methods including protein and DNA vaccinations. In BALB/c mice, we identified that LYPSHGIYIYI within No. 13 (gH) and RYLQMETFI within No. 157 (gQ2) are new H2K<sup>d</sup>-restricted CD8<sup>+</sup> T-cell epitopes, and No. 46 (gH), No. 79 (gL), and No. 147 (gQ2) are relatively strong CD4<sup>+</sup> T-cell-stimulating 20-mer peptides. Interestingly, LYPSHGIYIYI and YPSHGIYIYI within No. 13 (gH) were not stimulatory when they were pulsed on single H2K<sup>d</sup>, H2D<sup>d</sup>, or H2L<sup>d</sup>-expressing BW5147 cells (Figure 4(d)). On the other hand, gH protein-expressing BW5147-H2K<sup>d</sup> cells (transduced with gH-expressing retrovirus vector) were strongly stimulatory (Figure 4(e)), suggesting that this T-cell epitope is more stably presented on H2K<sup>d</sup> through the endogenous antigen processing pathway. By searching the mouse genome, mouse plexin-A3 contains LYPAFDIYIYI sequence, which only differs in the middle part of the LYPSHGIYIYI epitope, from SHG to AFD. This may contribute to the observed phenomenon, but further experiments are required to understand this.

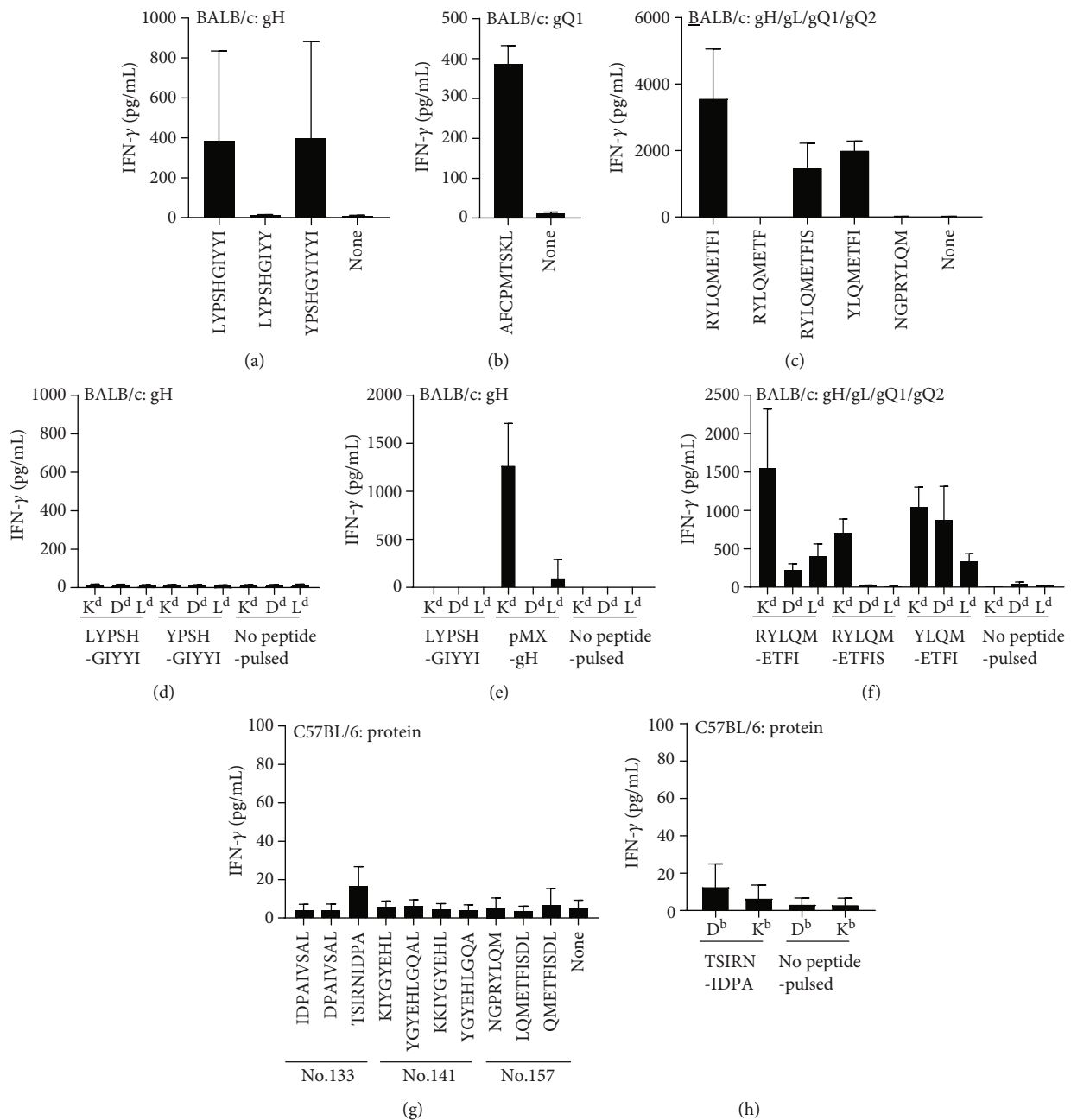


FIGURE 4: Short epitope determination for CD8<sup>+</sup> T-cell-responding 20-mer peptides. Undepleted splenocytes of BALB/c mice immunised with expression plasmid of gH (a, d, e), gQ1 (b), and a mixture of gH, gL, gQ1, and gQ2 (c, f), and C57BL/6 mice immunised with the tetrameric protein complex plus CpG adjuvant (g, h) were tested with short peptides shown in Table 1 (a-c) and Table 2 (g). The restricted MHC I molecules were determined by the peptide-pulsed BW5147 cell lines expressing each of the H2d molecules (d-f) or H2b molecules (h). For LYP SHGIYYI restricted MHC I molecule determination, gH-expressing BW5147 cell lines were also examined (e). The production of IFN- $\gamma$  after 20 h of stimulation was measured by ELISA. Data are presented in pg/mL and shown as mean  $\pm$  SD.

In a previous study, we examined T-cell epitopes within gQ1 in BALB/c mice by DNA vaccination and found that AFCPMTSKL within P17 (No. 113 peptide in the library of this study) was the H2K<sup>d</sup>-restricted CD8<sup>+</sup> T-cell epitope, and P43 (No. 139 peptide in this study) stimulated CD4<sup>+</sup> T-cell responses. This study also confirmed these findings of a CD8<sup>+</sup> T-cell response against No. 113 peptide and a CD4<sup>+</sup> T-cell response against No. 139 peptide (Figures 1 and 2).

In C57BL/6 mice, we found that TSIRNIDPA within No. 133 (gQ1) is the CD8<sup>+</sup> T-cell epitope, but we could not clearly determine the restricted H2b molecule for TSIRNIDPA short peptide. For No. 141 and No. 157, we consistently observed CD8<sup>+</sup> T-cell responses against these 20-mer peptides, but these responses were somehow too weak to further determine the short peptide epitopes for them. No. 6, No. 39, No. 47, No. 51, No. 55, No. 66 (gH), No. 75 (gL),

TABLE 2: CD8<sup>+</sup> T-cell short epitope peptide prediction in C57BL/6 mice.

Peptide no. (glycoprotein)	Length (aa)	Amino acid sequence*1	Estimated scores for restriction molecules*2		%rank	
			BIMAS		NetMHC	
			D <sup>b</sup>	K <sup>b</sup>	D <sup>b</sup>	K <sup>b</sup>
No. 133 (gQ1)	20	QRGTSIRNIDPAIVSALWHS				
	9	<u>IDPAIVSAL</u>	0.017	<b>3.3</b>	26	18
	8	<u>DPAIVSAL</u>	—	1.1	65	70
	8	RGTSIRNI	—	0.475	48	30
	10	NIDPAIVSAL	0.05	0.24	27	46
	8	RNIDPAIV	—	0.174	48	19
	10	RNIDPAIVSA	0.119	0.158	55	50
	9	AIVSALWHS	0.022	0.132	35	40
	9	<b><u>TSIRNIDPA</u></b>	<b>1047.388</b>	0.12	<b>0.01</b>	<b>11</b>
No. 141 (gQ1)	20	MFEKKIYGYEHLGQALCEGG				
	8	<u>KIYGYEHL</u>	—	<b>132</b>	9	<b>0.03</b>
	10	<u>YGYEHLGQAL</u>	<b>3.024</b>	8.64	<b>1.2</b>	<b>1.8</b>
	9	<u>KKIYGYEHL</u>	0.899	6	4.5	5
	10	EKKIYGYEHL	0.011	1.2	13	22
	8	YEHLGQAL	—	1	21	43
	9	<u>YGYEHLGQA</u>	0.108	0.72	7.5	3.5
	9	GYEHLGQAL	0.006	0.24	35	34
	8	EHLGQALC	—	0.11	95	80
No. 157 (gQ2)	20	NGPRYLQMETFISDLFRYEC				
	8	<u>NGPRYLQM</u>	—	<b>103.68</b>	23	4.5
	10	<u>LQMETFISDL</u>	<b>15.459</b>	1.32	<b>3.5</b>	6
	8	METFISDL	—	1.1	37	28
	10	NGPRYLQMET	0.108	0.432	36	60
	10	YLQMETFISD	0.059	0.3	28	43
	8	LQMETFIS	—	0.264	39	37
	9	<u>QMETFISDL</u>	1.175	0.24	16	<b>2.5</b>
	10	RYLQMETFIS	0.003	0.22	4	36

\*1 Underlined peptides were synthesised and used for experiments. Bold type peptides indicate determined short CD8<sup>+</sup> T-cell epitope. \*2 No binding score.

and No. 103 (gQ1) were CD4<sup>+</sup> T-cell-stimulating 20-mer peptides in C57BL/6 mice.

By using two strains of mice (BALB/c and C57BL/6) and immunising them with two different methods (using protein and DNA), we also observed different T-cell responses between BALB/c and C57BL/6 mice, and between protein vaccine and DNA vaccine. Overall, T-cell responses were stronger in BALB/c mice than in C57BL/6 mice, irrespective of the immunisation method (Figures 1–3).

BALB/c and C57BL/6 mice have different MHC haplotypes. MHC haplotype of BALB/c is H-2d and that of C57BL/6 is H-2b. Different MHC haplotype molecules present different peptides to the T cells, so that T cells from BALB/c or C57BL/6 respond to different peptides is expected result from the view of MHC haplotype. Another possible factor that contributes the difference of T-cell responses between BALB/c and C57BL/6 mice is their preferences to develop Th1 or Th2 type cytokine response, respectively. They are regarded as prototypes of Th1 or Th2 mouse strains [25]. Recent papers also showed BALB/c mice have a tendency of Th2 type

immune responses, and C57BL/6 mice Th1 type immune responses, especially in innate and immunometabolic phases [26, 27]. These innate responses usually affect the adaptive immune responses, too. However, there is a report that BALB/c and C57BL/6 mice do not show default Th1 and Th2 preference in adaptive immune response by allergen immunisation [28]. The observed T-cell response difference between BALB/c and C57BL/6 in this study is mainly a result of MHC haplotype differences; however, it could be also influenced by Th1/Th2-related genetic background differences of these two strains.

In terms of the difference of vaccination methods, we observed a general tendency that protein vaccination preferentially induced CD4<sup>+</sup> T-cell responses even with CpG adjuvants, and DNA vaccination preferentially induced CD8<sup>+</sup> T-cell responses. This fits with the classical view of antigen presentation pathway that internal antigen preferentially presented on MHC-I for inducing CD8<sup>+</sup> T-cell responses, and that external antigen preferentially presented on MHC-II for CD4<sup>+</sup> T-cell responses. In other words, the

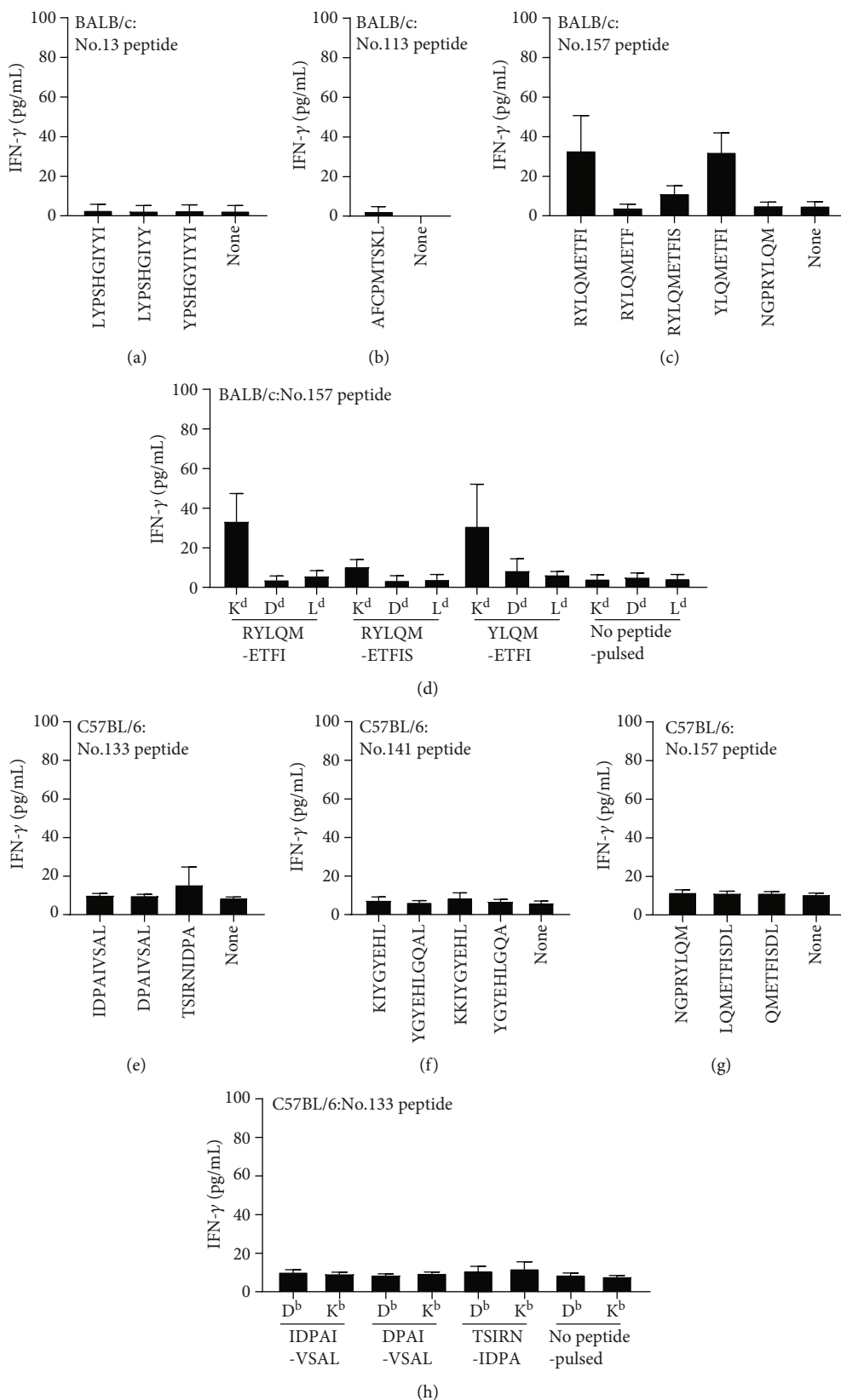


FIGURE 5: T-cell response inductions with 20-mer peptide plus CpG adjuvant. Whole splenocytes of BALB/c mice immunised with No. 13 (a), No. 113 (b), or No. 157 (c) peptide plus CpG adjuvant, and whole splenocytes of C57BL/6 mice immunised with No. 133 (e), No. 141 (f), or No. 157 (g) peptide plus CpG adjuvant were tested for the reactivity to CD8<sup>+</sup> T-cell short epitope candidates. After 20 h of stimulation, the production of IFN- $\gamma$  was measured by ELISA. Data are presented in pg/mL and shown as mean  $\pm$  SD.



DNA vaccination can provide internal antigen, and the protein vaccination largely provides external antigen. However, many reports also demonstrated that alternative “cross-presentation pathway” is a physiologically important pathway to induce CD8<sup>+</sup> T-cell responses to infectious disease and cancer, in which external antigen is presented on MHC-I for inducing CD8<sup>+</sup> T-cell responses [29, 30]. It is also known that using an adjuvant such as CpG in protein vaccination, the immunised protein antigen (this is external antigen) was also efficiently processed and induced CD8<sup>+</sup> T-cell responses via this cross-presentation pathway.

We initially expected the induction of CD8<sup>+</sup> T-cell response with protein + CpG adjuvant immunisation, because it has been shown that CpG adjuvant can induce strong CD8<sup>+</sup>T-cell responses for many protein vaccines, and we also observed the induction of CD8<sup>+</sup> T-cell responses with CpG adjuvant for a variety of antigens (Suppl. Figure 1). This expectation was true for C57BL/6 mice. gH/gL/gQ1/gQ2 tetrameric protein + CpG adjuvant immunisation induced detectable CD8<sup>+</sup> T-cell responses against No. 133, No. 141, and No. 157 peptides (Figure 1(f)). In C57BL/6 mice, CD8<sup>+</sup> T-cell responses to the same three peptides were also similarly induced by the DNA vaccination method (Figure 3(e)). In contrast, this expectation was not met in BALB/c mice. Specifically, protein vaccination did not induce any consistently detectable CD8<sup>+</sup> T-cell responses in these mice (Figure 1(c)). Instead, DNA vaccination induced consistently detectable CD8<sup>+</sup> T-cell responses against No. 13, No. 113, and No. 157 peptides (Figure 2(e)). Interestingly, T-cell responses against No. 13 were only detected by single gH DNA immunisation in BALB/c mice. In contrast, T-cell responses against No. 157 in BALB/c mice were only induced by immunisation with a mixture of DNA (Figure 2(b)), but not with single gQ2 DNA (Figure 2(a)). In C57BL/6 mice, only immunisation with a mixture of DNA led to consistently detectable T-cell responses (Figure 3(b)). This may reflect the status differences of gH/gL/gQ1/gQ2 complex protein structures between single and mixed expression, and the antigen processing and presentation may be influenced by these protein structure-dependent effects. Although these issues need to be examined in future experiments, consistent CD8<sup>+</sup> T-cell responses were only induced by DNA vaccination in BALB/c mice (Figure 2(e)). Similar phenomena have been reported for a tuberculosis vaccine model in mice. In this tuberculosis model, immunisation with rTB10.4 antigen + CAF05 adjuvant (potentially CD8<sup>+</sup> T-cell response-inducing adjuvant composed of DDA/TDB/poly I: C) resulted in only CD4<sup>+</sup> T-cell responses rather than the expected CD8<sup>+</sup> T-cell responses, while the same antigen induced strong CD8<sup>+</sup> T-cell responses with *M. tuberculosis* infection [31], suggesting that recombinant protein vaccination even with a potentially cross-presentation-activating adjuvant like CAF05 or CpG cannot always successfully induce the expected CD8<sup>+</sup> T-cell responses. On the other hand, in a similar tuberculosis model using a different antigen, immunisation with a recombinant adenovirus vector induced mostly CD8<sup>+</sup> T-cell responses and only weak CD4<sup>+</sup> T-cell responses [32]. This situation is similar to the protein vs. DNA immunisation in

this study. Importantly, in the tuberculosis model, CD4<sup>+</sup> T-cell but not CD8<sup>+</sup> T-cell responses were protective against challenge with *M. tuberculosis* infection [31, 32].

Although we could not examine the protective efficacy of the newly identified T-cell epitopes due to the lack of an established animal model for HHV-6B infection, our results demonstrated that an HHV-6B gH/gL/gQ1/gQ2 tetramer complex-targeted vaccine approach can induce multiple CD4<sup>+</sup> and CD8<sup>+</sup> T-cell responses irrespective of the immunised mouse strain, supporting that HHV-6B gH/gL/gQ1/gQ2 tetramer complex is a promising candidate to develop an HHV-6B vaccine.

## 4. Methods

**4.1. Preparation of gH/gL/gQ1/gQ2 Protein Complex.** The preparation of the gH/gL/gQ1/gQ2 tetrameric complex was described in another paper (Wang et al., PLoS Pathogen, in press). In brief, 293 GnTI- cells were transfected with the dual-expression plasmids (pCAGGS-pur-gQ1/gQ2 and pCAGGS-neo-gHFchHis/gL), and the single clone derived tetramer-expressing cell line was established. The cells were cultivated in a chemically defined protein-free medium, CD293 Medium (ThermoFisher Scientific, Waltham, MA) supplemented with 1 µg/ml puromycin and 20 µg/ml gentamicin at 37°C, 5% CO<sub>2</sub> for 2 days, and then the culture supernatant was collected, and the tetramer was further purified by Ni-NTA agarose (Qiagen) and size exclusion column chromatography using a Superdex 200 pg column (GE Healthcare, Buckinghamshire, UK).

**4.2. CpG Adjuvant for Protein Vaccination.** CpG containing adjuvant D35/DOTAP was prepared with NanoAssemblr Benchtop (Precision NanoSystems Inc., BC, Canada), which can mediate bottom-up self-assembly for nanoparticle synthesis with microfluidic mixing technology. D35 (an A-type CpG ODN) [33, 34] was dissolved at 500 µg/mL in 25 mM sodium acetate at pH 4.0. One volume of D35 solution and three volumes of 10 mg/mL DOTAP in ethanol were injected into the microfluidic mixer with a combined final flow rate of 15 mL/min (3.75 mL/min ethanol, 11.25 mL/min aqueous). The D35/DOTAP mixtures were immediately dialysed (50 kDa MWCO dialysis tubing; Repligen Corporation, MA) against 5% glucose solution to remove ethanol and unload D35. D35/DOTAP was filtered through a 0.22-µm PVDF filter (Merck KGaA).

For protein immunisation, 10 µg of the gH/gL/gQ1/gQ2 tetrameric complex and 10 µg of D35/DOTAP (containing D35 amount) were mixed and then made up to a volume of 100 µL with phosphate-buffered saline (PBS).

**4.3. Preparation of PEI-DNA Complex for DNA Vaccination.** The construction of expression plasmids for gH, gL, gQ1, and gQ2 (pCAGGS-gH, pCAGGS-gL, pCAGGS-gQ1, and pCAGGS-gQ2) was described previously [11]. The plasmid was amplified in DH5a *Escherichia coli* and purified using QIAGEN EndoFree Plasmid Maxi Kit (QIAGEN), following the manufacturer’s instructions. The plasmid DNA was complexed with PEI (87 kDa linear; Polysciences Inc.) based on a

method described previously [35]. PEI stock solution was diluted to 1 mg/mL with 5% glucose solution and mixed with an equal volume of glucose solution containing 0.2 mg/mL plasmid DNA to achieve a nitrogen-to-phosphate ratio (N/P) of 7.5. The mixture was incubated for at least 15 min at room temperature for complex formation before use.

**4.4. Peptide Synthesis.** A library containing a total of 162 peptides (No. 1–162) spanning the entire 694-amino-acid (aa) gH sequence, 250-aa gL sequence, 516-aa gQ1 sequence, and 182-aa gQ2 sequence of the HHV-6B HST strain was synthesised by Eurofins Genomics (Tokyo, Japan) as 20-mers overlapping by 10 residues (Supplementary Table 1). All peptides were dissolved in dimethyl sulfoxide (DMSO) at a concentration of 1 mg/ml and stored at  $-80^{\circ}\text{C}$  until use. For peptide vaccination, 10  $\mu\text{g}$  of 20-mer peptide and 10  $\mu\text{g}$  of D35/DOTAP were mixed and then made up to a volume of 100  $\mu\text{L}$  with PBS.

**4.5. Animals and Immunisations.** BALB/c and C57BL/6 mice were purchased from CLEA Japan, Inc., and maintained under specific-pathogen-free conditions in accordance with institutional guidelines. Mice of 5–19 weeks of age were used in all of the experiments. All animal experiments were conducted under the approval of the Animal Research Committee of the Research Institute for Microbial Diseases at Osaka University.

Mice were immunised intradermally with 100  $\mu\text{L}$ /dose of the HHV6B tetrameric complex+ D35/DOTAP as protein vaccination or intravenously with 100  $\mu\text{L}$ /dose of PEI-DNA complex as plasmid DNA vaccination. In addition, mice were immunised intradermally with 100  $\mu\text{L}$ /dose of 20-mer peptide + D35/DOTAP as peptide vaccination.

**4.6. Cell Stimulation with 162 Peptides and IFN- $\gamma$  Assay.** One week after the immunisation, spleens were collected and a single-cell suspension was prepared. Red blood cells were lysed at room temperature with 5 mL of ACK lysing buffer for 3 min and washed with RPMI1640. Then, some of the splenocytes were depleted for CD4<sup>+</sup> or CD8<sup>+</sup> T cells using the MACS system with mouse CD4 microbeads (L3T4; Miltenyi Biotec) or CD8 $\alpha$  microbeads (Ly-2; Miltenyi Biotec), in accordance with the manufacturer's instructions. CD4<sup>+</sup>- or CD8<sup>+</sup>-depleted splenocytes and undepleted splenocytes were resuspended in R-10 (RPMI 1640 containing 10% FBS and 5% penicillin and streptomycin) at a concentration of  $1 \times 10^7$  cells/mL. The splenocytes were seeded at 100  $\mu\text{L}$ /well in 96-well half-area plates (#3696; Corning), in the presence of 10  $\mu\text{g}$ /mL of each of No. 1–162 peptides or 5  $\mu\text{g}$ /mL concanavalin A (Con A) and then cultured at  $37^{\circ}\text{C}$  for 20 h in a 5% CO<sub>2</sub> incubator. The production of IFN- $\gamma$  in each well was assayed in the supernatants using Mouse IFN-gamma DuoSet ELISA kits (R&D Systems). One experiment for detection of the CD4<sup>+</sup> or CD8<sup>+</sup> T-cell response against 162 peptides was assessed using three culture plates. We repeated the experiment at least three times to see the consistency of the responses to each peptide stimulation. For graphical presentation, IFN- $\gamma$  (pg/mL) of each peptide from three culture plates was normalised to the Z score

( $Z = x - \text{mean}/\text{SD}$ , where  $x$  is the quantity of IFN- $\gamma$  for each peptide), and the median Z score from the three independent experiments was calculated for each peptide. A Z score of less than 0.01 was considered to indicate that no response had been detected.

**4.7. Cell Line.** The BW5147 (H2k) lymphoma cell line was transduced retrovirally with a gene encoding one of H2K<sup>d</sup>, H2D<sup>d</sup>, H2L<sup>d</sup>, H2D<sup>b</sup>, and H2K<sup>b</sup>, as described previously [21, 36], and used to determine the CD8<sup>+</sup> T-cell epitope presenting MHC Ia molecule. The cells were maintained in R-10 in an incubator with a humidified atmosphere containing 5% CO<sub>2</sub>.

**4.8. Determination of the Restricted MHC Ia Molecule.** The CD8<sup>+</sup> T-cell epitope presenting H2d molecules including H2K<sup>d</sup>, H2D<sup>d</sup>, and H2L<sup>d</sup> for BALB/c mice, or presenting H2b molecules including H2K<sup>b</sup> and H2D<sup>b</sup> for C57BL/6 mice were determined as previously reported [36]. Briefly, BW5147-H2K<sup>d</sup>, -H2D<sup>d</sup>, -H2L<sup>d</sup>, -H2K<sup>b</sup>, or -H2D<sup>b</sup> cells ( $4 \times 10^6$  cells) were cocultured with each peptide (10  $\mu\text{g}$ /mL) at  $37^{\circ}\text{C}$  for 1 h. The cells were washed three times with RPMI 1640 medium and resuspended in R-10 at a concentration of  $4 \times 10^6$  cells/mL. Splenocytes ( $1 \times 10^6$  cells) from immunised mice were stimulated with each peptide-pulsed BW5147 cell line ( $2 \times 10^5$  cells) in 100  $\mu\text{L}$  of R-10 for 20 h at  $37^{\circ}\text{C}$ , and the IFN- $\gamma$  production was determined by ELISA. BW5147-H2K<sup>d</sup>, -H2D<sup>d</sup>, and -H2L<sup>d</sup> cells were also retrovirally transduced with the gH gene to make BW5147-H2K<sup>d</sup>, -H2D<sup>d</sup>, and -H2L<sup>d</sup> cells internally expressing gH protein.

## Data Availability

All data generated or analysed during this study are included in this published article and its Supplementary Information files.

## Conflicts of Interest

Mie Okutani and Soichiro Kuwabara are employed by the Research Foundation for Microbial Diseases of Osaka University. Yasunari Haseda, Lisa Munakata, Ryo Suzuki, Yasuko Mori, and Taiki Aoshi have filed a patent application related to the content of this manuscript. The remaining authors declare no conflicts of interest.

## Authors' Contributions

M.O and T.A. designed the research; M.O., S.K., and Y.S. conducted the research; A.K., M.N., S.N., S.K., L.M., R.S., and Y.M. contributed critical reagents/tools used for the study; M.O. and T.A. analysed the data; and M.O. and T.A. wrote the paper. All authors reviewed the manuscript.

## Acknowledgments

We thank Jie Meng and Asako Kubota for experimental support, and Saiko Ito for secretarial assistance. We also acknowledge financial support from the Japan Agency for

Medical Research and Development (AMED; grant numbers 16im0210601h0101 and 17im0210601h0102).

## Supplementary Materials

Supplementary Table 1: peptide library used in this study. Supplementary Figure 1: (a) C57BL/6 mice were immunised at the tail base with 40  $\mu\text{g}$  of influenza HA split vaccine with or without D35/DOTAP (D35: 10  $\mu\text{g}$ ) adjuvant. Seven days after immunisation, splenocytes were stimulated with 5  $\mu\text{g}/\text{mL}$  A/California/7/2009 (X-179A) (H1N1) pdm09 or 5  $\mu\text{g}/\text{mL}$  epitope peptide ASNENMETM, which is the H2-Db restricted epitope peptide within the NP of influenza A/PR/8/34 (H1N1). After 20 h of stimulation, the production of IFN- $\gamma$  was measured by ELISA, and data are presented in pg/mL. Note that influenza HA split vaccine is a mixture of equal amounts of A/California/7/2009 (X179A) (H1N1) pdm09, A/Hong Kong/4801/2014 (X-263) (H3N2), B/Phuket/3073/2013 (Yamagata), and B/Texas/2/2013 (Victoria) provided from the Research Foundation for Microbial Diseases of Osaka University. (b) BALB/c mice were immunised at the tail base with 10  $\mu\text{g}$  of LLO91-99 peptide (GYKDG-NEYI) with or without D35/DOTAP (D35: 10  $\mu\text{g}$ ) adjuvant. Seven days after immunisation, splenocytes were stimulated with 5  $\mu\text{g}/\text{mL}$  LLO91-99 peptide. After 20 h of stimulation, the production of IFN- $\gamma$  was measured by ELISA, and data are presented in pg/mL. Supplementary Figure 2: short peptide stimulation and the restricted MHC I molecule determination after expression plasmid DNA vaccination in C57BL/6 mice. (a) C57BL/6 splenocytes immunised with a mixture of gH, gL, gQ1, and gQ2 expression plasmids were stimulated with the indicated CD8+ T-cell short epitope candidate peptides. After 20 h of stimulation, IFN- $\gamma$  (pg/mL) of each peptide was measured by ELISA (A; left). The restricted MHC I molecules were examined by each peptide-pulsed BW5147 cell line expressing H2Db or H2Kb (a; right). (b) C57BL/6 splenocytes immunised with a mixture of gH, gL, gQ1, and gQ2 expression plasmids were first depleted of CD4+ T cells (to increase the detection sensitivity of CD8+ T-cell responses) and then stimulated with the indicated CD8+ T-cell short epitope candidate peptides. After 20 h of stimulation, IFN- $\gamma$  (pg/mL) of each peptide was measured by ELISA (b; left). The restricted MHC I molecules were examined with each peptide-pulsed BW5147 cell line expressing H2Db or H2Kb (b; right). (*Supplementary Materials*)

## References

- [1] L. De Bolle, L. Naesens, and E. De Clercq, "Update on human herpesvirus 6 biology, clinical features, and therapy," *Clinical Microbiology Reviews*, vol. 18, no. 1, pp. 217–245, 2005.
- [2] D. V. Ablashi, N. Balachandran, S. F. Josephs et al., "Genomic polymorphism, growth properties, and immunologic variations in human herpesvirus-6 isolates," *Virology*, vol. 184, no. 2, pp. 545–552, 1991.
- [3] B. Chandran, S. Tirawatnpong, B. Pfeiffer, and D. V. Ablashi, "Antigenic relationships among human herpesvirus-6 iso-
- [4] D. Ablashi, H. Agut, R. Alvarez-Lafuente et al., "Classification of HHV-6A and HHV-6B as distinct viruses," *Archives of Virology*, vol. 159, no. 5, pp. 863–870, 2014.
- [5] H. Agut, P. Bonnafous, and A. Gautheret-Dejean, "Mise au point sur les herpesvirus humains 6A, 6B et 7," *Médecine et Maladies Infectieuses*, vol. 47, no. 2, pp. 83–91, 2017.
- [6] K. Yamanishi, T. Okuno, K. Shiraki et al., "Identification of human herpesvirus-6 as a causal agent for exanthem subitum," *Lancet*, vol. 331, no. 8594, pp. 1065–1067, 1988.
- [7] T. Yoshikawa, M. Ohashi, F. Miyake et al., "Exanthem subitum-associated encephalitis: nationwide survey in Japan," *Pediatric Neurology*, vol. 41, no. 5, pp. 353–358, 2009.
- [8] P. Ljungman, F. Z. Wang, D. A. Clark et al., "High levels of human herpesvirus 6 DNA in peripheral blood leucocytes are correlated to platelet engraftment and disease in allogeneic stem cell transplant patients," *British Journal of Haematology*, vol. 111, no. 3, pp. 774–781, 2000.
- [9] M. Ogata, T. Fukuda, and T. Teshima, "Human herpesvirus-6 encephalitis after allogeneic hematopoietic cell transplantation: what we do and do not know," *Bone Marrow Transplantation*, vol. 50, no. 8, pp. 1030–1036, 2015.
- [10] T. Okuno, K. Takahashi, K. Balachandra et al., "Seroepidemiology of human herpesvirus 6 infection in normal children and adults," *Journal of Clinical Microbiology*, vol. 27, no. 4, pp. 651–653, 1989.
- [11] H. Tang, S. Serada, A. Kawabata et al., "CD134 is a cellular receptor specific for human herpesvirus-6B entry," *Proceedings of the National Academy of Sciences of the United States of America*, vol. 110, no. 22, pp. 9096–9099, 2013.
- [12] H. Tang, J. Wang, N. F. Mahmoud, and Y. Mori, "Detailed study of the interaction between human herpesvirus 6B glycoprotein complex and its cellular receptor, human CD134," *Journal of Virology*, vol. 88, no. 18, pp. 10875–10882, 2014.
- [13] N. Babic, B. G. Klupp, B. Makoschey, A. Karger, A. Flamand, and T. C. Mettenleiter, "Glycoprotein gH of pseudorabies virus is essential for penetration and propagation in cell culture and in the nervous system of mice," *The Journal of General Virology*, vol. 77, no. 9, pp. 2277–2285, 1996.
- [14] S. van Drunen Littel-van den Hurk, S. Khatat, S. K. Tikoo et al., "Glycoprotein H (gH/gp 108) and glycoprotein L form a functional complex which plays a role in penetration, but not in attachment, of bovine herpesvirus 1," *Journal of General Virology*, vol. 77, no. 7, pp. 1515–1520, 1996.
- [15] G. Dominguez, T. R. Dambaugh, F. R. Stamey, S. Dewhurst, N. Inoue, and P. E. Pellett, "Human herpesvirus 6B genome sequence: coding content and comparison with human herpesvirus 6A," *Journal of Virology*, vol. 73, no. 10, pp. 8040–8052, 1999.
- [16] U. A. Gompels, J. Nicholas, G. Lawrence et al., "The DNA sequence of human herpesvirus-6: structure, coding content, and genome evolution," *Virology*, vol. 209, no. 1, pp. 29–51, 1995.
- [17] Y. Isegawa, T. Mukai, K. Nakano et al., "Comparison of the complete DNA sequences of human herpesvirus 6 variants A and B," *Journal of Virology*, vol. 73, no. 10, pp. 8053–8063, 1999.
- [18] S. F. Josephs, D. V. Ablashi, S. Z. Salahuddin, L. L. Jagodzinski, F. Wong-Staal, and R. C. Gallo, "Identification of the human herpesvirus 6 glycoprotein H and putative large tegument

- protein genes," *Journal of Virology*, vol. 65, no. 10, pp. 5597–5604, 1991.
- [19] K. Takeda, T. Okuno, M. Haque, Y. Isegawa, K. Yamanishi, and T. Sunagawa, "Identification of a variant B-specific neutralizing epitope on glycoprotein H of human herpesvirus-6," *The Journal of General Virology*, vol. 78, no. 9, pp. 2171–2178, 1997.
- [20] A. Kawabata, H. Oyaizu, T. Maeki, H. Tang, K. Yamanishi, and Y. Mori, "Analysis of a neutralizing antibody for human herpesvirus 6B reveals a role for glycoprotein Q1 in viral entry," *Journal of Virology*, vol. 85, no. 24, pp. 12962–12971, 2011.
- [21] S. Nagamata, T. Aoshi, A. Kawabata et al., "Identification of CD4 and H-2K<sup>d</sup>-restricted cytotoxic T lymphocyte epitopes on the human herpesvirus 6B glycoprotein Q1 protein," *Scientific Reports*, vol. 9, no. 1, p. 3911, 2019.
- [22] Y. Haseda, L. Munakata, J. Meng, R. Suzuki, and T. Aoshi, "Microfluidic-prepared DOTAP nanoparticles induce strong T-cell responses in mice," *PLoS One*, vol. 15, no. 1, article e0227891, 2020.
- [23] T. H. Thatcher, D. P. O'Brien, S. Altuwajjri, and R. K. Barth, "Increasing the frequency of T-cell precursors specific for a cryptic epitope of hen-egg lysozyme converts it to an immunodominant epitope," *Immunology*, vol. 99, no. 2, pp. 235–242, 2000.
- [24] C. Cheadle, M. P. Vawter, W. J. Freed, and K. G. Becker, "Analysis of Microarray Data Using Z Score Transformation," *Journal of Molecular Diagnostics*, vol. 5, no. 2, pp. 73–81, 2003.
- [25] F. P. Heinzl, M. D. Sadick, B. J. Holaday, R. L. Coffman, and R. M. Locksley, "Reciprocal expression of interferon gamma or interleukin 4 during the resolution or progression of murine Leishmaniasis. Evidence for expansion of distinct helper T cell subsets," *Journal of Experimental Medicine*, vol. 169, no. 1, pp. 59–72, 1989.
- [26] N. Jovicic, I. Jetic, I. Jovanovic et al., "Differential Immunometabolic phenotype in Th1 and Th2 dominant mouse strains in response to high-fat feeding," *PLoS One*, vol. 10, no. 7, pp. e0134089–e0134089, 2015.
- [27] H. Watanabe, K. Numata, T. Ito, K. Takagi, and A. Matsukawa, "INNATE immune response in Th1- and Th2-dominant mouse strains," *Shock*, vol. 22, no. 5, pp. 460–466, 2004.
- [28] K. T. HayGlass, B. Nashed, S. Haile, A. J. Marshall, and W. Thomas, "C57Bl/6 and BALB/c mice do not represent default Th1 and Th2 strains in allergen-driven immune responses," *Journal of Allergy and Clinical Immunology*, vol. 115, no. 2, Supplement, p. S258, 2005.
- [29] K. Hildner, B. T. Edelson, W. E. Purtha et al., "Batf3 deficiency reveals a critical role for CD8+ dendritic cells in cytotoxic T cell immunity," *Science*, vol. 322, no. 5904, pp. 1097–1100, 2008.
- [30] L. J. Sigal, S. Crotty, R. Andino, and K. L. Rock, "Cytotoxic T-cell immunity to virus-infected non-haematopoietic cells requires presentation of exogenous antigen," *Nature*, vol. 402, no. S6763, pp. 25–29, 1999.
- [31] T. Lindenstrøm, C. Aagaard, D. Christensen, E. M. Agger, and P. Andersen, "High-frequency vaccine-induced CD8+ T cells specific for an epitope naturally processed during infection with *Mycobacterium tuberculosis* do not confer protection," *European Journal of Immunology*, vol. 44, no. 6, pp. 1699–1709, 2014.
- [32] T. Bennekov, J. Dietrich, I. Rosenkrands, A. Stryhn, T. M. Doherty, and P. Andersen, "Alteration of epitope recognition pattern in Ag85B and ESAT-6 has a profound influence on vaccine-induced protection against *Mycobacterium tuberculosis*," *European Journal of Immunology*, vol. 36, no. 12, pp. 3346–3355, 2006.
- [33] T. Aoshi, Y. Haseda, K. Kobiyama et al., "Development of Nonaggregating Poly-a Tailed Immunostimulatory a/D Type CpG Oligodeoxynucleotides Applicable for Clinical Use," *Journal of Immunology Research*, vol. 2015, 20 pages, 2015.
- [34] D. Verthelyi, K. J. Ishii, M. Gursel, F. Takeshita, and D. M. Klinman, "Human peripheral blood cells differentially recognize and respond to two distinct CPG motifs," *Journal of Immunology*, vol. 166, no. 4, pp. 2372–2377, 2001.
- [35] M. Thomas, J. J. Lu, Q. Ge, C. Zhang, J. Chen, and A. M. Klibanov, "Full deacylation of polyethylenimine dramatically boosts its gene delivery efficiency and specificity to mouse lung," *Proceedings of the National Academy of Sciences of the United States of America*, vol. 102, no. 16, pp. 5679–5684, 2005.
- [36] T. Aoshi, M. Suzuki, M. Uchijima, T. Nagata, and Y. Koide, "Expression mapping using a retroviral vector for CD8<sup>+</sup> T cell epitopes: Definition of a *Mycobacterium tuberculosis* peptide presented by H2-D<sup>d</sup>," *Journal of Immunological Methods*, vol. 298, no. 1-2, pp. 21–34, 2005.

## Review Article

# The Pathogenesis of Coronavirus Disease 2019 (COVID-19): Evaluation and Prevention

Hayat Ouassou <sup>1</sup>, Loubna Kharchoufa <sup>1</sup>, Mohamed Bouhrim <sup>1</sup>,  
Nour Elhouda Daoudi <sup>1</sup>, Hamada Imtara <sup>2</sup>, Nouredine Bencheikh <sup>1</sup>,  
Amine ELbouzidi <sup>3</sup>, and Mohamed Bnouham <sup>1</sup>

<sup>1</sup>Laboratory of Bioresources, Biotechnology, Ethnopharmacology and Health, Faculty of Sciences, Mohammed First University, Oujda, Morocco

<sup>2</sup>Faculty of Arts and Sciences, Arab American University Palestine, P. O. Box 240, Jenin, State of Palestine

<sup>3</sup>Faculty of sciences, Mohammed First University, Morocco

Correspondence should be addressed to Mohamed Bnouham; mbnouham@yahoo.fr

Received 23 March 2020; Accepted 5 May 2020; Published 10 July 2020

Academic Editor: Roberta Antonia Diotti

Copyright © 2020 Hayat Ouassou et al. This is an open access article distributed under the Creative Commons Attribution License, which permits unrestricted use, distribution, and reproduction in any medium, provided the original work is properly cited.

Coronavirus Disease 2019 (COVID-19) has become a major health problem causing severe acute respiratory illness in humans. It has spread rapidly around the globe since its first identification in Wuhan, China, in December 2019. The causative virus is called severe acute respiratory syndrome coronavirus 2 (SARS-CoV-2), and the World Health Organization (WHO) named the new epidemic disease Coronavirus Disease (COVID-19). The incidence of COVID-19 continues to increase with more than three million confirmed cases and over 244,000 deaths worldwide. There is currently no specific treatment or vaccine against COVID-19. Therefore, in the absence of pharmaceutical interventions, the implementation of precautions and hygienic measures will be essential to control and to minimize human transmission of the virus. In this review, we highlight the epidemiology, transmission, symptoms, and treatment of this disease, as well as future strategies to manage the spread of this fatal coronavirus.

## 1. Introduction

Coronaviruses belong to the Coronaviridae family in the Nidovirales order. Corona represents crown-like spikes on the outer surface of the virus; thus, it was named coronavirus. Coronaviruses are minute in size (65-125 nm in diameter) and contain a single-stranded RNA as nucleic material, with a size ranging from 26 to 32 kilobases (kb) in length. The subgroups of the coronavirus family are alpha ( $\alpha$ ), beta ( $\beta$ ), gamma ( $\gamma$ ), and delta ( $\delta$ ) [1]. Several coronaviruses can infect humans, like the globally endemic human coronaviruses HCoV-229E, HCoV-NL63, HCoV-HKU1, and HCoV-OC43 that tend to cause mild respiratory disease, and the zoonotic Middle East respiratory syndrome coronavirus (MERS-CoV) and severe acute respiratory syndrome coronavirus (SARS-CoV) that have a higher case fatality rate [2]. In

late December 2019, a cluster of patients was admitted to hospitals with an initial diagnosis of pneumonia of an unknown etiology. These patients were epidemiologically linked to a seafood and wet animal wholesale market in Wuhan, Hubei Province, China [3, 4]. The pathogen has been identified as a novel coronavirus. Initially tentatively named 2019 novel coronavirus (2019-nCoV), the virus has now been named SARS-CoV-2 by the International Committee of Taxonomy of Viruses (ICTV) [5]. This virus can cause the disease named coronavirus disease 2019 (COVID-19) [5]. The SARS-CoV-2 belongs to the same coronavirus group (Betacoronavirus) as SARS and MERS viruses that caused two of the more severe epidemics in recent years. As with SARS and MERS, this new coronavirus, 2019-nCoV, is believed to be of zoonotic origin, but may also be transmitted through the respiratory tract, by direct contact, and possibly

via patients excreta which may contain the living virus [6]. Since the emergence of the 2019 novel coronavirus (2019-nCoV) infection in Wuhan, China, it has rapidly spread across China and many other countries [7]. The outbreak of COVID-19 has affected more than three million patients in 187 countries, areas, or territories with a mortality rate of 4.20% and has become a major global health concern [8]. Based on the evidence of a rapidly increasing incidence of infections and the possibility of transmission by asymptomatic carriers [9, 10], SARS-CoV-2 can be transmitted effectively among humans and exhibits high potential for a pandemic [11–13]. To date, the disease has spread worldwide and become a serious infectious disease affecting human health worldwide [14]. In the absence of specific therapeutic drugs or vaccines for 2019 novel coronavirus disease (COVID-19), it is essential to detect the diseases at an early stage and immediately isolate the infected person from the healthy population. In this paper, we attempt to review and document the current data related to Corona Virus Disease 2019 (COVID-19) including etiology, epidemiology, clinical characteristics, and measures of treatment of COVID-19, with a special focus on infection control and prevention.

## 2. Epidemiology of COVID-19

In December 2019, Wuhan City, Province of China, became the center of an outbreak of novel contagious coronavirus disease (COVID-19) of unknown etiology [11, 15]. Efforts are underway to continue to better understand more about transmissibility, severity, and other features associated with COVID-19 [16]. It appears that an infected animal may have first transmitted the virus to humans at a seafood market [17, 18]. Soon, a secondary source of infection was found to be human-to-human transmission of the COVID-19 virus [19]. It became clear that the COVID-19 infection occurs among close contacts and exposure to the virus [17]. Recent studies showed that people aged  $\geq 60$  years and the population with poor immune function such as diabetes, cardiovascular disease, chronic respiratory disease, cancer, renal, and hepatic dysfunction are at higher risk for severe COVID-19 than children who might be less likely to become infected or, if so, may show milder symptoms or even asymptomatic infection [20]. Coronavirus disease 2019 (COVID-19) is spreading rapidly across China and is being exported to a growing number of countries, some of which have seen onward transmission. According to the World Health Organization (WHO), COVID-19 continues to emerge and represents a serious problem to public health. On 2 May of March 2020, more than three million confirmed cases of COVID-19 reported by the World Health Organization. Of these, more than 240 000 have been fatal. About 83,959 cases were confirmed in China, and 4637 deaths were confirmed (Figure 1) [8]. The growing global tally includes spikes in Korea, Iran, Italy, Spain, France, and Germany. The virus is also continuing to spread to African countries including Algeria, South Africa, Senegal, Burkina Faso, Cameroon, Nigeria, and Côte d'Ivoire. In addition to the confirmed case,

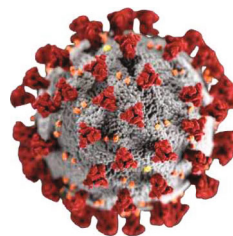


FIGURE 1: A graphical representation of the ultrastructural morphology of coronavirus (SARS-CoV-2). Source: Centers for Disease Control and Prevention—Public Health Image Library. Credit: Alissa Eckert, MS, Dan Higgins, MAM (Public Domain).

Moroccan's health ministry says that Morocco has more than 4500 confirmed cases of the coronavirus.

## 3. Origin and Transmission of COVID-19

The SARS-CoV-2 was found to be a positive-stranded RNA virus belonging to the genus Betacoronavirus with a crown due to the presence of spike glycoproteins on the envelope (Figure 2) [7]. Other than SARS-CoV-2, there are six types as humans coronaviruses have been identified, namely, HCoV-229E, HCoV-OC43, SARS-CoV, HCoV-NL63, HCoV-HKU1, and MERS-CoV [21]. Phylogenetic analysis revealed that the SARS-CoV-2 is closely related, with 88–89% similarity, to two bat-derived severe acute respiratory syndrome- (SARS-) like coronaviruses, bat-SL-CoVZC45 (accession no. MG772933.1), and bat-SL-CoVZXC21 (accession no. MG772934.1), but it is more distant from SARS-CoV, with about 79% similarity, and MERS-CoV, with about 50% similarity [22–24]. The SARS-CoV-2 has an envelope; its particles are round or elliptic and often polymorphic form, and a diameter of 60 nm to 140 nm [25]. Additional studies based on the genetic sequence identity and the phylogenetic reports confirmed that COVID-19 is different from SARS-CoV, and it can thus be considered as a new betacoronavirus that infects humans [26].

The source of the 2019-nCoV is still unknown. However, the growing outbreak has been linked to the Huanan South China Seafood Market [27]. Scientists are trying to find the animal host of this novel coronavirus in hopes of eradicating the spread, but so far, no one is certain. Most sources agree that the possible host of the 2019-nCoV is bats, pangolins, or seafood [3, 4, 25]. The task at hand is to find the intermediate host that is responsible for transmitting the coronavirus to humans. It is important to determine the source of the virus, to help the discovery of the zoonotic transmission patterns [25]. SARS-CoV-2 presents a high transmissibility and pathogenicity [28]. It could be transmitted from human to human by droplets and contact [28]. Several reports have suggested that symptomatic people are the most frequent source of COVID-19 spread. It primarily spreads between people through respiratory droplets by coughing or sneezing from an infected individual [26]. Moreover, there are suggestions that individuals who remain asymptomatic could transmit the virus. Further, studies are needed to clarify and understand the mechanisms of transmission, the incubation period, and the duration of infectivity of this virus.

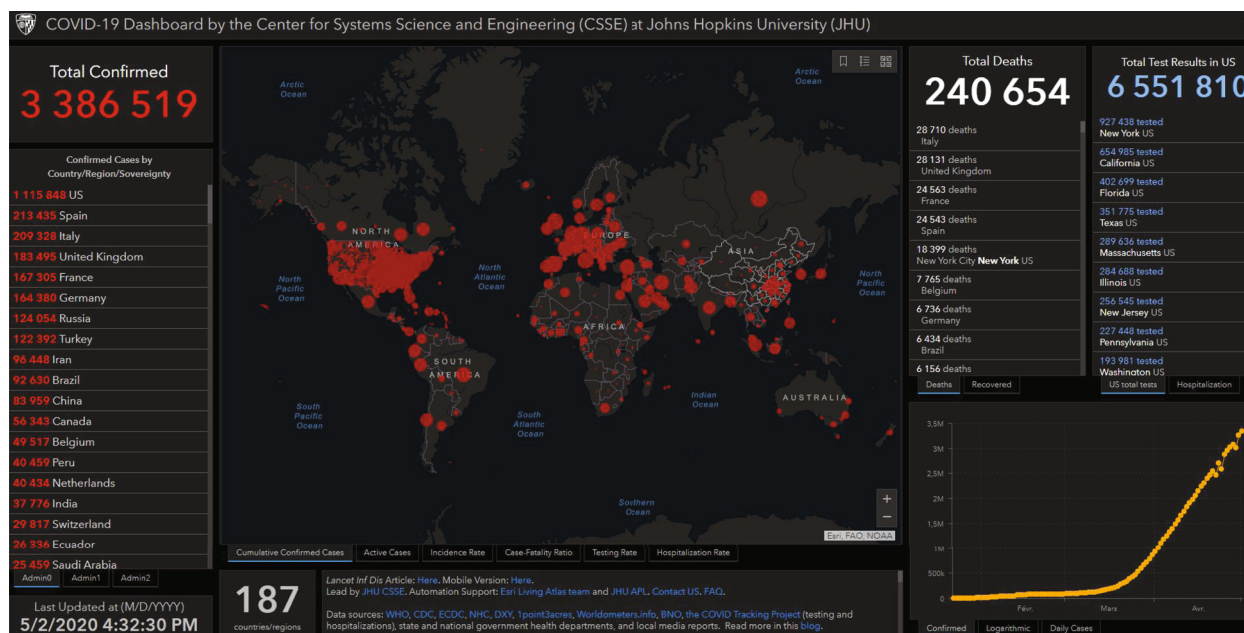


FIGURE 2: World map represents the geographical distribution of COVID-19 outbreaks. Data accurate as of 21 March 2020 [8].

#### 4. Clinical Characteristics of COVID-19

In patients with Coronavirus disease 2019 (COVID-19), the most common clinical symptoms are fever and cough, shortness of breath, and other breathing difficulties in addition to other nonspecific symptoms, including headache, dyspnea, fatigue, and muscle pain [29, 30]. Moreover, some patients also report digestive symptoms such as diarrhea and vomiting [11, 30]. COVID-19 was similar to SARS and MERS in some clinical manifestations [29]. Fever occurred in 98-100% of patients with SARS or MERS, compared to 81.3% of patients with COVID-19 [29, 31, 32]. 18.7% of patients had no fever at admission, suggesting that the absence of fever could not rule out the possibility of COVID-19 [29]. Although patients initially have fever with or without respiratory symptoms, various degrees of lung abnormalities develop later in all patients, and these can be seen on chest CT (CT) [11, 33]. Although diarrhea is present in approximately 20-25% of patients infected with MERS-Cov or SARS-Cov, intestinal symptoms have rarely been reported in patients with COVID-19 [34]. Patients receive chest CT scans that provide reliable data on the dynamic X-ray pattern. Typical mild COVID-19 pneumonia begins primarily with small, subpleural, unilateral, or bilateral frosted glass opacities in the lower lobes, which then develop into a crazy-paving pattern and subsequent consolidation. After more than two weeks, the lesions are gradually absorbed with residual frosted glass opacities and subpleural parenchymal bands. In these patients who have recovered from COVID-19 pneumonia [35]. At admission, the majority of patients had lymphopenia and platelet abnormalities, neutrophils, aspartate aminotransferase (AST), aspartate aminotransferase (AST), lactate dehydrogenase (LDH), and inflammatory biomarkers. According to the results of the CT or X-ray, the patients had bilateral pneumonia and pleural effusion that occurred in 10.3% of the patients. Compared to

patients in general, refractory patients had a higher level of neutrophils, AST, LDH, and reactive protein C and a lower level of platelets and albumin. In addition, refractory patients had a higher incidence of bilateral pneumonia and pleural effusion [36]. In general, hospitalized patients are classified in two categories, the general COVID-19 which has been defined according to the following criteria: obvious relief of respiratory symptoms (for example, cough, chest distress, and shortness of breath) after treatment, maintaining normal body temperature for more than three days without the use of corticosteroids or antipyretics, improving radiological abnormalities in the chest scanner or X-rays after treatment, a hospital stay of less than 10 days. Otherwise, it was classified as COVID-19 refractory. In the admission severity assessment, a serious illness was defined if it met at least one of the following: respiratory rate 30/min, pulse oximeter oxygen saturation (Spo<sub>2</sub>) 93% at rest, and partial arterial oxygen pressure (PaO<sub>2</sub>) at the inspired oxygen fraction (Fio<sub>2</sub>) 300 mmHg [29].

#### 5. Treatment of COVID-2019

After the diagnosis of SARS-Cov2 infection was made, the prevention and quarantine are considered as the most way to stop the fast spreading of the virus, because there is no effective vaccine, drugs, or antiviral to prevent and treat this disease despite the great efforts made by the scientists and researchers around the world to develop vaccines and treatments of coronavirus. Furthermore, several strategies were carried out to help patients with COVID-2019 as oxygen therapy (major treatment intervention), antivirals (Lopinavir, Ritonavir, Ribavirin, Favipiravir (T-705), remdesivir, oseltamivir, Chloroquine, and Interferon) [25, 37, 38]. Most importantly, unselective or inappropriate administration of antibiotics should be avoided. Moreover, corticosteroids treatment should not be given for the treatment of SARS-Cov2 [39]. Convalescent plasma can

be used to help people recover from viral infection without the occurrence of severe adverse events [40].

Among the difficulties that avoid finding the treatment for COVID-2019 is that the spike protein of the virus interacts with the host cell receptor including GRP78 (Glucose Regulating Protein 78). Consequently, the inhibition of this interaction would probably decrease the rate of the infection [41]. Lopinavir (protease inhibitor used to treat HIV) or Lopinavir/Ritonavir has shown *in vitro* anti-coronavirus activity [42]. In addition, the utilization of Lopinavir/Ritonavir showed a reduction of viral loads and it was found that it is able to improve virus symptoms during the treatment period [43]. Other reported antiviral treatments for human pathogenic CoVs include neuraminidase inhibitors like oral oseltamivir has been used in China hospitals for COVID-2019 cases [44]. No study has demonstrated the effectiveness of oseltamivir in the treatment of SARS-CoV-2 [42]. In Wuhan, on 6 February 2020, a clinical trial was initiated of remdesivir (Newly discovered antiviral drug) on SARS-CoV-2. This compound showed an inhibition of the replication of SARS-CoV and MERS-CoV in tissue cultures and efficacy in animal models [45]. However, given the related issues of security, safety, and efficacy, it is necessary to take some time to develop the vaccine and the antiviral drugs [46].

For a thousand years, Traditional Chinese medicine has gained an important experience in the infection healing. Currently, this kind of medicine has provided significant therapies for many current diseases as A H1N1 Influenza, A H7N9 Influenza, Ebola virus, and SARS-CoV [46–48]. Consequently, it can be also developed and applied in the treatment of COVID-2019. In fact, the decoction combination of Ma Xing Gan Shi (Combination includes *Ephedrae herba*, *Armeniacae semen amarum*, *Glycyrrhizae radix and rhizoma*, and *Gypsum fibrosum*) with Da Yuan Yin that includes *Arecae semen*, *Magnoliae officinalis cortex*, *Tsaoko fructus*, *Anemarrhenae rhizoma*, *Dioscoreae rhizoma*, *Scutellariae radix*, *Glycyrrhizae radix*, and *rhizoma* had showed in 2003 an important and a significant impact on SARS. The State Administration of Traditional Chinese Medicine advised on 6 February 2020, the utilization of Qing Fei Pai Du decoction that includes *Ephedrae herba*, *Gypsum fibrosum*, *Pinelliae rhizoma*, *Aurantii fructus immaturus*, and *Zingiberis rhizoma recen*. This decoction has been shown to be 90% effective in the treatment of SARS-CoV-2 [46, 49]. Besides, other Chinese herb combinations have been used to treat SARS-CoV infection like

- (i) Yin Qiao San composed with *Fructus Forsythiae*, *Flos Lonicerae*, *Radix Platycodonis*, *Herba Menthae*, *Herba Lophatheri*, *Radix Glycyrrhizae*, *Herba Schizonepetae*, *Fermented soybean*, *Fructus arctii*, and *Rhizoma Phragmitis*
- (ii) Yu Ping Feng San includes *Astragali radix*, *Astragalus membranaceus*, *Atractylodes macrocephala*, and *Saposhnikoviae Radix*
- (iii) Shuang Huang Lian includes *Lonicera japonica*, *Scutellaria baicalensis*, and *Forsythia suspensa*

- (iv) Lian Hua Qing Wen Capsule includes *Forsythia suspensa*, *Ephedra sinica*, *Lonicera japonica*, *Isatis indigotica*, *Mentha haplocalyx*, *Dryopteris crassirhizoma*, *Rhodiola rosea*, *Gypsum Fibrosum*, *Pogostemon cablin*, *Rheum palmatum*, *Houttuynia cordata*, *Glycyrrhizae, uralensis*, and *Armeniacae sibirica*. This treatment can be used to control fever, cough, and tired related with COVID-19 [49]

Actually, there is no specific treatment or vaccine of COVID-2019; all of the drug options come from experience treating influenza, HIV, SARS, or MERS. At present, current efforts are focused on developing vaccines or specific antiviral drugs for COVID-19.

## 6. Infection Control and Prevention of COVID-19

According to what was published by the World Health Organization and a number of international health institutes, there are many restrictions that must be followed, either on a personal level or on the environmental level, including early recognition by the patients; carrying out additional precautions for persons suspected of infection, as well as for people who had contact with patients before their patients were revealed; applying standard precautions for all patients and imposing administrative measures from various authorities, such as the environment and health authorities [50, 51]. In the current situation and to limit the spread of the COVID-19 virus, all countries should publish an awareness declaration of the symptoms of infection in all cities, especially in remote areas. Also, publish the easiest and fastest way for the methods that every patient should follow in the event of a patient. In addition, encourage HCWs to have a high level of clinical suspicion [52, 53]. The WHO confirmed that the rational, correct, and consistent use of personal protective equipment (PPE) also helps reduce the spread of pathogens. PPE effectiveness depends strongly on adequate and regular supplies, adequate staff training, appropriate hand hygiene, and appropriate human behaviour [51, 54, 55].

At the level of additional precautions for patients, patients should be isolated in private quarantine rooms; everyone who contact with the patients, whether family, friends, or visitors, should be placed in a quarantine and a distance for contacting between them should be established [56]; the patients should cover their mouth and nose during sneezing by using masks or tissue as well as the persons COVID-19 suspected should place medical masks in public places and closed rooms and after every sneeze; the patient must wash their hands well (with an alcohol-based hand rub or with soap and water), as a result of coming into contact with respiratory secretions; a proper and careful approach should be taken to eliminate all waste from patient uses [55], reducing as much as possible the exchange of equipment between patients and sterilizing them well when transporting them from one patient to another and after patient care, appropriate doffing and disposal of all PPE and hand hygiene should be carried out



[54]. At the level of additional precautions for health care workers (HCWs), a specialized team must be identified to deal with the patients to limit the spread of infection through protection methods, including the use of a medical mask, use of gloves, wearing of eye protection or facial protection, and wearing a clean, nonsterile, and long-sleeved gown; health care workers are prohibited from touching their eyes and nose with gloves or uncovered hands and limit the number of HCWs, family members, and visitors who are in contact with suspected or confirmed COVID-19 patients [54, 55]. At the level of additional precautions for the environment surrounding patients, the surfaces and places that patients come in contact with should be sterilized regularly; ensure adequate ventilation in the health care facility; separation of at least one meter should be maintained between all patients and manage laundry, food service utensils, and medical waste in accordance with safe routine procedures [57, 58]. The last section is on administrative policies and regulations that include educating caregivers on how to dealing patients, developing policies and plans through which early recognition of acute respiratory infection potentially caused by COVID-19 virus, preventing overcrowding in public places as much as possible, ensuring that the necessary equipment for health care is provided in sufficient quantities and permanently, providing protection to quarantine areas by the authorities to reduce patients' contact with healthy people, and imposing sanctions on those who violate the provisions that have been put in place by the authorities to limit the spread of the COVID-19 virus [56].

## 7. Conclusion

In conclusion, COVID-19 has become a high risk to the general population and healthcare workers worldwide. However, scientific research is growing to develop a coronavirus vaccine and therapeutics for controlling the deadly COVID-19. Hence, health education on knowledge for disease prevention and control is also important to control and reduce the coronavirus infection rate. Further research should be directed toward the study of SARS-CoV-2 on animal models for analyzing replication, transmission, and pathogenesis in humans.

## Abbreviations

WHO:	World Health Organization
Covid-19:	Coronavirus disease 2019
SASRS-Cov2:	Severe acute respiratory syndrome coronavirus 2
SARS-Coc:	Severe acute respiratory syndrome coronavirus
MERS-Cov:	Middle East respiratory syndrome coronavirus
HCov:	Human coronavirus
ICTV:	International Committee of Taxonomy of Viruses
CT:	Computed tomography
HIV:	Human immunodeficiency virus
PPE:	Personal protective equipment
HCW:	Health care workers.

## Conflicts of Interest

The authors declare that there is no conflict of interest regarding the publication of this article.

## Acknowledgments

This work was supported by grants from the CNRST of Morocco, (Project PPR2 /2016/14 PPR2).

## References

- [1] M. A. Shereen, S. Khan, A. Kazmi, N. Bashir, and R. Siddique, "COVID-19 infection: origin, transmission, and characteristics of human coronaviruses," *Journal of Advanced Research*, vol. 24, pp. 91–98, 2020.
- [2] World Health Organization, *Laboratory testing for coronavirus disease 2019 (COVID-19) in suspected human cases*, World Health Organization, 2020.
- [3] H. Lu, C. W. Stratton, and Y. W. Tang, "Outbreak of pneumonia of unknown etiology in Wuhan China: the mystery and the miracle," *Journal of Medical Virology*, vol. 92, no. 4, pp. 401–402, 2020.
- [4] I. I. Bogoch, A. Watts, A. Thomas-Bachli, C. Huber, M. U. G. Kraemer, and K. Khan, "Pneumonia of unknown aetiology in Wuhan, China: potential for international spread via commercial air travel," *Journal of Travel Medicine*, vol. 27, no. 2, 2020.
- [5] A. E. Gorbalenya, S. C. Baker, R. S. Baric et al., "Severe acute respiratory syndrome-related coronavirus: The species and its viruses – a statement of the Coronavirus Study Group," *BioRxiv*, 2020.
- [6] H.-W. Zhang, J. Yu, H. J. Xu et al., "Corona virus international public health emergencies: implications for radiology management," *Academic Radiology*, vol. 27, no. 4, pp. 463–467, 2020.
- [7] C. C. Lai, T.-P. Shih, W. C. Ko, H. J. Tang, and P.-R. Hsueh, "Severe acute respiratory syndrome coronavirus 2 (SARS-CoV-2) and coronavirus disease-2019 (COVID-19): The epidemic and the challenges," *International Journal of Antimicrobial Agents*, vol. 55, no. 3, article 105924, 2020.
- [8] World Health Organization, "Coronavirus disease 2019 (COVID-19): Situation Report 61," March 2020, <https://www.who.int/emergencies/diseases/novel-coronavirus-2019/situation-reports>.
- [9] C. Biscayart, P. Angeleri, S. Lloveras, T. . S. S. Chaves, P. Schlagenhauf, and A. J. Rodríguez-Morales, "The next big threat to global health? 2019 novel coronavirus (2019-nCoV): what advice can we give to travellers? – Interim recommendations January 2020, from the Latin-American society for travel medicine (SLAMVI)," *Travel Medicine and Infectious Disease*, vol. 33, article 101567, 2020.
- [10] S. Zhao, Q. Lin, J. Ran et al., "Preliminary estimation of the basic reproduction number of novel coronavirus (2019-nCoV) in China, from 2019 to 2020: a data-driven analysis in the early phase of the outbreak," *International Journal of Infectious Diseases*, vol. 92, pp. 214–217, 2020.
- [11] C. Huang, Y. Wang, X. Li et al., "Clinical features of patients infected with 2019 novel coronavirus in Wuhan, China," *The Lancet*, vol. 395, no. 10223, pp. 497–506, 2020.
- [12] W. G. Carlos, C. S. Dela Cruz, B. Cao, S. Pasnick, and S. Jamil, "Novel Wuhan (2019-nCoV) coronavirus," *American Journal of Respiratory and Critical Care Medicine*, vol. 201, no. 4, pp. P7–P8, 2020.

- [13] G. Chowell, F. Abdirizak, S. Lee et al., "Transmission characteristics of MERS and SARS in the healthcare setting: a comparative study," *BMC Medicine*, vol. 13, no. 1, p. 210, 2015.
- [14] C. Li, Y. Yang, and L. Ren, "Genetic evolution analysis of 2019 novel coronavirus and coronavirus from other species," *Infection, Genetics and Evolution*, vol. 82, p. 104285, 2020.
- [15] F. Wu, S. Zhao, B. Yu et al., "A new coronavirus associated with human respiratory disease in China," *Nature*, vol. 579, no. 7798, pp. 265–269, 2020.
- [16] S. P. Adhikari, S. Meng, Y. J. Wu et al., "Epidemiology, causes, clinical manifestation and diagnosis, prevention and control of coronavirus disease (COVID-19) during the early outbreak period: a scoping review," *Infectious Diseases of Poverty*, vol. 9, no. 1, p. 29, 2020.
- [17] Q. Li, X. Guan, P. Wu et al., "Early transmission dynamics in Wuhan, China, of novel coronavirus infected pneumonia," *New England Journal of Medicine*, vol. 382, no. 13, pp. 1199–1207, 2020.
- [18] P. Zhou, X. L. Yang, X. G. Wang et al., "Discovery of a novel coronavirus associated with the recent pneumonia outbreak in humans and its potential bat origin," *BioRxiv*, 2020.
- [19] H. Nishiura, S.-M. Jung, N. M. Linton et al., "The extent of transmission of novel coronavirus in Wuhan, China, 2020," *Journal of Clinical Medicine*, vol. 9, no. 2, p. 330, 2020.
- [20] T. P. Velavan and C. G. Meyer, "The COVID-19 epidemic," *Tropical Medicine & International Health*, vol. 25, no. 3, pp. 278–280, 2020.
- [21] F. A. Rabi, M. S. al Zoubi, G. A. Kasasbeh, D. M. Salameh, and A. D. al-Nasser, "SARS-CoV-2 and coronavirus disease 2019: what we know so far," *Pathogens*, vol. 9, no. 3, p. 231, 2020.
- [22] S. Jiang, L. Du, and Z. Shi, "An emerging coronavirus causing pneumonia outbreak in Wuhan, China: calling for developing therapeutic and prophylactic strategies," *Emerging Microbes & Infections*, vol. 9, no. 1, pp. 275–277, 2020.
- [23] L. L. Ren, Y. M. Wang, Z. Q. Wu et al., "Identification of a novel coronavirus causing severe pneumonia in human," *Chinese Medical Journal*, vol. 133, no. 9, pp. 1015–1024, 2020.
- [24] R. Lu, X. Zhao, J. Li et al., "Genomic characterisation and epidemiology of 2019 novel coronavirus: implications for virus origins and receptor binding," *The Lancet*, vol. 395, no. 10224, pp. 565–574, 2020.
- [25] Y.-H. Jin, L. Cai, Z.-S. Cheng et al., "A rapid advice guideline for the diagnosis and treatment of 2019 novel coronavirus (2019-nCoV) infected pneumonia (standard version)," *Military Medical Research*, vol. 7, no. 1, p. 4, 2020.
- [26] H. A. Rothan and S. N. Byrareddy, "The epidemiology and pathogenesis of coronavirus disease (COVID-19) outbreak," *Journal of Autoimmunity*, vol. 109, article 102433, 2020.
- [27] L. E. Gralinski and V. D. Menachery, "Return of the coronavirus: 2019-nCoV," *Viruses*, vol. 12, no. 2, p. 135, 2020.
- [28] Y. Han and H. Yang, "The transmission and diagnosis of 2019 novel coronavirus infection disease (COVID-19): a Chinese perspective," *Journal of Medical Virology*, vol. 92, no. 6, pp. 639–644, 2020.
- [29] P. Mo, Y. Xing, Y. Xiao et al., "Clinical characteristics of refractory COVID-19 pneumonia in Wuhan, China," *Clinical Infectious Diseases*, 2020.
- [30] W. Wang, J. Tang, and F. Wei, "Updated understanding of the outbreak of 2019 novel coronavirus (2019-nCoV) in Wuhan, China," *Journal of Medical Virology*, vol. 92, no. 4, pp. 441–447, 2020.
- [31] A. Assiri, J. A. al-Tawfiq, A. A. al-Rabeeh et al., "Epidemiological, demographic, and clinical characteristics of 47 cases of Middle East respiratory syndrome coronavirus disease from Saudi Arabia: a descriptive study," *The Lancet Infectious Diseases*, vol. 13, no. 9, pp. 752–761, 2013.
- [32] Y. Yin and R. G. Wunderink, "MERS, SARS and other coronaviruses as causes of pneumonia," *Respirology*, vol. 23, no. 2, pp. 130–137, 2018.
- [33] D. Wang, B. Hu, C. Hu et al., "Clinical characteristics of 138 hospitalized patients with 2019 novel coronavirus-infected pneumonia in Wuhan, China," *JAMA*, vol. 323, no. 11, pp. 1061–1069, 2020.
- [34] A. R. Sahin, A. Erdogan, P. M. Agaoglu et al., "2019 novel coronavirus (COVID-19) outbreak: a review of the current literature," *Eurasian Journal of Medicine and Oncology*, vol. 4, no. 1, pp. 1–7, 2020.
- [35] F. Pan, T. Ye, P. Sun et al., "Time course of lung changes on chest CT during recovery from 2019 novel coronavirus (COVID-19) pneumonia," *Radiology*, no. article 200370, 2020.
- [36] W. J. Guan, Z. Y. Ni, Y. Hu et al., "Clinical characteristics of 2019 novel coronavirus infection in China," *MedRxiv*, 2020.
- [37] N. Chen, M. Zhou, X. Dong et al., "Epidemiological and clinical characteristics of 99 cases of 2019 novel coronavirus pneumonia in Wuhan, China: a descriptive study," *The Lancet*, vol. 395, no. 10223, pp. 507–513, 2020.
- [38] L. Zhang and Y. Liu, "Potential interventions for novel coronavirus in China: a systematic review," *Journal of Medical Virology*, vol. 92, no. 5, pp. 479–490, 2020.
- [39] C. D. Russell, J. E. Millar, and J. K. Baillie, "Clinical evidence does not support corticosteroid treatment for 2019-nCoV lung injury," *The Lancet*, vol. 395, no. 10223, pp. 473–475, 2020.
- [40] L. Chen, J. Xiong, L. Bao, and Y. Shi, "Convalescent plasma as a potential therapy for COVID-19," *The Lancet Infectious Diseases*, vol. 20, no. 4, pp. 398–400, 2020.
- [41] I. M. Ibrahim, D. H. Abdelmalek, M. E. Elshahat, and A. A. Elfiky, "COVID-19 Spike-host cell receptor GRP78 binding site prediction," *Journal of Infection*, vol. 80, no. 5, pp. 554–562, 2020.
- [42] H. Lu, "Drug treatment options for the 2019-new coronavirus (2019-nCoV)," *Bioscience Trends*, vol. 14, no. 1, pp. 69–71, 2020.
- [43] J. Lim, S. Jeon, H. Y. Shin et al., "Case of the index patient who caused tertiary transmission of coronavirus disease 2019 in Korea: the application of lopinavir/ritonavir for the treatment of COVID-19 pneumonia monitored by quantitative RT-PCR," *Journal of Korean Medical Science*, vol. 35, no. 6, 2020.
- [44] S. Khaerunnisa, H. Kurniawan, R. Awaluddin, S. Suhartati, and S. Soetjipto, "Potential Inhibitor of COVID-19 Main Protease (Mpro) from Several Medicinal Plant Compounds by Molecular Docking Study," 2020.
- [45] M. A. Martinez, "Compounds with therapeutic potential against novel respiratory 2019 coronavirus," *Antimicrobial Agents and Chemotherapy*, vol. 64, no. 5, 2020.
- [46] H. T. Cui, Y. T. Li, L. Y. Guo et al., "Traditional Chinese medicine for treatment of coronavirus disease 2019: a review," *Traditional Medicine Research*, vol. 5, no. 2, pp. 65–73, 2020.
- [47] W. Chen, C. E. D. Lim, H.-J. Kang, and J. Liu, "Chinese herbal medicines for the treatment of type A H1N1 influenza: a systematic review of randomized controlled trials," *PLoS One*, vol. 6, no. 12, article e28093, 2011.

- [48] International Expert Meeting on the Treatment of SARS by Traditional Chinese Medicine, and the Integration of Traditional Chinese Medicine with Western Medicine, *SARS: clinical trials on treatment using a combination of traditional Chinese medicine and Western medicine: report of the WHO International Expert Meeting to review and analyse clinical reports on combination treatment for SARS, 8-10 October 2003*, World Health Organization, Beijing, People's Republic of China, 2004.
- [49] Y. Yang, M. S. Islam, J. Wang, Y. Li, and X. Chen, "Traditional Chinese medicine in the treatment of patients infected with 2019-new coronavirus (SARS-CoV-2): a review and perspective," *International Journal of Biological Sciences*, vol. 16, no. 10, pp. 1708–1717, 2020.
- [50] World Health Organization, *Minimum requirements for infection prevention and control programmes*, World Health Organization, 2019, <https://apps.who.int/iris/handle/10665/330080>.
- [51] World Health Organization, "Coronavirus disease (COVID-19) technical guidance: Infection prevention and control / WASH," March 2020, <https://www.who.int/emergencies/diseases/novel-coronavirus-2019/technical-guidance/infection-prevention-and-control>.
- [52] World Health Organization, "Coronavirus disease 2019 (COVID-19).events as they happen," March 2020, <https://www.who.int/emergencies/diseases/novel-coronavirus-2019/events-as-they-happen>.
- [53] W H Organization, *Managing Epidemics: Key Facts about Major Deadly Diseases*, WHO, World Health Organization, Geneva, 2018.
- [54] World Health Organization, *How to put on and take off personal protective equipment (PPE)*, World Health Organization, 2008.
- [55] World Health Organization, *WHO guidelines on hand hygiene in health care*, World Health Organization Press, Geneva, Switzerland, 2009.
- [56] World Health Organization, *Infection prevention and control of epidemic-and pandemic-prone acute respiratory infections in health care*, World Health Organization, Geneva, 2014.
- [57] World Health Organization, *Decontamination and Reprocessing of Medical Devices for Health-Care Facilities*, World Health Organization, Geneva, Switzerland, 2016.
- [58] T. Jefferson, C. B. Del Mar, L. Dooley et al., "Physical interventions to interrupt or reduce the spread of respiratory viruses," *Cochrane Database of Systematic Reviews*, 2011.

## Research Article

# Immunotherapy with IgY Antibodies toward Outer Membrane Protein F Protects Burned Mice against *Pseudomonas aeruginosa* Infection

Fatemeh Norouzi,<sup>1</sup> Bahador Behrouz,<sup>1</sup> Mahya Ranjbar,<sup>1,2</sup>  
and Seyed Latif Mousavi Gargari<sup>1</sup> 

<sup>1</sup>Department of Biology, Faculty of Basic Science, Shahed University, Tehran, Iran

<sup>2</sup>Department of Microbiology, Shahed University Faculty of Medical Sciences, Tehran, Iran

Correspondence should be addressed to Seyed Latif Mousavi Gargari; [slmousavi@shahed.ac.ir](mailto:slmousavi@shahed.ac.ir)

Received 8 February 2020; Revised 9 April 2020; Accepted 19 May 2020; Published 29 May 2020

Academic Editor: Roberta Antonia Diotti

Copyright © 2020 Fatemeh Norouzi et al. This is an open access article distributed under the Creative Commons Attribution License, which permits unrestricted use, distribution, and reproduction in any medium, provided the original work is properly cited.

Burn patients with multidrug-resistant *Pseudomonas aeruginosa* infections commonly suffer from high morbidity and mortality, which present a major challenge to healthcare systems throughout the world. Outer membrane protein F (OprF), as a main outer membrane porin, is required for full virulence expression of *P. aeruginosa*. The aim of this study was to evaluate the protective efficacy of egg yolk-specific antibody (IgY) raised against recombinant OprF (r-OprF) protein in a murine burn model of infection. The mice were immunized with r-OprF, and anti-r-OprF IgY was purified using salt precipitation. Groups of mice were injected with different regimens of anti-OprF IgY or control IgY (C-IgY). Infections were caused by subcutaneous injection of *P. aeruginosa* strain PAO1 at the burn site. Mice were monitored for mortality for 5 days. The functional activity of anti-OprF IgY was determined by *in vitro* invasion assays. Immunotherapy with anti-OprF IgY resulted in a significant improvement in the survival of mice infected by *P. aeruginosa* from 25% to 87.5% compared with the C-IgY and PBS. The anti-OprF IgY decreased the invasion of *P. aeruginosa* PAO1 into the A549. Passive immunization with anti-OprF IgY led to an efficacious protection against *P. aeruginosa* burn infection in the burn model.

## 1. Introduction

*P. aeruginosa* has emerged as a formidable pathogen that contributes to fatal infections among burn patients to a great extent, primarily because they are notoriously resistant to a broad array of antimicrobial agents, which rapidly disseminate throughout the burn units worldwide [1–3]. Moreover, nosocomially acquired multidrug-resistant (MDR) strains of *P. aeruginosa* can spread systemically from the site of burn wound infection to distant organs, in part due to the immunosuppressive effects of burn trauma, in addition to the production of virulence factors that confer invasiveness, which may result in life-threatening systemic infections [4]. The global rising trend of morbidity of burn patients, combined with the dwindling choices of effective therapeutic options

to treat MDR *P. aeruginosa* strains, has compelled researchers to investigate the merits of active as well as passive immunotherapy approaches in the treatment of severe burn wound infections.

Most clinical isolates of *P. aeruginosa* possess outer membrane protein F (OprF), encoded by the *oprF* gene which maintains the cell shape by anchoring the peptidoglycan to the outer membrane and is involved in host-pathogen interactions and also required for the expression of full virulence [5, 6]. For instance, studies have shown that non-OprF *P. aeruginosa* mutants have lower virulence in terms of impairment in ExoT and ExoS toxins through the type III secretion system (T3SS), *Pseudomonas* quinolone signal (PQS) synthesis, and production of the quorum-sensing-dependent virulence factors as well as biofilm development [7, 8].

Mounting evidence from several *in vitro* and *in vivo* studies supports the notion that OprF is surface exposed, is antigenically conserved, and could serve as a promising antigen for a vaccine against *P. aeruginosa* in various models of acute and chronic infections [9–13]. In addition, antibodies generated in response to OprF have been shown to exhibit potent antigen-binding, antibody-dependent, and complement-mediated opsonophagocytic killing activities against *P. aeruginosa* PAO1 [14], whose anti-OprF IgG activity level is correlated with the level of protection against *P. aeruginosa* in experimental animals and humans [15, 16]. Moreover, an adenovirus vector expressing OprF induces anti-OprF humoral and cellular immunity and provides protection against a lethal pulmonary challenge with *P. aeruginosa* [12].

Chicken egg yolk immunoglobulins (IgY) have been known as an extremely rich and economical source of polyclonal antibodies, which is not immunologically cross-reactive with the mammalian complement system and IgG [17]. Also, the high yield of specific antibodies along with simple and noninvasive collection method of IgY reveals a number of advantages over mammalian IgG antibodies to control infectious diseases [18]. IgY has been shown to prevent gastrointestinal [19] and influenza virus infections in both humans and animals without side effects [20, 21]. Oral immunotherapy with anti-*P. aeruginosa* IgY antibodies effectively declines chronic colonization of *P. aeruginosa* in CF patients [22, 23].

The present study evaluates the protective potential of anti-OprF IgY antibodies against *P. aeruginosa* in the burned mouse model of infection and determines the *in vitro* protective activity of elicited antibodies.

## 2. Materials and Methods

**2.1. Bacterial Strains and Growth Media.** *P. aeruginosa* PAO1 was used for the purification of the OprF protein and challenge. Luria-Bertani (LB) medium, trypticase soy agar (TSA), and tryptic soy broth (TSB; all from Merck, Germany) were used for routine culture of all bacterial strains.

**2.2. Animals.** Male 6–8-week-old BALB/C mice were purchased from the Royan Institute (Tehran, Iran). The 25 weeks old, shaver laying hens were purchased from a poultry farm (Alborz, Iran). All animal experiments were performed in compliance with the Animal Ethics Committee guidelines of Shahed University.

**2.3. Preparation of Recombinant Protein.** Recombinant OprF protein was purified as described previously. Briefly, the OprF gene (GenBank Accession No. NC\_002516.2), previously cloned into the pET-28a vector, was transformed into *Escherichia coli* BL21. The recombinant gene construct was expressed with isopropyl b-D thiogalactoside (IPTG, 1 mM), and protein was affinity purified by a Ni-NTA agarose column under denaturing procedures (Qiagen, Hilden, Germany). The purified recombinant protein was confirmed by Western blotting with mouse anti-His tag monoclonal antibody.

**2.4. Preparation of Anti-OprF IgY Antibodies.** Two hens were immunized with 150  $\mu$ g of the r-OprF in complete Freund's adjuvant (1:1; Sigma-Aldrich, USA), which was administered intramuscularly and boosted 3 times with 150  $\mu$ g of this protein in incomplete Freund's adjuvant (1:1; Sigma-Aldrich), while control hen received adjuvant only at 2-week intervals. Two weeks after the last injection, the laid eggs were collected daily for 5 to 6 months and stored at 4°C. Isolation of anti-OprF IgY antibodies was performed as described previously [24]. The separated egg yolk was diluted 7 times with distilled water (pH 5) and incubated at -70°C overnight and then filtered with Whatman cellulose filter paper (Sigma-Aldrich). The filtrate was mixed with 8.8% (*w/v*) NaCl at pH 4 for 2 h and then centrifuged at 3,380  $\times$  g for 20 min. The pellet was dissolved in PBS, and final IgY was stored at -20°C. The purity of IgY was evaluated by 9% SDS-PAGE, followed by Coomassie Brilliant Blue G-250 staining. The total amount of IgY was quantitatively measured by the Bradford method. The reactivity of IgY antibodies raised against the r-OprF was analyzed by immunoblotting r-OprF. The r-OprF was transferred onto the nitrocellulose membrane from SDS-PAGE by wet transfer blotting apparatus. The membrane was washed by PBS and blocked with PBS containing 5% (*w/v*) skim milk overnight. The membrane was washed and incubated with 1 mg of anti-OprF IgY for 2 h in order to recognize r-OprF. 1:10000 diluted rabbit anti-chicken IgY conjugated with HRP (Sigma-Aldrich) was added as a secondary antibody and incubated at 37°C for 2 h, then washed with 0.05% Tween PBS (T-PBS). The paper was submerged in a solution containing 50 mM Tris (pH 7.8) and 0.6 mg/mL 3,3'-diaminobenzidine substrate (DAB). The reaction was terminated with distilled water after color development.

**2.5. Evaluation of Anti-OprF IgY Titers.** Antigen-specific IgY titers against whole-cell *P. aeruginosa* PAO1 as well as r-OprF were assessed by ELISA, as described previously [25]. Briefly, each ELISA plate well (Nunc, USA) was coated with 10<sup>8</sup> CFU of *P. aeruginosa* PAO1 or 2.5  $\mu$ g r-OprF in 15 mM Na<sub>2</sub>CO<sub>3</sub> and 35 mM NaHCO<sub>3</sub> (pH 9.6), incubated overnight at 4°C, washed with 0.05% T-PBS, and blocked with PBS +5% skim milk. 100  $\mu$ L of 50  $\mu$ g/mL IgY antibodies was incubated in each well for 90 min at 37°C and washed three times with T-PBS, and then, 100  $\mu$ L of 1:1000-diluted HRP-conjugated rabbit anti-IgY antibody (HRP; Sigma-Aldrich) was added. After incubating for 1 h at 37°C, the plates were washed three times with T-PBS. Next, 100  $\mu$ L of TMB liquid substrate was added to each well. After color development for 20 min at room temperature, the reaction was stopped with 3 N H<sub>2</sub>SO<sub>4</sub> and the absorbance at 450 nm (OD<sub>450</sub>) was measured.

**2.6. Invasion Assay.** To test the inhibitory activity of anti-OprF IgY antibodies on *P. aeruginosa* invasion to the A549 cell line, a gentamicin protection assay was performed, and we followed the methods of Ranjbar et al. [25]. Briefly, anti-OprF IgY antibodies were mixed with PAO1 strain and then added to confluent A549 cells seeded in a 24-well plate (Nunc). Gentamicin was then added to the plate and

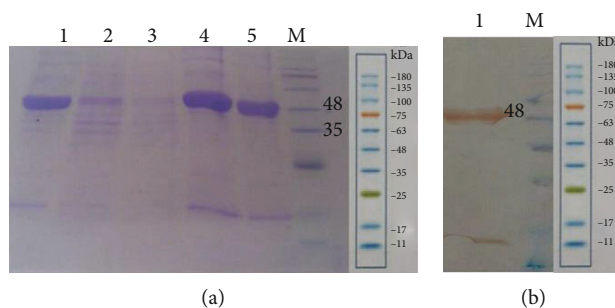


FIGURE 1: SDS-PAGE for detecting expressed and purified r-OprF. Lane M: low molecular weight protein size markers; Lane 1: precolumn lysate, Lane 2: flow through the matrix; Lane 3: washing with 20 mM imidazole; Lane 4: elution with 250 mM imidazole; Lane 5: purified r-OprF after dialysis (a). Western blotting results. Lane 1: r-OprF detected by monoclonal anti-His tag antibody; Lane M: low molecular weight protein size markers (b).

incubated for 1 h; then, cells were washed with PBS and lysed with 0.5% Triton X-100, and samples were serially diluted and grown on TSA plates (triplicates). Colony counting after 16 hours showed the number of PAO1 strain released from lysed cells.

**2.7. Murine Burn Infection Model.** The mice were burned and challenged as previously described by Neely et al. [26]. BALB/C mice ( $n = 56$ ) were randomized into 7 groups. Briefly, 10-15% total body surface area (TBSA) burn wound was created using ethanol flame (0.5 mL ethanol). All mice received 0.3 mL of sterile saline intraperitoneal immediately after burning. Acetaminophen (0.25 mg/mL) was used post burn as an analgesic. The mice were challenged subcutaneously at the burn site with *P. aeruginosa* neutralized by preincubating with 0.1 and 10 mg of anti-OprF IgY antibodies. In other groups, *P. aeruginosa* were preincubated with 1 mg of anti-OprF IgY antibodies and then mice received intravenously 0.5 mg of anti-OprF IgY antibodies 12 h after infection. Moreover, in other groups, mice received 1 mg of anti-OprF IgY antibodies 2 h before infection and 0.5 mg of anti-OprF IgY antibodies 12 and 24 h after infection. In the IgY control group, mice were challenged subcutaneously with *P. aeruginosa* that were preincubated 1 h with 1 mg of control IgY (C-IgY). Survival without treatment was monitored in the PBS-treated group. The burn control group comprised untreated mice with burn wounds that were not infected. The survival rate of experimental mice was monitored twice daily up to 5 days, which were analyzed using the Mantel-Cox log-rank test [25].

**2.8. Statistical Analysis.** All statistical analyses were performed using GraphPad Prism 6 (GraphPad Software, Inc., USA). The data were analyzed by one-way analysis of variance with Tukey's multiple comparison tests. Survival analysis for different mouse groups was performed using the Kaplan Meier survival curve with the Mantel-Cox log-rank test [25]. All results were expressed as the mean  $\pm$  standard deviation (SD). The  $P$  values less than 0.05 were considered statistically significant.

### 3. Results

**3.1. Expression and Purification of r-OprF.** The protein expression of *E. coli* BL21 (DE3) carrying a recombinant vector was induced with IPTG (1 mM). Based on the SDS-PAGE, the expression product of r-OprF protein was approximately 48 kDa. The OprF was successfully purified by Ni-NTA affinity chromatography under denaturing procedures (Figure 1(a)). As illustrated in Figure 1(b), based on Western blot analysis, anti-His monoclonal antibody reacted specifically with a ~48 kDa purified protein, corresponding to r-OprF.

**3.2. The Reactivity and Specificity of IgY Antibodies Raised against OprF.** The reactivity and specificity of IgY antibodies were evaluated using immunoblots of OprF. The IgY raised against r-OprF was precipitated by NaCl, and 50 mg of anti-OprF IgY was obtained per egg (Figure 2(a)). IgY antibodies from immunized egg yolk reacted with ~48 kDa r-OprF protein (Figure 2(b)). The specificities of IgY antibodies raised against r-OprF were further verified using an indirect ELISA to analyze whole cell lysates as well as r-OprF. As shown in Figures 2(c) and 2(d), the IgY levels of r-OprF-immunized hen against whole live cells of *P. aeruginosa* PAO1 strain or recombinant protein were significantly ( $P < 0.01$ ) higher than those of C-IgY over a period of time.

**3.3. Anti-OprF IgY Antibodies Reduce *P. aeruginosa* Invasion.** Anti-OprF IgY antibodies decrease the invasion to A549 cells by *P. aeruginosa*. The invasion efficiency of PAO1 in the presence of PBS was 100%. In contrast, in the presence of 1 and 2 mg/mL of anti-OprF IgY antibodies, invasion efficiencies of PAO1 were 33.72% and 35.08%, respectively, which were significantly higher than that of controls ( $P < 0.05$ , Figure 3). There was no significant difference between 1 and 2 mg/mL of anti-OprF IgY ( $P < 0.05$ ). In the presence of C-IgY antibodies, the invasion efficiency of PAO1 was 58.02%, which was significantly higher than that of PBS ( $P < 0.05$ ) (Figure 3).

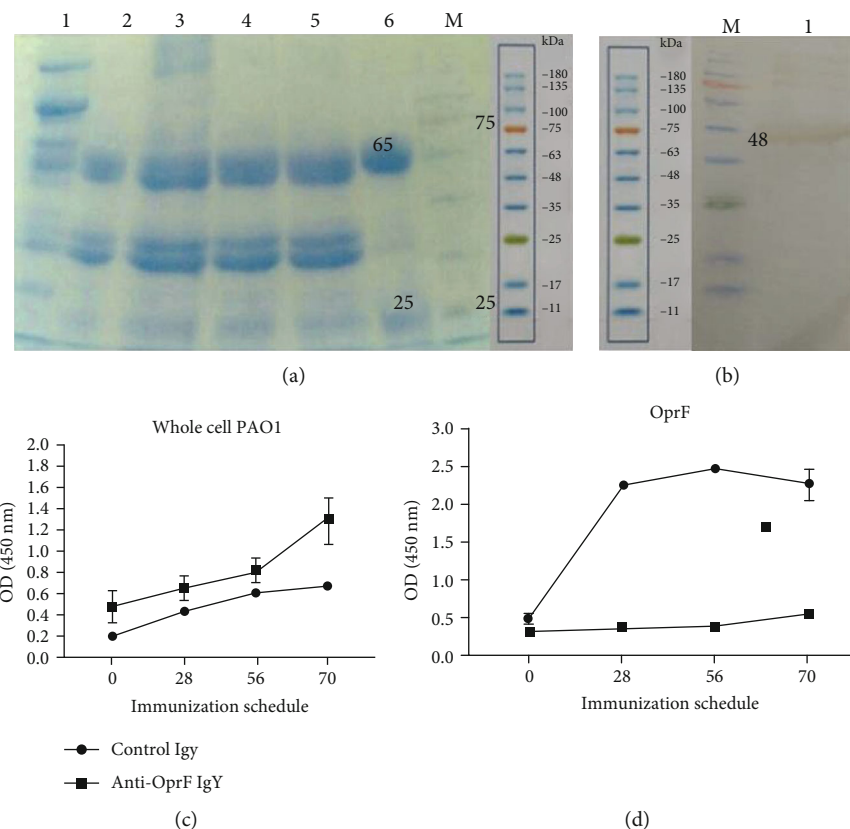


FIGURE 2: Precipitation and reactivity of anti-OprF IgY antibodies. SDS-PAGE of IgY precipitated with NaCl under acidic conditions. Lane 1: egg yolk; Lane 2: filtered diluted egg yolk, Lane 3: add NaCl; Lane 4: adjust pH 4; Lane 5: precipitated at room temperature for 2 h; Lane 6: purified IgY; Lane M: protein marker (a). R-OprF induced specific IgY binding to *P. aeruginosa* target antigen. IgY immunoreacted with r-OprF (~48) protein (b). An indirect ELISA was used to determine the reactivity of IgY antibodies against r-OprF with *P. aeruginosa* strain PAO1 (c) and r-OprF (d). C-IgY served as negative controls. Values represent the mean of triplicate independent experiments  $\pm$  standard deviation (SD).

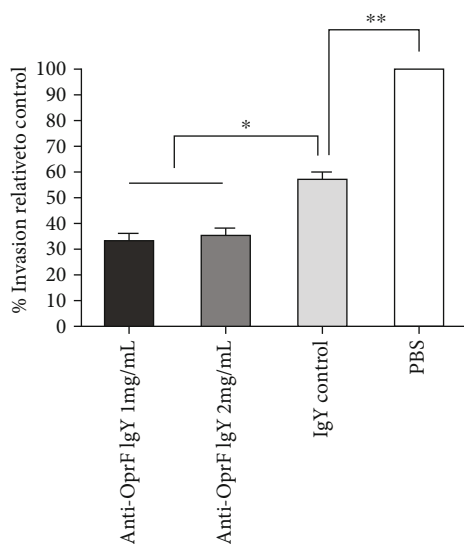


FIGURE 3: The inhibitory effects of anti-OprF IgY antibodies on the invasion of *P. aeruginosa* to A549 cells. PAO1 strain was incubated with different amounts of IgY antibodies (1 and 2 mg/mL). C-IgY and PBS served as controls. Values represent the mean of triplicate independent experiments  $\pm$  SD. \* $P < 0.05$  and \*\* $P < 0.01$ .

3.4. *Anti-OprF IgY Antibodies Increased the Survival of P. aeruginosa* Infected Mice. To assess the efficacy of anti-OprF IgY in rising protection against *P. aeruginosa* infection, we compared the survival rates of passively immunized mice with the anti-OprF IgY versus C-PBS- and C-IgY-infected mice (Table 1). The survival rates of infected mice with neutralized *P. aeruginosa* with both 0.1 and 10 mg of anti-OprF IgY were determined to be 25% (Figure 4(a)). Moreover, the survival rate of infected mice with neutralized *P. aeruginosa* with 1 mg of anti-OprF IgY and those that received 0.5 mg of anti-OprF IgY intravenously 12 h after infection was 50% (Table 1, Figure 4(b)). In addition, the survival rate of infected mice received 1 mg of anti-OprF IgY subcutaneously 2 h before infection as prophylaxis and treated with 0.5 mg of anti-OprF IgY intravenously 12 and 24 h after infection was 87.5%. None of the C-PBS and C-IgY mice survived *P. aeruginosa* wound infections (Table 1, Figure 4(c)). All noninfected burned mice survived.

#### 4. Discussion

The foremost challenge in controlling *P. aeruginosa* burn wound infections is a limited success in antimicrobial therapy due to the emergence of MDR strains, which are highly

TABLE 1: The effect of different regimens of anti-OprF IgY antibodies on the survival of *P. aeruginosa*-infected mice ( $n = 8$ ). Survival was assessed in infected mice with burn wounds days after subcutaneous injection of *P. aeruginosa*.

Group	Challenge	Intravenous treatment	No. of dead mice/total no. of mice on day					Survival (%)
			1	2	3	4	5	
I	Neutralized <i>P. aeruginosa</i> with 0.1 mg of anti-OprF IgY	—	1/8	6/8	6/8	6/8	6/8*	25
II	Neutralized <i>P. aeruginosa</i> with 10 mg of anti-OprF IgY	—	0/8	0/8	4/8	6/8	6/8*	25
III	Neutralized <i>P. aeruginosa</i> with 1 mg of anti-OprF IgY	0.5 mg of anti-OprF IgY (12 h after infection)	0/8	2/8	4/8	4/8	4/8**	50
IV	Prophylaxis 1 mg of anti-OprF IgY 2 h before infection with <i>P. aeruginosa</i>	0.5 mg of anti-OprF IgY (12 h and 24 h after infection)	0/8	0/8	1/8	1/8	1/8**	87.5
V	Neutralized <i>P. aeruginosa</i> with 1 mg of control IgY	—	0/8	6/8	8/8			0
VI	<i>P. aeruginosa</i>	—	8/8					0
VII	—	—	0/8	0/8	0/8	0/8	0/8**	100

\* $P < 0.05$  and \*\* $P < 0.01$  (Mantel-Cox log-rank test).

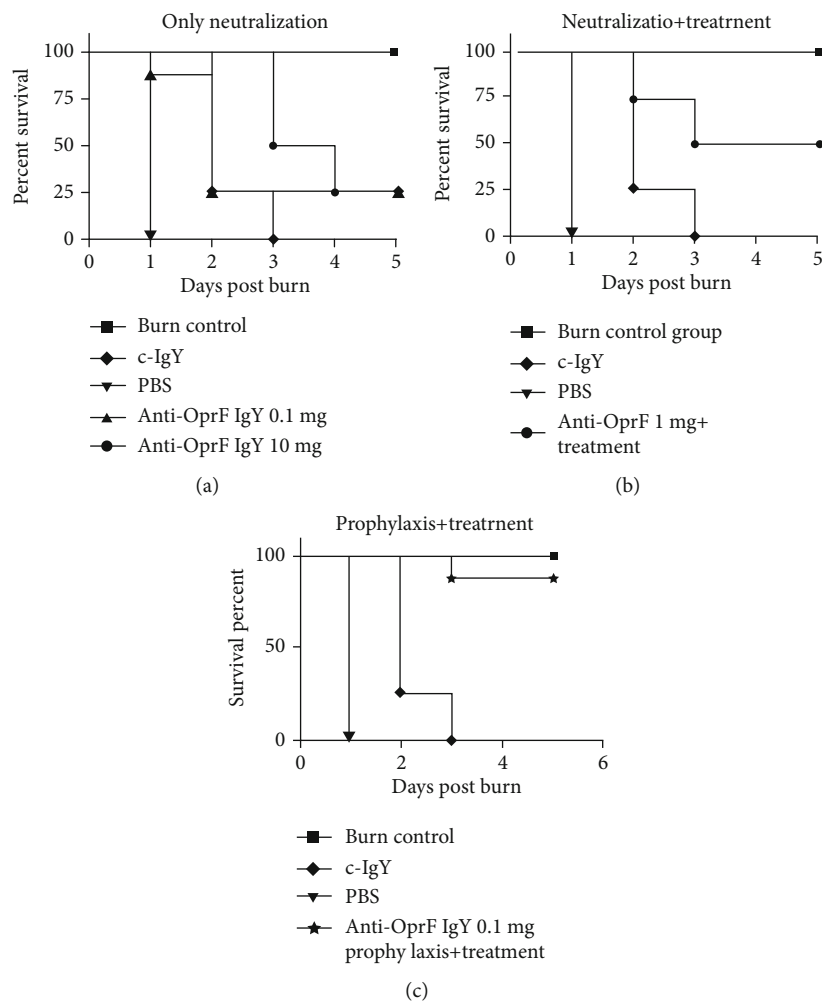


FIGURE 4: Protective effect of different anti-OprF IgY regimens on the survival of infected mice ( $n = 8$ ) in comparison to control groups 5 days after subcutaneous inoculation of  $10^8$  CFU *P. aeruginosa*. Mice received specific IgY as neutralized with bacteria (a), neutralized with bacteria treated with IgY after 12 h (b), and prophylaxis and treatment (c).



resistant to virtually all available antimicrobial agents. Moreover, *P. aeruginosa* commonly evades the immune response and produces a wide array of virulence factors, which further damages the patient's organ systems. This further complicates patient treatment and leads to the exclusion of antibody-based immunotherapy. Although several *P. aeruginosa* antigens have been evaluated as possible vaccine candidates, OprF is known as a feasible target antigen because it is expressed and conserved antigenically in clinical isolates as well as having important functions during infection and providing protective antibody responses. In the current study, the burn wound mouse model has used to demonstrate that anti-OprF IgY antibodies afford protection against lethal *P. aeruginosa* infections. Our result showed that burned challenged mice were protected and their survival rates were higher than control groups. The results of the burned mouse model indicated that prophylaxis of *P. aeruginosa* infection by anti-OprF IgY antibodies and intravenous injection of anti-OprF IgY antibodies as treatment led to an increase of 87.5% in the survival rate of mice compared to the control group. Our findings are consistent with Matthews-Greer and Gilleland [5], who showed active immunization with isolated OprF from cell envelope led to an increase of 83% in the survival rate of burned mice after challenge with *P. aeruginosa*. Additionally, Worgall et al. demonstrated that active immunization with adenovirus expressing *P. aeruginosa* OprF increased the survival rate of infected mice in acute pneumonia model to 80% [12]. This also accords with our earlier observation where preincubation of *P. aeruginosa* with anti PcrV IgY enhanced the survival rate of burned mice to 33% as our 25% in the same preincubated group [25]. It is crucial to consider this statement, especially in the era of increasing number of drug-resistant bacteria and predominant MDR-*P. aeruginosa* strains in numerous hospitals, principally in burn units. In addition, the complex issue of successfully eradicating virulent and highly resistant bacterial strains within burn patients is further exacerbated with the issue of dwindling number of newly approved antimicrobial agents against such strains. Fortunately, mounting evidence has indicated that immunotherapy is a promising treatment option that holds potential as an independent therapeutic strategy, alone or in combination with antimicrobial therapy [27, 28]. It seems rational to consider that antibody-based immunotherapy prevents MDR-*P. aeruginosa* burden among the burn patient in whom infection is being established, which ultimately causes high morbidity and mortality. However, inhibition of *P. aeruginosa* virulence factor OprF by IgY antibodies shows a specific antibacterial effect without triggering the development of resistant strains.

In this study, we found that bacterial invasion to A549 cells was inhibited by anti-OprF IgY antibodies, which indicated a key role in reducing the local and systemic distribution of *P. aeruginosa*. It was previously found that high hydrophobicity of anti-OprF IgY antibodies aggregates bacteria, therefore facilitating clearance by the host immune cells [29]. The findings of the current study are consistent with that of our previous report of 25% invasion of *P. aeruginosa* to A549 cells in the presence of 1 mg anti-PcrV IgY [25].

The observed substantial clinical efficacy of IgY immunotherapy may be associated with interference interactions between pathogen and host epithelial cells [30, 31]. Furthermore, anti-OprF IgGs exhibit potent antibody-dependent complement-mediated killing of the *P. aeruginosa* strain PAO1 [14], and the levels of antibodies correlate with the levels of protection against *P. aeruginosa* in burned mice [16]. In addition, it was suggested that IgY antibodies have inhibitory effects on bacterial pathogenesis and can be considered an adjunct therapy to improve antibiotic action. Thus, anti-OprF IgY antibodies showed a great activity against *P. aeruginosa* and interfered with the *P. aeruginosa* virulence factor to inhibit cell invasion. The moderate inhibitory activity of C-IgY having a nonsignificant reduction in the invasion of *P. aeruginosa* and improvement in the survival of infected mice compared to anti-OprF IgY could be due to the exposition of chickens with *P. aeruginosa*, which is a ubiquitous environmental bacterium and also polyclonal nature of IgY. These findings are consistent with previous studies [25, 29, 32–37].

## 5. Conclusion

In conclusion, these results offer evidence that anti-OprF IgY antibodies can confer protection against burn wound infection caused by *P. aeruginosa* through the inhibition of bacterial invasion to host cells and tissues. Our data show that *P. aeruginosa*-infected treated mice are protected against burn wound sepsis, further supporting the conclusion that IgY against OprF provides approaches to develop a protective treatment. Supposedly, anti-OprF IgY antibodies may be used in combination with antibiotic therapies as an adjunct approach to prevent *P. aeruginosa* infections.

## Data Availability

No data were used to support this study.

## Conflicts of Interest

There are no conflicts of interest.

## Acknowledgments

This work was supported by Shahed University.

## References

- [1] I. A. Bahemia, A. Muganza, R. Moore, F. Sahid, and C. N. Menezes, "Microbiology and antibiotic resistance in severe burns patients: a 5 year review in an adult burns unit," *Burns*, vol. 41, no. 7, pp. 1536–1542, 2015.
- [2] E. F. Keen, B. J. Robinson, D. R. Hospenthal et al., "Prevalence of multidrug-resistant organisms recovered at a military burn center," *Burns*, vol. 36, no. 6, pp. 819–825, 2010.
- [3] M. A. Albrecht, M. E. Griffith, C. K. Murray et al., "Impact of Acinetobacter infection on the mortality of burn patients," *Journal of the American College of Surgeons*, vol. 203, no. 4, pp. 546–550, 2006.

- [4] D. Church, S. Elsayed, O. Reid, B. Winston, and R. Lindsay, "Burn wound infections," *Clinical Microbiology Reviews*, vol. 19, no. 2, pp. 403–434, 2006.
- [5] J. M. Matthews-Greer and H. E. Gilleland, "Outer membrane protein F (porin) preparation of *Pseudomonas aeruginosa* as a protective vaccine against heterologous immunotype strains in a burned mouse model," *The Journal of Infectious Diseases*, vol. 155, no. 6, pp. 1282–1291, 1987.
- [6] H. E. Gilleland Jr., L. B. Gilleland, and J. M. Matthews-Greer, "Outer membrane protein F preparation of *Pseudomonas aeruginosa* as a vaccine against chronic pulmonary infection with heterologous immunotype strains in a rat model," *Infection and Immunity*, vol. 56, no. 5, pp. 1017–1022, 1988.
- [7] E. Bouffartigues, J. A. Moscoso, R. Duchesne et al., "The absence of the *Pseudomonas aeruginosa* OprF protein leads to increased biofilm formation through variation in c-di-GMP level," *Frontiers in Microbiology*, vol. 6, p. 630, 2015.
- [8] L. Fito-Boncompte, A. Chapalain, E. Bouffartigues et al., "Full virulence of *Pseudomonas aeruginosa* requires OprF," *Infection and Immunity*, vol. 79, no. 3, pp. 1176–1186, 2011.
- [9] L. Peluso, C. de Luca, S. Bozza et al., "Protection against *Pseudomonas aeruginosa* lung infection in mice by recombinant OprF-pulsed dendritic cell immunization," *BMC Microbiology*, vol. 10, no. 1, p. 9, 2010.
- [10] A. W. Cripps, M. L. Dunkley, D. C. Taylor, S. Cousins, and R. L. Clancy, "Immunity to *Pseudomonas aeruginosa* induced by OprF following intestinal immunization," *Advances in Experimental Medicine and Biology*, vol. 371B, pp. 761–763, 1995.
- [11] B. M. Price, D. R. Galloway, N. R. Baker, L. B. Gilleland, J. Staczek, and H. E. Gilleland Jr., "Protection against *Pseudomonas aeruginosa* chronic lung infection in mice by genetic immunization against outer membrane protein F (OprF) of *P. aeruginosa*," *Infection and Immunity*, vol. 69, no. 5, pp. 3510–3515, 2001.
- [12] S. Worgall, A. Krause, J. P. Qiu, J. Joh, N. R. Hackett, and R. G. Crystal, "Protective immunity to *pseudomonas aeruginosa* induced with a capsid-modified adenovirus expressing *P. aeruginosa* OprF," *Journal of Virology*, vol. 81, no. 24, pp. 13801–13808, 2007.
- [13] U. Baumann, E. Mansouri, and B.-U. Von Specht, "Recombinant OprF–OprI as a vaccine against *Pseudomonas aeruginosa* infections," *Vaccine*, vol. 22, no. 7, pp. 840–847, 2004.
- [14] E. T. Weimer, S. E. Ervin, D. J. Wozniak, and S. B. Mizel, "Immunization of young African green monkeys with OprF epitope 8–OprI–type A- and B-flagellin fusion proteins promotes the production of protective antibodies against nonmucoid *Pseudomonasaeruginosa*," *Vaccine*, vol. 27, no. 48, pp. 6762–6769, 2009.
- [15] T. R. Anderson and T. C. Montie, "Flagellar antibody stimulated opsonophagocytosis of *Pseudomonas aeruginosa* associated with response to either a- or b-type flagellar antigen," *Canadian Journal of Microbiology*, vol. 35, no. 9, pp. 890–894, 1989.
- [16] T. R. Anderson and T. C. Montie, "Opsonophagocytosis of *Pseudomonas aeruginosa* treated with antflagellar serum," *Infection and immunity.*, vol. 55, no. 12, pp. 3204–3206, 1987.
- [17] G. W. Warr, K. E. Magor, and D. A. Higgins, "IgY: clues to the origins of modern antibodies," *Immunology Today*, vol. 16, no. 8, pp. 392–398, 1995.
- [18] M. Tini, U. R. Jewell, G. Camenisch, D. Chilov, and M. Gassmann, "Generation and application of chicken egg yolk antibodies," *Comparative Biochemistry and Physiology. Part A, Molecular & Integrative Physiology*, vol. 131, no. 3, pp. 569–574, 2002.
- [19] S. Rahman, K. Higo-Moriguchi, K. W. Htun et al., "Randomized placebo-controlled clinical trial of immunoglobulin Y as adjunct to standard supportive therapy for rotavirus-associated diarrhea among pediatric patients," *Vaccine*, vol. 30, no. 31, pp. 4661–4669, 2012.
- [20] H. H. Nguyen, T. M. Tumpey, H. J. Park et al., "Prophylactic and therapeutic efficacy of avian antibodies against influenza virus H5N1 and H1N1 in mice," *PLoS One*, vol. 5, no. 4, article e10152, 2010.
- [21] M. G. Wallach, R. J. Webby, F. Islam et al., "Cross-protection of chicken immunoglobulin Y antibodies against H5N1 and H1N1 viruses passively administered in mice," *Clinical and Vaccine Immunology*, vol. 18, no. 7, pp. 1083–1090, 2011.
- [22] E. Nilsson, A. Larsson, H. V. Olesen, P. E. Wejaker, and H. Kollberg, "Good effect of IgY against *Pseudomonas aeruginosa* infections in cystic fibrosis patients," *Pediatric Pulmonology*, vol. 43, no. 9, pp. 892–899, 2008.
- [23] H. Kollberg, D. Carlander, H. Olesen, P. E. Wejaker, M. Johannesson, and A. Larsson, "Oral administration of specific yolk antibodies (IgY) may prevent *Pseudomonas aeruginosa* infections in patients with cystic fibrosis: a phase I feasibility study," *Pediatric Pulmonology*, vol. 35, no. 6, pp. 433–440, 2003.
- [24] E. M. Akita and S. Nakai, "Comparison of four purification methods for the production of immunoglobulins from eggs laid by hens immunized with an enterotoxigenic *E. coli* strain," *Journal of Immunological Methods*, vol. 160, no. 2, pp. 207–214, 1993.
- [25] M. Ranjbar, B. Behrouz, F. Norouzi, and S. L. M. Gargari, "Anti-PcrV IgY antibodies protect against *Pseudomonas aeruginosa* infection in both acute pneumonia and burn wound models," *Molecular Immunology*, vol. 116, pp. 98–105, 2019.
- [26] A. N. Neely, I. A. Holder, and G. D. Warden, "Then and now: studies using a burned mouse model reflect trends in burn research over the past 25 years," *Burns: journal of the International Society for Burn Injuries*, vol. 25, no. 7, pp. 603–609, 1999.
- [27] J.-P. Pirnay, D. De Vos, C. Cochez et al., "Molecular epidemiology of *Pseudomonas aeruginosa* colonization in a burn unit: persistence of a multidrug-resistant clone and a silver sulfadiazine-resistant clone," *Journal of Clinical Microbiology*, vol. 41, no. 3, pp. 1192–1202, 2003.
- [28] N. P. Singh, R. Goyal, V. Manchanda, S. Das, I. Kaur, and V. Talwar, "Changing trends in bacteriology of burns in the burns unit, Delhi, India," *Burns*, vol. 29, no. 2, pp. 129–132, 2003.
- [29] K. Thomsen, L. Christophersen, T. Bjarnsholt, P. O. Jensen, C. Moser, and N. Hoiby, "Anti-*Pseudomonas aeruginosa* IgY antibodies induce specific bacterial aggregation and internalization in human polymorphonuclear neutrophils," *Infection and Immunity*, vol. 83, no. 7, pp. 2686–2693, 2015.
- [30] X. Li, L. Wang, Y. Zhen, S. Li, and Y. Xu, "Chicken egg yolk antibodies (IgY) as non-antibiotic production enhancers for use in swine production: a review," *Journal of Animal Science and Biotechnology*, vol. 6, no. 1, p. 40, 2015.
- [31] S. Rahman, S. Van Nguyen, F. C. Icatlo Jr., K. Umeda, and Y. Kodama, "Oral passive IgY-based immunotherapeutics: a novel solution for prevention and treatment of alimentary

- tract diseases,” *Human Vaccines & Immunotherapeutics*, vol. 9, no. 5, pp. 1039–1048, 2014.
- [32] K. Thomsen, L. Christophersen, T. Bjarnsholt, P. Ø. Jensen, C. Moser, and N. Højby, “Anti- *Pseudomonas aeruginosa* IgY antibodies augment bacterial clearance in a murine pneumonia model,” *Journal of Cystic Fibrosis*, vol. 15, no. 2, pp. 171–178, 2016.
- [33] K. Thomsen, L. Christophersen, P. Ø. Jensen, T. Bjarnsholt, C. Moser, and N. Højby, “Anti-*Pseudomonas aeruginosa* IgY antibodies promote bacterial opsonization and augment the phagocytic activity of polymorphonuclear neutrophils,” *Human Vaccines & Immunotherapeutics*, vol. 12, no. 7, pp. 1690–1699, 2016.
- [34] H. Ahmadi, B. Behrouz, G. Irajian, N. Amirmozafari, and S. Naghavi, “Bivalent flagellin immunotherapy protects mice against *Pseudomonas aeruginosa* infections in both acute pneumonia and burn wound models,” *Biologicals*, vol. 46, pp. 29–37, 2017.
- [35] M. Saffari, S. Behbood, G. Irajian, A. Khorshidi, R. Moniri, and B. Behrouz, “Antibodies raised against divalent type b flagellin and pilin provide effective immunotherapy against *Pseudomonas aeruginosa* infection of mice with burn wounds,” *Biologicals*, vol. 45, pp. 20–26, 2017.
- [36] B. Behrouz, N. Amirmozafari, N. Khoramabadi, M. Bahroudi, P. Legae, and M. Mahdavi, “Cloning, expression, and purification of *Pseudomonas aeruginosa* flagellin, and characterization of the elicited anti-flagellin antibody,” *Iranian Red Crescent Medical Journal*, vol. 18, no. 6, p. e28271, 2016.
- [37] M. Mousavi, B. Behrouz, G. Irajian, M. Mahdavi, F. Korpi, and M. Motamedifar, “Passive immunization against *Pseudomonas aeruginosa* recombinant PilA in a murine burn wound model,” *Microbial Pathogenesis*, vol. 101, pp. 83–88, 2016.